Measuring Underwater noise exposure from shipping

Merchant, Nathan

Award date:
2014

Awarding institution:
University of Bath

Measuring underwater noise exposure from shipping

submitted by

Nathan Daniel Merchant

for the degree of Doctor of Philosophy

of the

University of Bath

Department of Physics

October 2013

Summary

Levels of underwater noise in the open ocean have been increasing since at least the 1960s due to growth in global shipping traffic and the speed and propulsion power of vessels. This rise in noise levels reduces the range over which vocal marine species can communicate, and can induce physiological stress and behavioural responses, which may ultimately have population-level consequences. Although long-term noise trends have been studied at some open-ocean sites, in shallower coastal regions the high spatiotemporal variability of noise levels presents a substantial methodological challenge, and trends in these areas are poorly understood.

This thesis addresses this challenge by introducing new techniques which combine multiple data sources for ship noise assessment in coastal waters. These data include Automatic Identification System (AIS) ship-tracking data, shore-based time-lapse footage, meteorological data, and tidal data. Two studies are presented: in the first, AIS data and acoustic recordings from Falmouth Bay in the western English Channel are combined using an adaptive threshold, which separates ship passages from background noise in the acoustic data. These passages are then cross-referenced with AIS vessel tracks, and the noise exposure associated with shipping activity is then determined. The second study, at a site in the Moray Firth, Scotland, expanded the method to include shore-based time-lapse footage, which enables visual corroboration of vessel identifications and the production of videos integrating the various data sources.

Two further studies examine and enhance basic analysis techniques for ambient noise monitoring. The first study examines averaging metrics and their applicability to the assessment of noise from shipping. Long-term data from the VENUS observatory are empirically assessed for different averaging times and in the presence of outliers. It is concluded that the mean sound pressure level averaged in linear space is most appropriate, in terms of both standardisation and relevance to impacts on marine fauna. In the second study, a new technique for the statistical analysis of long-term passive acoustic datasets, termed spectral probability density (SPD), is introduced. It is shown that the SPD can reveal characteristics such as multimodality, outlier influence, and persistent self-noise, which are not apparent using conventional techniques. This helps to interpret long-term datasets, and can indicate whether an instrument's dynamic range is appropriate to field conditions.

Taken together, the contributions presented in this thesis help to establish a stronger methodological basis for the assessment of shipping noise. These methods can help to inform emerging policy initiatives, efforts to standardise underwater noise measurements, and investigation into the effects of shipping noise on marine life.

To Mum and Dad
for supporting me all the way,
and to Julia
for putting up with me.

In the beginner's mind there are many possibilities,
in the expert's there are few.

— SHUNRYU SUZUKI

μέγα βιβλίον μέγα κακόν
Mega biblion, mega kakon.

— CALLIMACHUS

Acknowledgements

First of all, and most of all, I'd like to thank my supervisor, Philippe Blondel, who has supported me selflessly and unconditionally throughout these three years. The more I learn about academia, the more I realise how fortunate I've been to find a supervisor so positive and so willing to make time in a very busy schedule. None of this work would have been possible without your patience, good humour, and (mercifully!) tactful guidance.

Next, I'd like to thank my principal collaborators, all of whom invested considerable time early on in my PhD to make projects happen which would depend on my unproven abilities: Matthew Witt and Brendan Godley (University of Exeter), Tom Dakin and John Dorocicz (University of Victoria), and Paul Thompson and Enrico Pirotta (Universiy of Aberdeen). I hope you'll agree that the risk has paid off, and I can't thank you enough for putting in all the hard work by collecting the data presented here. I especially thank Matthew Witt, who has set a great (and, to me, unobtainable) example as an early career role model, and Paul Thompson for generously hosting me at the Lighthouse Field Station in Cromarty more than once.

Technical support has been key to this data-intensive project, and I've particularly relied on the excellent IT knowhow of Simon Dodd and Adrian Hooper in the Department of Physics at Bath to churn through the multiple terabytes in various formats. Tim Barton at the University of Aberdeen has been equally indispensable in managing the data and equipment for our collaborations in the Moray Firth.

Thanks to Kim Juniper for letting me join the ONC 'Wiring the Abyss 2013' cruise aboard the *R/V Thompson* in the Northeast Pacific, and to Maia Hoeberechts, Steve Mihaly, and the rest of the cruise team for an enjoyable and memorable experience. Thanks also to Becky Hewitt and Rachael Plunkett for a fun couple of days in the Moray Firth on the *M/V Solstice*.

Various elders (and not so elders!) from the underwater acoustics scene in the UK and further afield have been kind enough to offer advice and encouragement during my PhD, and I'd par-

ticularly like to thank Stephen Robinson, Paul Lepper, Pete Theobald, Michel André, Dick Hazelwood, Mike Ainslie, Victor Humphrey, Ben Wilson, Christine Erbe, Ross Chapman, Jakob Tougaard and Annie Linley.

I'd also like to thank my fellow travellers at various events and at our various stages along the PhD path. Be it earnestly sharing research experiences or dancing incompetently till daybreak in Budapest nightclubs, moped-ing round Greek islands or stopping for 1 a.m. Montreal bagels, the journey wouldn't have been half as rewarding without you. Roughly in order of appearance: Stephanie Moore, Astrid Harendza, David Barclay, Jen Wladichuk, Sophie Holles (now Nedelec), Paul Barker, Caroline Carter, Enrico Pirotta (again!), Julius Piercy, Irene Völlmy, Errol Neo, Jo Garrett, Daphne Cuvelier, Françoise Gervais, Guangyu Xu, Ilaria Spiga, Louise Roberts and Jamie McWilliam.

Friends in Bath who have made it a great place to live include: Andre Müller, Ashok Chauhan, Aleksandra Kruss, Juanjo Riquelme, Douglas Shanks, Kamil Wezka, Keiron Pizzey, Dean Whittaker, David Tregurtha, Peter Lewis, Gavin Jones, Le Zhao, Hazel Garvie-Cook, Charlene Edwardson, Ed Wright, Ruth Rowlands and Kristina Rusimova.

Finally, I thank Julia, my partner, who has tirelessly proofread all of my work and helped me to rethink many of my more wayward ideas. Thank you for putting things in perspective and making me take a break once in a while – all of the credit for keeping me tolerably compos mentis goes to you.

Contents

List of Publications

The following publications were authored or co-authored by the author during the PhD. Four of these appear as sections in the thesis (see footnotes).

Peer-Reviewed Journal Articles

*Merchant, N.D., Pirotta, E., Barton, T.R., and Thompson, P.M. (2014). Monitoring ship noise to assess the impact of coastal developments on marine mammals. Marine Pollution Bulletin 78 (1-2), 85-95.

Thompson, P.M., Brookes, K.L., Graham, I.M., Barton, T.R., Needham, K., Bradbury, G., Merchant, N.D. (2013). Short-term disturbance by a commercial two-dimensional seismic survey does not lead to long-term displacement of harbour porpoises. Proceedings of the Royal Society B: Biological Sciences 280 (1771), 20132001.

†Merchant, N.D., Barton, T.R., Thompson, P.M., Pirotta, E., Dakin, D.T., Dorocicz, J. (2013). Spectral probability density as a tool for ambient noise analysis. Journal of the Acoustical Society of America 133 (4), EL262-EL267.

‡Merchant, N.D., Blondel, P., Dakin, D.T., Dorocicz, J. (2012). Averaging underwater noise levels for environmental assessment of shipping. Journal of the Acoustical Society of America 132 (4), EL343-EL349.

§Merchant, N.D., Witt, M.J., Blondel, P., Godley, B.J., Smith, G.H. (2012). Assessing sound exposure from shipping in coastal waters using a single hydrophone and Automatic Identification System (AIS) data. Marine Pollution Bulletin 64 (7), 1320-1329.

*Section 4.2, p72.
†Section 3.2, p46.
‡Section 3.1, p39.
§Section 4.1, p55.

Reports

Merchant, N.D. and Blondel, P. (2013). Underwater noise measurements in Mayumba National Park, Gabon, during the VAALCO/Harvest Etame-Marin seismic surveys in October/November 2011. Report commissioned by VAALCO Energy, Inc. 33pp.

Conference Papers

Merchant, N.D., Dakin, D.T., Dorocicz, J., Blondel, P. (2013). Remote performance assessment of cabled observatory hydrophone systems. Journal of the Acoustical Society of America 134 (5), 3973 (presented by D.T. Dakin at the 166th Meeting of the Acoustical Society of America, 2-6 December 2013, San Francisco, USA).

Merchant, N.D., Pirotta, E., Barton, T.R., Thompson, P.M. (2013). Soundscape and noise exposure monitoring in a marine protected area using shipping data and time-lapse footage. 3rd International Conference on the Effects of Noise on Aquatic Life, 11-16 August 2013, Budapest, Hungary.

Merchant, N.D., Barton, T.R., Thompson, P.M., Pirotta, E., Dakin, D.T., Dorocicz, J. (2013). Spectral probability density as a tool for marine ambient noise analysis. Journal of the Acoustical Society of America 133 (5), 3494 (presented at International Congress on Acoustics, 2-7 June 2013, Montreal, Canada).

Merchant, N.D., Witt, M.J., Blondel, P., Godley, B.J., Smith, G.H. (2012). Long-term monitoring of sound exposure from shipping in coastal waters. 11th European Conference on Underwater Acoustics (ECUA), 2-6 July 2012, Edinburgh, Scotland.

Merchant, N.D., Witt, M.J., Blondel, P., Godley, B.J., Smith, G.H. (2011). Ambient noise in the western English Channel: Temporal variability due to shipping and biological sources. Proceedings of the Institute of Acoustics 33 (5), 27-29 (presented at Ambient noise in north-European seas: Monitoring, impact and management, 3-5 October 2011, National Oceanography Centre, Southampton).

Merchant, N.D., Blondel, P., Wladichuk, J.L., Megill, W.M. (2011). Acoustic interaction of humpback whales and recreational fishing vessels in a temperate fjord: Measurements in Rivers' Inlet, British Columbia. 4th International Conference and Exhibition on Underwater Acoustic Measurements: Technologies and Results, 20-24 June 2011, Kos, Greece.

Table of Figures

Glossary of Acronyms and Abbreviations

Term	Definition	Page
ADC	Analogue-to-Digital Converter	28
AIS	Automatic Identification System	58
AMAR	Autonomous Multichannel Acoustic Recorder	58
ASW	Anti-Submarine Warfare	26
ATL	Adaptive Threshold Level	61
CPA	Closest Point of Approach	62
DFT	Discrete Fourier Transform	29
DP	Dynamic Positioning	80
EIA	Environmental Impact Assessment	3
GUI	Graphical User Interface	62
MMSI	Maritime Mobile Service Identity	62
MPA	Marine Protected Area	54
MRED	Marine Renewable Energy Device	19
MSFD	Marine Strategy Framework Directive	40
NOAA	National Oceanic and Atmospheric Administration	98
ONC	Ocean Networks Canada	38
ONCCEE	ONC Centre for Enterprise and Engagement	40
PAM	Passive Acoustic Monitoring	24
PCAD	Population Consequences of Acoustic Disturbance	2
PD	Probability Density	41
PSD	Power Spectral Density	29
SAC	Special Area of Conservation	74
SEL	Sound Exposure Level	44
SPD	Spectral Probability Density	47
SPL	Sound Pressure Level	32
WAV	WAVeform audio format	28
WEC	Wave Energy Converter	19

Chapter 1

Introduction

1.1 Setting the Scene

The threats to marine ecosystems from human activities are manifold: chemical and biological pollution, climate change and acidification, oil spillages, radioactive waste, heavy metals, and plastic debris are imposing unprecedented pressures on Earth's oceanic environment (Shahidul Islam and Tanaka, 2004). One form of pollution that is increasingly recognised as a substantial threat to marine life is anthropogenic noise (Richardson et al., 1995; National Research Council, 2005). Anthropogenic noise is generated – intentionally or otherwise – by activities such as shipping, offshore construction, and military sonar operations, and probably reached significant levels with the mechanisation of ship propulsion in the 19th century.

Anthropogenic noise was first posited as a threat to marine life in 1971 (Payne and Webb, 1971) in relation to the masking of long-range acoustic communication among baleen whales by noise from shipping. In subsequent decades, significant progress was made to document responses to noise (mostly concerning cetaceans), but it was not until the 1990s that this work was amalgamated and key knowledge gaps identified (Myrberg, 1990; Richardson et al., 1995; Richardson and Würsig, 1997). In the following years, the field was pursued with greater urgency, and by the early 2000s, several high-profile whale strandings linked to military sonar testing (Frantzis, 1998; Evans and England, 2001) had raised the issue in the public consciousness, and the research effort received widespread attention.

Assessing the impact of anthropogenic noise is a complex task, and establishing appropriate criteria remains a work in progress. This work is hampered by a lack of information in sev-

eral key areas. For example, the auditory sensitivities of most marine species (including all baleen whales) are still unknown (Au and Hastings, 2008), and long-term population-scale effects have yet to be characterised (National Research Council, 2005). Further obstacles are presented by the multidisciplinary nature of the field, as the differing methodologies and perspectives of several long-established disciplines have to be overcome. These knowledge gaps and the uncertainty in how to quantify environmental impacts make it more difficult to build a case for the regulation of anthropogenic noise in the near term (Horowitz and Jasny, 2007).

Efforts to address these deficits are proceeding on several fronts. Basic research into the responses of marine fauna to anthropogenic noise is becoming more sophisticated, as studies have progressed from describing short-term behavioural responses by cetaceans to exceptionally loud events (e.g. Richardson et al., 1986), to observing other taxa [such as fish (e.g. McCauley et al., 2003) and invertebrates (e.g. André et al., 2011b)]; lower-amplitude sources such as ship noise (e.g. Rolland et al., 2012; Holles et al., 2013); longer-term – often subtle – responses (Parks et al., 2007; Picciulin et al., 2010); effects on larval development (Aguilar de Soto et al., 2013); and physiological changes in response to noise (e.g. Wysocki et al., 2006; Wale et al., 2013a). Such observations are being fed into models which seek to predict the population-level consequences of acoustic disturbance (PCAD; e.g. New et al., 2013). At the same time, advances are being made in 'top-down' management of underwater noise pollution, with some legislatures moving towards statutory regulation of underwater noise (European Commission, 2008) and attempts to map underwater noise levels at a regional and national scale (Erbe et al., 2012; NOAA, 2012). One thing these developments have in common is their need for metrics and methodologies to describe underwater noise which are relevant to interpreting its potential effects on marine life. However, acoustical metrics are often misapplied (as discussed by, e.g. Madsen, 2005; Ainslie, 2011), and the development of suitable noise monitoring methodologies is ongoing (e.g. Van der Graaf et al., 2012).

This thesis focuses on these methodological issues, with a particular emphasis on shipping. Noise from shipping is the most pervasive source of anthropogenic noise (Hildebrand, 2009), and has been increasing in magnitude in the deep ocean since at least the 1960s (Andrew et al., 2002), in line with global economic growth (Frisk, 2012). The persistence and ubiquity of shipping noise suggest it may have chronic effects on marine species (Wright et al., 2007a; Tyack, 2008), both through repeated exposures to vessel passages and a more diffuse heightening of background noise levels. This can induce a variety of effects, including physiological stress (Wysocki et al., 2006; Rolland et al., 2012) and communication masking (Vasconcelos et al., 2007; Clark et al., 2009). There is now a need to quantify levels of noise exposure from shipping in marine environments to better understand the potential severity of impacts on marine ecosystems. Long-term monitoring of ship noise has hitherto focused on deep-water

environments (e.g. Andrew et al., 2002; McDonald et al., 2006; Chapman and Price, 2011), but the concentration of shipping activity and sensitive marine ecosystems in coastal waters means there is also a need to develop methodologies for these shallow-water areas. This presents a significant challenge, since noise levels in coastal waters exhibit high spatiotemporal variability and sound propagation is highly dependent on environmental factors (Jensen et al., 2011).

An eventual aim of studying noise exposure from shipping is to inform regulation and mitigation measures where harmful levels are identified. In the terrestrial domain, assessment of human noise exposure to transport, construction and industrial activities is a well-established field (Harris, 1991), and an analogous industry is developing around environmental impact assessment (EIA) of underwater noise from offshore construction and oil and gas exploration. Regulation of shipping noise is more problematic, since shipping routinely traverses international jurisdictions, and measures such as mandatory ship-quieting technology would require broad international agreement (Southall, 2005). Nevertheless, by quantifying levels and variability of shipping noise, initial steps can be taken towards regulation of shipping noise through the identification of areas of greatest concern. With this in mind, the work presented in this thesis also considers how methodologies can inform large-scale marine environmental management as well as specific EIAs.

1.2 Research Objectives

There is a clear need to better understand the scale and severity of our acoustic impact on the marine environment, and to manage and mitigate these impacts in a precautionary manner where they are identified. Much of the current knowledge deficit concerns the effects of anthropogenic noise on marine ecosystems, and progress in this area will depend on the application of research methods which are consistent and appropriate. This thesis pursues the development of such methods for the study of noise exposure from shipping in coastal areas. Multiple data sources from three study sites are analysed and integrated, with the aim of achieving the following objectives:

i. To examine and build upon methodologies for acoustic habitat monitoring in marine environments.

ii. To develop ways of measuring the contribution of ships to noise exposure in coastal habitats.

iii. To explore how these methods can inform emerging policy initiatives to monitor and regulate underwater noise from shipping.

In pursuing these objectives, it is hoped that the work presented here will contribute to the understanding of noise exposure from shipping, and help to overcome some of the methodological obstacles outlined above.

1.3 Structure of the Thesis

Chapter 2 provides the necessary background in basic underwater acoustics and research methods for the subsequent studies of shipping noise, as well as reviewing underwater sound sources and the responses they have elicited in marine organisms.

The main body of the thesis consists of four published manuscripts presented in Chapters 3 and 4. This work resulted from collaborations initiated during the PhD with the University of Exeter, the University of Aberdeen, and the University of Victoria (Canada). Chapter 3 comprises two contributions to the analysis of passive acoustic datasets: Section 3.1 (Merchant et al., 2012a) concerns the application of appropriate averaging metrics to the assessment of shipping noise, while Section 3.2 (Merchant et al., 2013) presents the *spectral probability density* as a new analysis method. The use of ship-tracking data and other ancillary data sources is explored in Chapter 4 through two studies at different sites in the UK: Section 4.1 (Merchant et al., 2012b) introduces a method of identifying vessel passages and linking them with ship movements, and Section 4.2 (Merchant et al., 2014) elaborates on the technique by incorporating shore-based time-lapse footage and assessing the noise exposure contribution of tracked and untracked vessels.

The Synthesis and Discussion (Chapter 5) draws out the main themes from Chapters 3 and 4, and examines the principal findings and implications for future work with a broader outlook than that of the individual manuscripts. Finally, a brief conclusion (Chapter 6) summarises the key outcomes of the project.

Chapter 2

Background

This chapter provides an overview of the science that underpins the study of underwater sound (Section 2.1), as well as reviewing sources of sound in the ocean (Section 2.2) and the effects of shipping noise on marine organisms (Section 2.3). The practice of measuring underwater noise and processing acoustical data is covered in the final section (Section 2.4).

2.1 Underwater Acoustics

Electromagnetic radiation is rapidly attenuated in seawater (Woźniak and Dera, 2007), but sound can traverse entire ocean basins (Colosi et al., 1999). This relative transparency of the ocean to sound makes it a tool of choice for sensing the oceans, both for humans and marine organisms. Though the propagation of sound through the ocean is generally complex, a few basic principles govern most phenomena. This section briefly reviews these fundamentals, providing a foundation for subsequent discussion of ship noise propagation.

2.1.1 The ocean as an acoustic waveguide

In a fluid, acoustic waves are compressional disturbances causing small fluctuations in hydrostatic pressure (Kinsler et al., 1999). The rate at which these pressure perturbations propagate through the medium is the sound speed, c, which varies depending on the density, ρ, and compressibility, $\varkappa$, of the fluid:

$$c = \sqrt{\frac{1}{x\rho}} \tag{2.1}$$

In seawater, the compressibility is determined by the temperature, T, salinity, S, and hydrostatic pressure, P. Several expressions describe c in seawater with varying degrees of precision. A relatively simple formula valid for most applications (Medwin, 1975) is:

$$c = 1449.2 + 4.6T - 0.055T^2 + 0.00029T^3 + (1.34 - 0.010T)(S - 35) + 0.016z \tag{2.2}$$

where c is in metres per second, z is the depth [m], T is expressed in °C, and S in parts per thousand [‰]. The pressure depends directly on the depth, and the two can be used interchangeably given an appropriate conversion formula for the relevant latitude (e.g. Fofonoff and Millard, 1983).

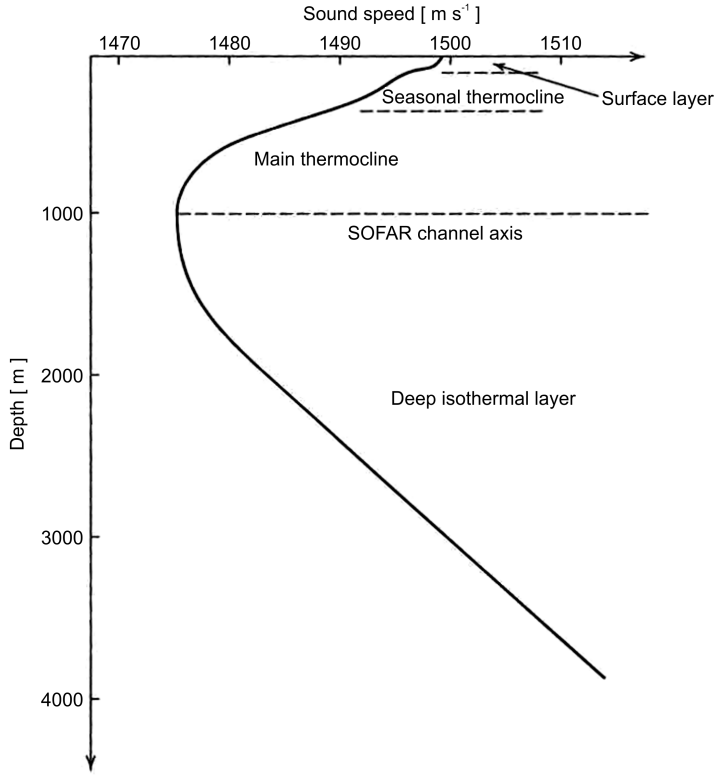

Figure 2.1: A typical sound speed profile for mid-latitude open ocean showing the key regions affecting deep-water sound propagation (see text for details; adapted from Kinsler et al., 1999).

The sound speed in the ocean varies between around 1,450 and 1,550 m s^{-1} (Lurton, 2010).

Changes in salinity are caused by evaporation and precipitation, changes in temperature by weather processes, and both are affected by ocean currents. From the surface to a depth of $\sim$1 km, the temperature decreases, leading to a negative gradient in the sound speed profile (Fig. 2.1). While there is a pressure gradient throughout the water column, temperature and salinity vary little below $\sim$1 km, in what is known as the *deep isothermal layer*. At these depths the sound speed profile tends toward a constant positive gradient due to the increasing pressure. This results in a minimum in the profile in all but the highest latitudes (where the surface temperature is cooler than at depth). The refraction caused by the sound speed gradient leads to a focusing of acoustic waves propagating along this minimum, known as the SOund Fixing And Ranging (SOFAR) channel, so called as it acts as a waveguide, eliminating propagation loss due to boundary interactions at the surface and seafloor (see below).

2.1.2 Spreading, absorption, and scattering losses

The amplitude of waves propagating from an acoustic source is diminished by geometrical spreading, attenuation by the medium, and scattering of sound in the water column and at the sea surface and bottom (Medwin and Clay, 1998).

Geometrical spreading losses occur as sound propagates away from a source and the energy is spread over an ever greater area. The propagation loss, PL, due to spreading can be expressed in the form (Urick, 1983):

$$\mathrm{PL} = \beta \log R \tag{2.3}$$

where PL is expressed in decibels relative to a reference range of one metre [dB re 1 m], and β depends on the spreading geometry: a value of 20 corresponds to spherical spreading (deep water) and 10 to cylindrical spreading (shallow water). Other geometries include 'semispherical' spreading ($\beta = 15$), often used as an approximate rule of thumb in shallow waters, and 'combined' spreading, where spherical spreading is assumed to a distance of one water depth, and cylindrical thereafter.

Absorption in the water column also diminishes the amplitude of sound waves as they propagate. In seawater, sound below $\sim 10^5$ Hz is primarily absorbed through the viscosity of water and by molecular relaxation of dissolved magnesium sulphate ($MgSO_4$) and boric acid ($B(OH)_3$; Medwin and Clay, 1998). Various models have been proposed to describe the attenuation coefficient, α. A simplified model applicable below 50 kHz (Thorp, 1967) is widely

used:

$$\alpha = \left[\frac{0.11}{(1+f^2)} + \frac{44}{(4100+f^2)} \right] f^2 \tag{2.4}$$

where α is expressed in decibels per kilometre [dB km^{-1}] and f is the frequency of interest [kHz]. Sound is also attenuated as it propagates through the seabed. This varies depending on the absorption coefficients of the seabed for compressional and shear (in the case of a rigid medium) waves.

Sound is scattered by inhomogeneities in the sea surface, bottom and water column, resulting in attenuation of coherent acoustic signals (Jensen et al., 2011). Scattering at the sea surface is caused by surface roughness due to the presence of surface waves, whose magnitude increases with wind speed. Surface scattering can also be caused by layers of bubbles at the surface generated by breaking waves (Leighton, 1994). Seabed roughness and inhomogeneities in seabed sediments scatter sound at the bottom boundary. Scattering in the water column is known as volume scattering, and is largely caused by biological organisms, including fish with air-filled swim bladders and zooplankton (Medwin and Clay, 1998).

2.1.3 Propagation modelling

With sufficient information on environmental parameters and an appropriate modelling approach, propagation of sound in the ocean can be accurately modelled (Etter, 1991; Jensen et al., 2011). Ideally, data such as seabed composition and sound speed profile would be sampled at sufficiently high spatial resolution for the frequencies in question (i.e. of the order of the wavelength of sound, e.g. $\sim$150 m at 100 Hz), and time-varying oceanographic parameters such as those determining the sound speed profile (temperature, pressure, and salinity; see above) sampled concurrently. In practice, the accuracy of propagation modelling is typically constrained by limited environmental data, since sampling of seabed composition, bathymetry, sound speed profile, etc., is costly and time intensive.

There are a number of modelling approaches widely in use, the more common being ray tracing, normal modes, parabolic equation, and wavenumber integration (also known as fast field; Etter, 1991). Some models are based on a direct physical interpretation of acoustic propagation (e.g. ray tracing, normal modes), while others are more approximate solutions to the wave equation (e.g. parabolic equation). A detailed discussion of these models is beyond the scope of this thesis, but it is important to note that the accuracy of model predictions

depends on the use of an appropriate model. In selecting a modelling approach, consideration should be given to the frequencies of sound in question, the depth of the water column, and whether the bathymetry and other environmental parameters vary significantly with range (Jensen et al., 2011). A brief summary of the applicability of the main modelling approaches is given in Fig. 2.2. Widely used models implementing these approaches include BELLHOP (ray tracing; Porter, 2011), KRAKEN (normal modes; Porter, 1992), and RAM (parabolic equation; Collins, 1995).

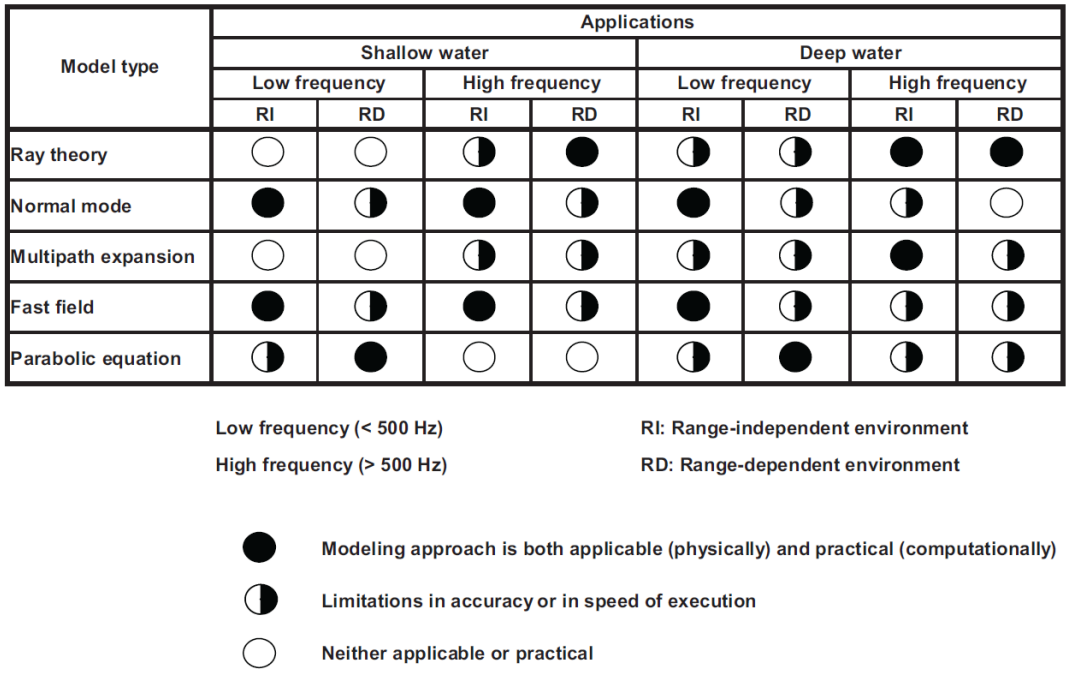

Figure 2.2: Applicability of propagation modelling approaches to deep- and shallow-water problems, high- and low-frequency propagation, and range-dependent and range-independent environments (Etter, 2009).

2.2 Sources of Sound in the Sea

Sound sources in the ocean can be divided into three main groups: natural physical processes (*abiotic*), biological organisms (*biotic*), and human activities (*anthropogenic*). Here, the principal sources of each type are presented, providing an overview of the main contributors to marine soundscapes.

2.2.1 Abiotic sources

During World War II, Knudsen and others observed that underwater noise spectra vary with wind speed (Knudsen et al., 1948). Since then, subsequent researchers have described the underwater acoustic signatures of weather and other physical processes in increasing detail. This section briefly summarises their results.

Wind

The pioneering work of Knudsen was expanded on by Wenz, whose now canonical 1962 paper (Wenz, 1962) describes a series of curves (since referred to as 'Wenz curves') corresponding to generic ambient noise spectra for different wind speeds. An updated version, in SI units and encompassing more recent research, is presented in Fig. 2.3. The Wenz curves show a characteristic peak at around 500 Hz, followed by a constant negative gradient with increasing frequency. The measurements on which the curves are based were made in the open ocean, where wind noise can be the dominant source between 500 Hz and 20 kHz. In shallow waters, the relationship between wind speed and ambient noise spectra is less predictable, possibly due to propagation effects associated with the seafloor and increased anthropogenic noise (Vagle et al., 1990).

Precipitation

The underwater noise due to even light rainfall is loud compared to that of wind (Ma and Nystuen, 2005). At low rainfall rates (less than around 5 mm/h), a distinctive peak is observed at 15 kHz attributed to bubbles generated by small (0.8–1.2 mm) raindrops ('R1' in Fig. 2.3). 'Medium-sized' raindrops (1.2–2.0 mm) do not exhibit this bubble-generating mechanism, and their signatures tend to be quieter ('R2' in Fig. 2.3). Large ($>$ 2.0 mm) drops characteristic of heavy rainfall produce turbulent splashes which produce a variety of bubble sizes, and a correspondingly wide noise spectrum (Nystuen, 2001). Hail produces a characteristic peak in the noise spectrum between 2.3 and 5 kHz ('H' in Fig. 2.3; Scrimger et al., 1987), whilst snow is unique among reported weather spectra as the level increases with frequency (Scrimger, 1985; Scrimger et al., 1987; Alsarayreh and Zedel, 2011). Lightning strikes also produce sound underwater, in the form of short pulses concentrated at low frequencies (Dubrovskiy and Kosterin, 1993).

Ice

A variety of mechanisms in both icebergs and pack ice contribute to the underwater soundscape in polar regions. Cracking, melting, the motion of ice masses themselves and interac-

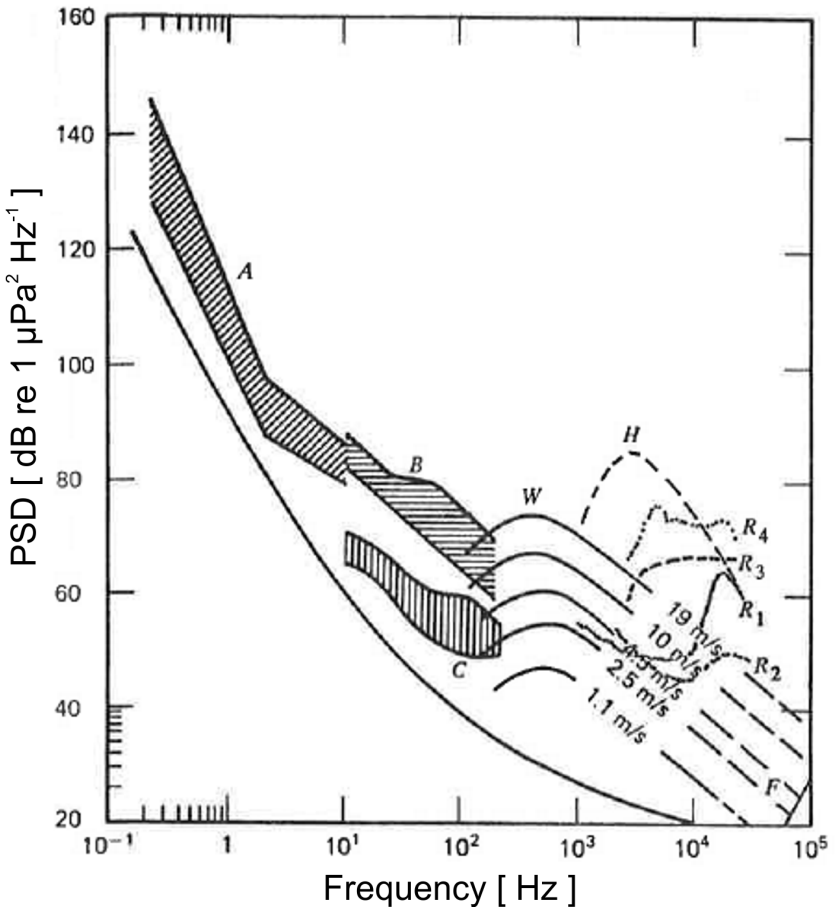

Figure 2.3: Spectral density levels of physical sounds from various studies (Medwin and Clay, 1998). The heavy solid line at the bottom is the minimum level at sea. A: seismic noise; B: ship noise; C: wave turbulence interactions; H: hail; W: sea surface levels at five different wind speeds; R1: drizzle (∼1 mm/h) with 0.6 m/s wind over lake; R2: drizzle with 2.6 m/s wind over lake; R3: heavy rain (15 mm/h) at sea; R4: very heavy rain (100 mm/h) at sea; F: thermal noise.

tions with waves all produce noise at a range of frequencies and amplitudes (Lurton, 2010). Dramatic events such as glacier calving can generate loud and abrupt broadband noise (Pettit, 2012; Tegowski et al., 2012), while smaller icebergs ('growlers' and 'bergy bits') generate sound through collisions, scraping and melting (Collins, 2011). The composition of the ice, its size and its structure all affect the signature produced. Ice coverage also reduces surface noise from wind and precipitation.

Surf noise

The noise generated by waves breaking on the shore is concentrated between 200 and 500

Hz (Wilson et al., 1985; Bass and Hay, 1997), and has been shown to scale with the root mean square of the wave height between 0.1 and 1 kHz (Deane, 2000). The noise level also varies depending on how the wave breaks: differences of 5–10 dB have been observed between 'spilling' and 'plunging' breakers (Means and Heitmeyer, 2002). The directionality of surf noise and the distinct acoustic signatures of different beaches could provide an orientation cue for some marine species (Wladichuk, 2010).

Seismic noise, wave interactions and thermal noise

At the extremes of the frequency spectrum dwell acoustic phenomena not generally of concern for the transmission of biologically significant sounds (Fig. 2.3). Between 0.1 and 5 Hz, volcanic and seismic activity are recorded, and between 5 and 20 Hz, noise due to wave interactions (Medwin and Clay, 1998). Above ∼100 kHz, thermal noise associated with molecular agitation dominates (Mellen, 1952).

2.2.2 Biotic sources

Sounds are produced by marine organisms for a variety of purposes, including communication, navigation, and prey detection. This section provides an overview of these sounds arranged according to three broad taxonomic groups: marine mammals, fish, and invertebrates.

Marine mammals

Cetaceans, commonly known as whales, dolphins and porpoises, consist of two surviving suborders – *Mysteceti* (baleen whales) and *Odontoceti* (dolphins and toothed whales) – that exhibit distinct sound production behaviours. Sounds produced by mysticetes are grouped into two categories: *calls* and *songs* (Clark, 1990). Four of the eleven species of mysticete produce songs (Au and Hastings, 2008), including the well-known humpback whale song (Payne and McVay, 1971), associated with the mating season. Their frequencies range from as low as 15 Hz for blue and fin whales (Širović et al., 2004; McDonald et al., 2009), to harmonics of at least 24 kHz for humpback whales (Au et al., 2006). 'Call' covers a multitude of social sounds with a wide range of characteristics, variously termed 'clicks', 'pulses', 'grunts', 'moans', 'gunshots', and so on (Parks et al., 2005; Dunlop et al., 2007; Stimpert et al., 2011). Odontocetes produce social sounds broadly referred to as *whistles* and *clicks* (Au and Hastings, 2008). Whistles mostly fall in the range 5 to 15 kHz, while burst pulses (series of broadband clicks) can have frequency components that exceed 100 kHz. Many odontocetes are also known to produce sound for echolocation. Frequencies reported range from around 30 to 130 kHz, with

source levels of up to 228 dB re 1 μPa^2 at 1 m.

The vocalisations of other marine mammals have also been studied, including pinnipeds and sirenians. Pinnipeds include species commonly known as seals, sea lions and walruses. As amphibious mammals, they exhibit vocal behaviour in both air and water. In water, dominant frequencies in the range 0.1 to 7 kHz are reported, with components as low as 20 Hz (Au and Hastings, 2008). Few studies have documented the vocalisations of manatees and dugongs (of the order *Sirenia*), but available data indicate frequency ranges of 1–8 kHz (Sousa-Lima et al., 2002) for manatees, and 0.5–18 kHz for dugongs, with components extending to around 22 kHz (Ichikawa et al., 2006).

Fish

Fishes are known to produce sound by two mechanisms: stridulation (scraping together parts of the body) and manipulation of the swim bladder (Zelick et al., 1999). The swim bladder acts as a resonance chamber to amplify sound, and sounds produced by this mechanism tend to have greater levels than those produced by stridulation, though neither type is intense.

Figure 2.4: Snapping shrimp *Alpheus euphrosyne*[*], approx. total length: 5 cm.

Invertebrates

Perhaps the most impressive sounds produced by a marine invertebrate are the high intensity 'snaps' produced by snapping shrimp (Everest et al., 1948). This group of crustacean species

[*] http://mangrove.nus.edu.sg/research/teoyenling/gallery/Alpheus%20euphrosyne_19feb2004

produces loud [189 dB re 1 μPa^2 (peak-to-peak)†] impulses using their large claw (they have a smaller, silent claw; see Fig. 2.4) which snaps shut producing a water jet. This jet leaves a region of negative pressure in its wake, forming a bubble that then cavitates, producing a broadband impulse from zero to more than 200 kHz (Au and Banks, 1998; Versluis et al., 2000). The aggregate noise produced by ensembles of snapping shrimp can dominate marine soundscapes in some areas (Johnson et al., 1947).

Less intense sounds are produced by other invertebrate species, such as sea urchins, whose scraping sounds made during feeding are amplified by their roughly spherical skeletons which act as Helmholtz resonators (Radford et al., 2008). The combined effect of biotic sound sources in shallow water reefs has been associated with distinct acoustic signatures (Radford et al., 2010) which are used as a navigational cue by coral fish larvae when finding a reef in which to settle (Simpson et al., 2005). Sound production has also been observed in aquatic insects (Aiken, 1985), though their contribution to aquatic soundscapes is likely to be highly localised.

2.2.3 Noise from shipping

The mechanisation of marine propulsion in the 19th century introduced the world's waterways to what is now an almost ubiquitous feature of the marine soundscape: shipping noise. This noise is caused primarily by cavitation induced by the ship's propeller (Ross, 1976). The force applied to the fluid by the propeller creates fluctuations in hydrostatic pressure, which can create bubbles in low-pressure regions. When these bubbles collapse and return to fluid, energy is released, including broadband noise.

Interest in the study of noise from shipping began long before its potential impact on marine fauna was fully recognised. During World War II, noise from ships was used by submarines to detect convoys (Lurton, 2010), and, particularly during the Cold War, noise from shipping was of military significance as the background noise field against which submarines might be detected. A strategic advantage might be gained through an understanding of the relationship between ambient noise characteristics and the presence and distribution of vessels in the area. It was similarly advantageous to invest in understanding the mechanics of propeller cavitation and radiated noise from vessels, both to improve submarine quieting technologies and to infer characteristics of vessels (on or below the surface) from their acoustic signatures.

A second and subsequent strand of ship noise research has focused on understanding the po-

†See Eq. 2.17, p34, for definition.

tential impacts of shipping noise on marine fauna. The potential for such negative impacts was first postulated as early as 1971 (Payne and Webb, 1971) in the context of long-range whale communication, but it was not until a quarter of a century later that the study of these potential effects gained momentum. This new impetus was generated in part by the publication of a book building on recent progress on the topic (Richardson et al., 1995) and the subsequent publication of measurements from the Northeast Pacific (Andrew et al., 2002) confirming Ross's prediction (Ross, 1976) that noise from shipping would continue to rise in the latter half of the 20th century.

The motivations and objectives of these two bodies of research – here termed *military era* and *ecological era* – are clearly distinct, and it is perhaps not surprising that methodologies developed in a military context are often not well suited to environmental impact assessment. Though it has, to a limited extent, been useful to draw on the military era literature in understanding shipping noise in the ecological era, its apparent focus on deep-water scenarios and relatively short timeframes contrasts with the need, for example, to be able to assess cumulative, long-term noise exposure in shallow, coastal waters where the coincidence of marine fauna and anthropogenic noise is greatest. It is therefore important to emphasise that biologically relevant metrics are needed when assessing potential impacts of shipping noise, and though the study of noise from shipping has a long history, the development of biologically relevant methodologies is still in its infancy.

Source characteristics of large vessels

One area of common ground between the military and ecological literature is the need to measure source levels (or radiated noise levels) of surface vessels for input to acoustic propagation models. Tankers, cargo ships and large passenger vessels are the loudest of ocean-going craft, and are thought to account for the majority of deep-ocean noise from the global fleet. The spectral energy of their noise signatures is concentrated at low frequencies (below 100 Hz), where attenuation by seawater is relatively low and sound can propagate thousands of kilometres under certain conditions. They are consequently of primary concern in efforts to reduce noise from shipping. However, there is only one detailed study (Arveson and Vendittis, 2000) of a large ocean-going vessel in the published literature. Based on measurements of a 173-m cargo ship, it was originally commissioned by the US Navy in 1980. The measurements were made at a Navy test facility and include detailed measurements of the directionality of radiated noise. The third-octave plot (Fig. 2.5) has a wide peak of 175–185 dB re 1 μPa^2 at 1 m between 30 and 100 Hz, followed by a linear reduction as frequency increases above 1 kHz. This linear roll-off above a few hundred Hertz is thought to be characteristic of ship spectra (Ross, 1976), though authors disagree as to the variability of its gradient among dif-

ferent ships. There are likely to be many more such detailed measurements in the classified literature, though measurements made at these advanced naval test ranges are not without their own methodological issues: a recent NATO exercise was conducted to help standardise vessel noise measurements among NATO allies, whereby the same test vessel was evaluated at facilities in each country (C. de Jong, pers. comm., 2013). Significant differences were found among the facilities, with implications for the transferability of acoustic intelligence.

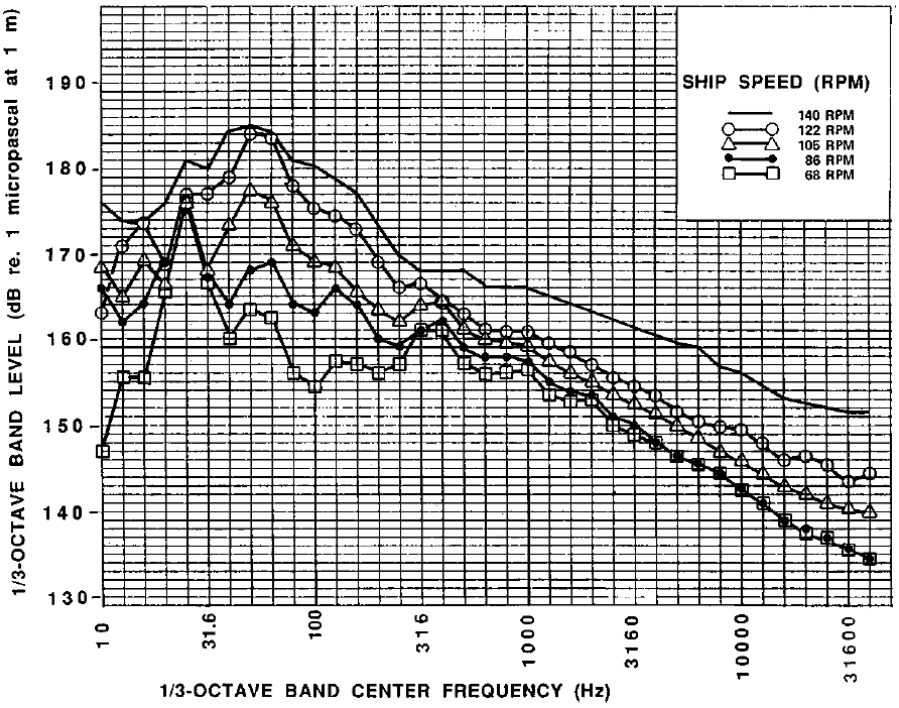

Figure 2.5: Keel-aspect third-octave bandwidth spectra of M/V Overseas Harriette at several speeds (Arveson and Vendittis, 2000).

Less detailed source level measurements have also been made, including military measurements dating from World War II (Ross, 1976) and measurements of ships-of-opportunity (Scrimger and Heitmeyer, 1991; Wales and Heitmeyer, 2002; McKenna et al., 2012, 2013). A consistent aim of these studies has been to identify relationships between vessel characteristics and ship source spectra, and there has been considerable debate over whether ship speed and length correlate with source level as proposed by Ross (1976). Measurements by Scrimger and Heitmeyer (1991) agreed well with this prediction, and found that the mean levels and standard deviations were comparable among different classes of ship (tankers, cargo ships and passenger vessels). However, Wales and Heitmeyer (2002) subsequently found negligible correlation to ship speed and length in their measurements of 54 vessels, and proposed an alternative and more complex source spectrum model that reduced the prediction errors

in their dataset. More recently, McKenna and others found no clear general relationship between ship speed and source level, and considerable differences between vessels of the same tonnage but different type (McKenna et al., 2012). Subsequent analyses of radiated noise characteristics separated by vessel type found the most significant factors were ship speed, size, and oceanographic conditions (McKenna et al., 2013).

Modelling noise from shipping

Early attempts to model ambient noise from shipping (e.g. Dyer, 1973) aimed to describe the statistical distribution of the background noise field at a particular site to optimise signal detection by sonar systems. These became more sophisticated in the following decades to include directional characteristics and more complex propagation environments (Hamson, 1997).

The first models to address potential impacts of shipping noise on marine life were based on the concept of 'zones of influence': areas defined by the radius from an anthropogenic source (in the case of cylindrical symmetry) in which a particular severity of impact might be expected (Richardson et al., 1995). A model using this technique (Erbe and Farmer, 2000b) was applied to risk assessment of noise from an icebreaker vessel (Erbe and Farmer, 2000a), and also to whale-watching boats (Erbe, 2002) with implications for the regulation of stand-off distances for whale-watching vessels in the study area. Later models attempted to generate more dynamic noise exposure scenarios using moving sound sources and cetaceans (Frankel et al., 2002; Gisiner et al., 2006), though these were largely designed for risk assessment of military sonar operations.

The main limitation of these early approaches is the focus on a discrete event or source: in the case of noise from shipping, there are generally multiple sources with varying characteristics and distances from a real or hypothesised animal. From an ecological perspective, the relevant spatial and temporal scales are also much greater than those considered in these localised noise impact studies: some cetacean species migrate thousands of kilometres each year (Stone et al., 1990), and may be exposed to noise from shipping for much of their lifetime. For these reasons, and also as a result of the growing policy interest in the issue, there has recently been a shift towards a more large-scale and long-term outlook, with preliminary efforts to map cumulative underwater noise levels at a national scale. These include mapping of predicted noise levels from shipping in the Canadian Northeast Pacific (Erbe et al., 2012), and CetSound (NOAA, 2012), a project to map predicted noise levels and cetacean distributions in United States territorial waters. These studies highlight the need to substantiate spatiotemporal models with acoustical measurements, and establish a basis and impetus for future work in this

area.

2.2.4 Other sources of anthropogenic noise

Small vessels and naval exotica

Peak frequencies of ship noise signatures tend to increase as vessel size diminishes. Consequently, small vessels such as recreational and fishing boats generally radiate noise at higher frequencies than large commercial vessels, with peak frequencies up to a few kHz for small vessels with outboard motors (Matzner et al., 2010). Though these higher frequencies are more rapidly attenuated in water (Lurton, 2010), they are still of concern due to the proximity of recreational boating traffic and cetacean-watching vessels to some marine mammal populations (Williams et al., 2002; Bejder et al., 2006).

The noise characteristics of less common seafaring craft are little studied (or less published, in the case of submarines and military vessels), though noise levels produced by hovercraft (Blackwell and Greene, 2005), racing powerboats (Amoser et al., 2004), and jet skis (Roussel, 2002; Erbe, 2013) have been reported. Radiated noise from research vessels has also been relatively well studied (e.g. Mitson, 1995; Bahtiarian and Fischer, 2006; De Robertis et al., 2013), particularly fisheries vessels, since their noise characteristics can affect fish avoidance behaviour, with consequences for measurements of fish abundance (De Robertis et al., 2013). To reduce these effects on abundance estimation, the International Council for the Exploration of the Sea (ICES) has specified noise emission recommendations (plotted in red in Fig. 2.6). Ships used for research in other areas (e.g. oceanography) have similar requirements for low self-noise.

Industrial activities

High levels of noise are generated by activities associated with the offshore industry, such as seismic surveys, pile driving and drilling (Hildebrand, 2009). The expansion of this sector in recent years and the increased interest in acoustic impacts on marine life have made the study of noise generated by offshore construction and resource extraction a fertile research area. A brief summary of each source is presented below.

Marine geophysical surveys, often in search of oil and gas deposits, use seismic airguns to probe the Earth's subsurface. Seismic airguns release compressed air into the water, creating a seismic pressure pulse concentrated at low frequencies and directed towards the seafloor (Caldwell and Dragoset, 2000). The sound reflected by different layers of the seabed is recorded

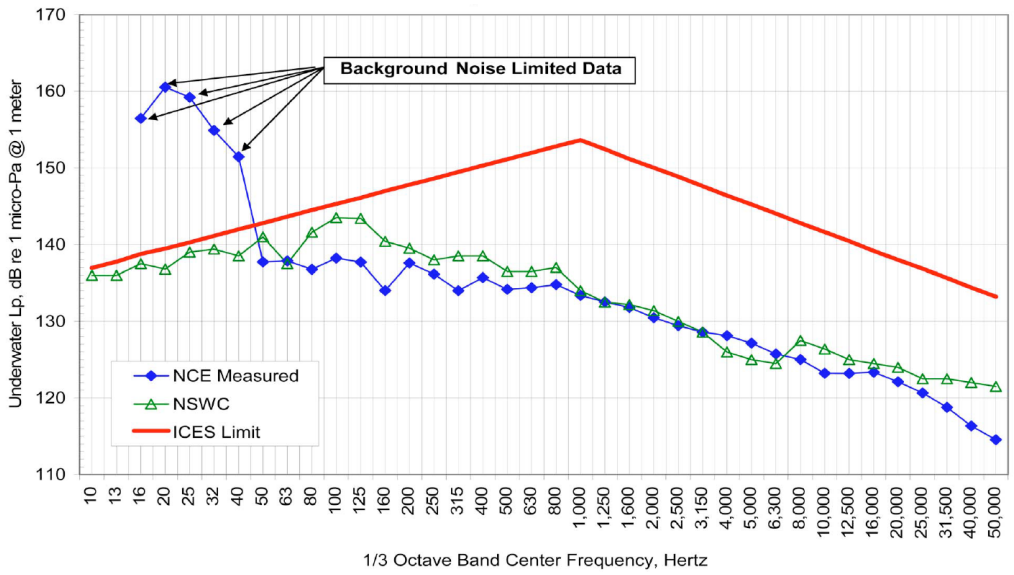

Figure 2.6: Radiated noise from R/V Oscar Dyson (Bahtiarian and Fischer, 2006).

by a towed array, and analysed to reveal the structure of the seabed and possible oil and gas deposits. As the airgun is highly directional, source level estimates based on omnidirectional spreading are inherently unsound. Notional source levels of 259 dB re μPa^2 at 1 m have been reported for the more powerful airgun arrays (Richardson et al., 1995; Tolstoy et al., 2009).

Pile driving is a common construction method for the foundations of offshore structures, such as platforms and wind turbines (Madsen et al., 2006). A hollow steel cylinder is driven into the seabed using a hydraulic ram, producing source levels of up to 235 dB re 1 μPa^2 (Tougaard et al., 2009b) at 1 m. Recent modelling and measurements suggest that the primary noise mechanism is a supersonic wave caused by the radial expansion of the cylinder (Reinhall and Dahl, 2011), with peak frequencies between 350 and 600 Hz.

Relatively few studies have reported noise from drilling and dredging activities. Drilling noise levels of up to 143 dB re 1 μPa^2 in the 20-Hz to 1-kHz range (received level at 1 km) have been reported (Greene, 1987), while dredging noise was found to be comparable to that of a cargo ship below 500 Hz, though higher above 1 kHz, and varied with the type of aggregate being extracted (Theobald et al., 2011). Despite the similarity of noise level between dredging and shipping, avoidance behaviour linked to dredging has been observed in bottlenose dolphins in an already urbanised waterway (Pirotta et al., 2013).

Marine Renewable Energy Devices (MREDs) are an emerging technology. While large-scale offshore wind farms are already operational, Wave Energy Converters (WECs) and tidal en-

ergy devices are still at the development stage. Noise assessment of MREDs is likewise in its infancy, especially for wave and tidal converters. Few *in situ* measurements of full-scale wave or tidal energy extractors have yet been published in the open literature [e.g. Haikonen et al., 2013; see also Bassett et al., 2011; Garrett et al., (In Press)], and most work to date has focused on modelling likely noise-generating mechanisms (e.g. Richards et al., 2007; Patricio et al., 2009; Lloyd et al., 2011). Offshore wind turbines do generate some noise during their operational phase: underwater acoustic measurements of wind farms (Tougaard et al., 2009a) found that turbine noise only exceeded background levels below 500 Hz, with a maximum third-octave level in the 25-Hz band of 126 dB re 1 μPa^2 at 14 m distance.

Figure 2.7: Pelamis wave energy converter, length 150 m.[‡]

Active sonar systems

Perhaps the first events to raise public awareness of the acoustic impacts of underwater human activities were mass strandings of marine mammals associated with military sonar exercises (e.g. Frantzis, 1998; Evans and England, 2001). The specifications of military sonar devices are generally classified, so source characteristics are hard to ascertain. Active sonar systems are also used for civilian purposes, notably in fisheries (MacLennan and Simmonds, 1992) and seabed mapping (Blondel and Murton, 1997; Kenny et al., 2003), and also as simple echo-sounders and acoustic deterrent devices.

[‡]http://www.fotosimagenes.org/imagenes/emec-3.jpg

2.3 Effects of Vessel Noise on Marine Fauna

Prior to industrialisation, it is likely that marine soundscapes were relatively undisturbed by human activity. Biological organisms evolved over many millions of years in this natural acoustical context, developing acoustic 'niches' (Mossbridge and Thomas, 1999) for communication and hearing that adapted to the naturally varying acoustic conditions in their habitats. Over a relatively short evolutionary timescale, however, shipping and industrial activity have transformed these soundscapes, raising levels of noise in the world's oceans, while whaling and overexploitation of fisheries have almost certainly diminished levels of biotic sound to a degree which is now impossible to ascertain.

The major component of this transformation has been the introduction of noise from mechanised ships, and marine organisms have been observed to respond to such noise in a number of ways. Through observations in the wild or by playback of ship noise in tank experiments, responses including avoidance behaviour, changes to vocal behaviour, and physiological responses in the form of heightened respiration rate, heart rate, and levels of stress hormones have been documented. This section gives an overview of some of this work, though it is inevitably an incomplete summary. As this evidence of responses to anthropogenic noise accumulates, the question arises: how can we determine whether these effects are biologically significant? Preliminary efforts to frame and address this complex issue are discussed in the final subsection.

2.3.1 Masking

Masking occurs when a listener is unable to detect, recognise, or interpret an acoustic signal due to the presence of some other confounding sound source (Clark et al., 2009). The interfering noise may render the signal inaudible, or may obfuscate information contained within it. In the context of underwater noise from shipping, the potential for masking of long-range acoustic communication in baleen whales has long been recognised (Payne and Webb, 1971) and remains an active area of investigation (Parks et al., 2007; Clark et al., 2009; Hatch et al., 2012). However, direct observation of masking in the wild is challenging, since sound perception cannot be measured directly (disregarding the startle reflex and overt behavioural responses, which tend to be in response to loud noise rather than communication signals). Detailed study of masking can only be achieved through behavioural responses of trained, captive animals, or measurement of auditory nerve signals in captive animals (Nachtigall et al., 2007). These difficulties mean that studies of masking in realistic conditions rely

on indirect approaches.

For wild animals, the presence of masking can be inferred through vocal modifications (see Section 2.3.2) which are attempts to overcome the effect of masking – such as calling louder, at a different frequency, or with a greater repetition rate – collectively known as the Lombard effect (Hotchkin and Parks, 2013). Another approach is to speculate on the degree to which ship noise limits acoustic communication, based on estimated noise levels in the absence of shipping and the presumed ability of animals to detect a signal in noise (e.g. Clark et al., 2009; Jensen et al., 2009; Hatch et al., 2012).

If controlled experiments can be conducted on the target species, then the potential for masking can be determined more directly by measuring the threshold of audibility (audiogram) with and without the presence of vessel noise. Such experiments have shown that for some fish species, the frequency range of best hearing coincides with peak frequencies of boat noise observed in their habitats, with implications for masking of vocalisations and detection of biologically significant sounds (Vasconcelos et al., 2007; Codarin et al., 2009).

2.3.2 Behavioural responses

Behavioural responses to vessel noise include vocal modifications, overt short-term responses (e.g. avoidance manoeuvres), and more subtle longer-term responses (e.g. reduced presence in an area). Vocal modifications in response to vessel noise have been observed in mysticetes (Norris, 1995; Parks et al., 2007, 2011a; Castellote et al., 2012) and odontocetes (Lesage et al., 1999; Buckstaff, 2004; Foote et al., 2004), which suggests that vessel noise can interfere with communication.

Avoidance responses in the wild can be difficult to characterise, since this behaviour may be due not only to noise from a vessel, but also the physical presence of the vessel or some other unrelated factor. Short-term avoidance responses have been documented in mysticetes (e.g. Richardson et al., 1985; Scheidat et al., 2004), odontocetes (e.g. Richardson and Würsig, 1997; Nowacek et al., 2001; Constantine et al., 2004) and fish [both due to vessel noise (Sara et al., 2007) and the ship's echosounder (Vabøet al., 2002; Handegard et al., 2003)].

More subtle and longer-term behavioural responses to vessel noise have also been observed, with wider implications for ecosystem dynamics. Examples include: changes in fish behaviour, such as time spent caring for nests (Picciulin et al., 2010) or response time to defend nests from predators (Bruintjes and Radford, 2013); avoidance of areas of intense shipping by bottlenose dolphins (Lusseau, 2005; Rako et al., 2013); and delayed predator avoidance

behaviour in crabs (Wale et al., 2013b). This disruption to habitat use and predator-prey interactions may have a profound influence on ecosystem dynamics in areas affected by high levels of vessel noise.

2.3.3 Physiological effects

A relatively recent area of study has been the physiological effects that exposure to vessel noise may have on marine species. Evidence of physiological stress can be found in levels of the stress hormone hydrocortisone (also known as cortisol) in faecal samples of animals exposed to noise. Studies measuring cortisol levels with and without the presence of vessel noise have found significantly higher stress levels in fish (Wysocki et al., 2006) and whales (Rolland et al., 2012) exposed to ship noise. Other physiological responses include increased heart rate (in fish; Graham and Cooke, 2008) and respiration (in crabs; Wale et al., 2013a). These physiological responses have evolved to enhance animals' ability to react to short-term threats in their natural environment, but may be maladaptive in the context of repeated or chronic elicitation by anthropogenic noise (Wright et al., 2007a). In the long term, heightened metabolic rate and physiological stress induced by vessel noise may be detrimental to individual fitness and survival, with potential ramifications for population levels.

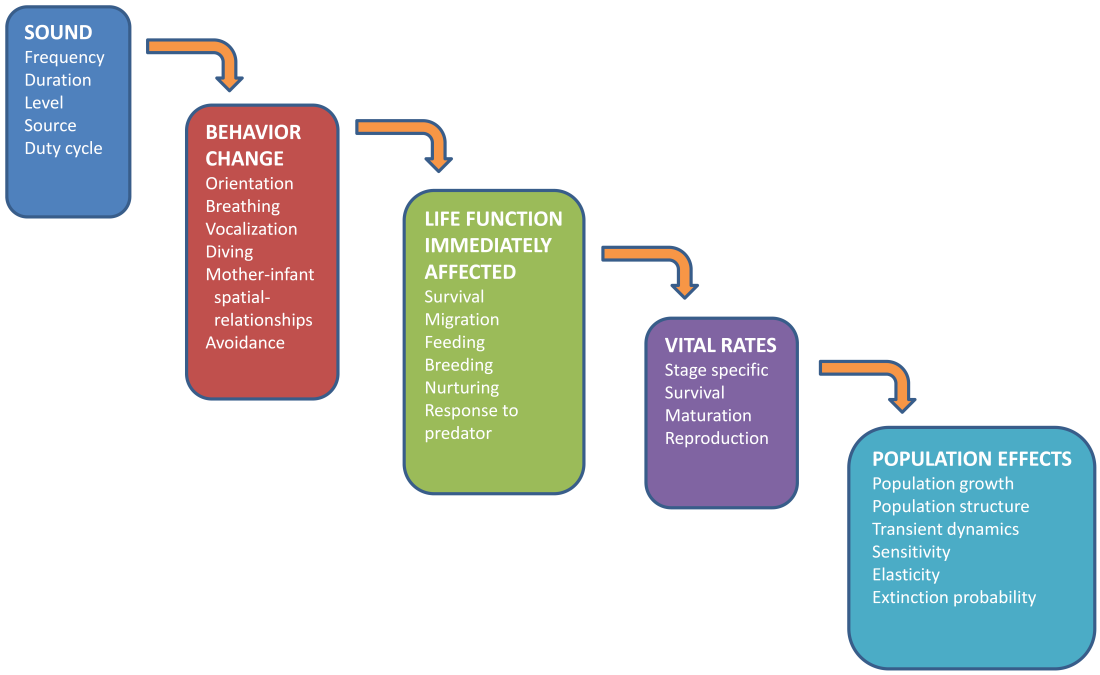

Figure 2.8: Overview of PCAD concept, which relates behavioural responses to noise to possible effects at the population level (National Research Council, 2005).

2.3.4 Population consequences

Though there is mounting evidence of behavioural disturbance by vessel noise, it is not clear how significant this disturbance is, or even which criteria are relevant to assessing the significance and severity of acoustic disturbance. Some have taken the view that disturbance from anthropogenic noise is significant insofar as it has a downstream effect on population growth rates, and have formulated a modelling framework known as Population Consequences of Acoustic Disturbance (PCAD; National Research Council, 2005). In short, the framework assumes that disturbance from anthropogenic noise leads to a change in behaviour or a physiological response. This affects the health of the individual animal, which in turn affects vital rates (e.g. reproduction, survival), which, finally, have effects at the population level (see Fig. 2.8). The challenge then is to determine the transfer functions between each stage in the framework for a particular species to make an estimate of the population consequences of a particular acoustic disturbance scenario. Given the limited data available, a comprehensive PCAD assessment is a long-term aspiration for most species, though some authors have already modelled the predicted effect of disturbance from vessel noise on a bottlenose dolphin population (New et al., 2013).

2.4 Passive Acoustic Monitoring of Aquatic Habitats

The many sources of sound in the ocean and the effects ship noise can have on marine life were described in previous sections; here, we examine the instrument platforms used to measure underwater noise, and the signal processing steps required to produce calibrated acoustical measurements. Analysis and presentation approaches for different applications are then discussed.

2.4.1 Monitoring platforms

All passive acoustic monitoring (PAM) systems include hydrophones as a basic component, but the deployment platforms on which they are mounted vary considerably. These platforms can be broadly divided into *fixed* and *mobile* systems; each system has its own benefits and limitations depending on the application.

Fixed platforms

Traditionally, underwater noise measurements have been at fixed locations and made using

cabled, bottom-mounted hydrophones (e.g. Wenz, 1961) or by lowering a hydrophone over the side of a stationary vessel (e.g. Tavolga, 1958). Though the latter approach is still used in contemporary studies (e.g. Rolland et al., 2012; Rako et al., 2013), this method is often avoided as it constrains data collection to short-term deployments in fair weather conditions, and can be limited by extraneous noise from waves slapping against the hull of the survey vessel and by cable strum. In contrast, cabled systems have seen a resurgence in recent years with the expansion of cabled ocean observatories, for example the NEPTUNE, VENUS and RSN networks in the Northeast Pacific (Martin Taylor, 2009; Cowles et al., 2010) and the LIDO project which sources data globally (André et al., 2011a). Cabled systems set up by the US Navy at the height of the Cold War to monitor submarines have since been largely decommissioned but remain in place, providing insight into trends in ambient noise over the last few decades in the Northeast Pacific (Andrew et al., 2002). This ability to make continuous measurements over long time periods is the principal advantage of cabled systems, though the associated costs of deployment, maintenance, and management of the large volumes of data generated can be high.

A relatively recent development is the use of autonomous PAM devices: self-contained, battery-powered recording units which can be deployed on the scale of weeks to months (Fig. 2.9). These are generally more cost-effective than cabled systems, and can be recovered using acoustic release devices and redeployed as needed, though acoustic release malfunction and trawling by fishing vessels are common pitfalls (Dudzinski et al., 2011). Multiple units can be deployed to track and localise sound sources (Van Parijs et al., 2009) or to investigate spatial characteristics of underwater noise (e.g. Hatch et al., 2012). Deployment longevity is limited by battery life and data storage capacity, though both have seen dramatic improvements through technological advances in recent years. Autonomous PAM units are already relatively inexpensive, and the increasingly competitive market (Sousa-Lima et al., 2013) is further driving down the cost of these systems. However, for many systems, performance issues such as limited dynamic range (Section 3.2.3, p50) and system noise (Wiggins, 2003) still need to be addressed.

Mobile platforms

Measuring ambient noise from a moving platform can be problematic, since turbulence around the hydrophone can cause flow noise – flow-dependent broadband noise with a negative spectral gradient as frequency increases (Strasberg, 1979). All of the mobile devices detailed below have to contend with this self- or pseudo-noise – noise caused by the presence of the recording apparatus. Flow noise can be reduced through streamlining, acoustic deflectors (Urick, 1986), and by limiting the speed of travel. Motion is, of course, relative, and in the

reference frame of fixed platforms, tidal flow can induce the same effects. One solution in high tidal flow environments such as proposed tidal energy sites has been to deploy freely drifting platforms (e.g. Wilson et al., 2011). These drifters consist of a hydrophone attached to a float containing a GPS tag. When the drifter is subsequently recovered, sound levels can be mapped through the deployment path.

Figure 2.9: Wildlife Acoustics SM2M PAM unit, length 0.8 m.[§]

The first mobile PAM platforms were towed arrays – multiple hydrophones towed behind a moving vessel – developed as early as the First World War (Gershman et al., 2000). They were employed initially for anti-submarine warfare (ASW) applications, though these became less effective with the development of submarine quieting technology in the late 1960s. Extensive towed arrays are also used in seismic surveys to detect the reflections of seismic sources from the seabed. As platforms for ambient noise monitoring, they can be limited by noise from the towing vessel if not towed far enough from the vessel (Urick, 1986), as well as flow noise caused by turbulence around the hydrophones at low frequencies.

A goal of marine mammal bioacoustics has been to understand the vocal behaviour of species in their natural context, but techniques such as boat-based monitoring can elicit their own behavioural responses (Nowacek et al., 2007), and some species such as deep-diving sperm whales vocalise at depths where it is difficult to monitor associated behaviour (Papastavrou et al., 1989). To address some of these issues, acoustic tags have been developed which are fixed to marine mammals via suction cups and can record sound for up to a few days (Johnson and Tyack, 2003). These devices have been used to study vocalisations in several species, including sperm whales (Watwood et al., 2006), humpback whales (Stimpert et al., 2007), right whales (Parks et al., 2011b), and beaked whales (Aguilar de Soto et al., 2012). They have also been recently employed to study animal responses to anthropogenic noise such as

[§]http://i1.ytimg.com/vi/jaMilQSTxlM/maxresdefault.jpg

navy sonar (DeRuiter et al., 2013; Goldbogen et al., 2013). For monitoring the ambient noise environment in an animal's habitat, however, these tags are quite limited since flow noise over the sensor contaminates low frequencies (Johnson and Tyack, 2003), and noise generated at the surface by waves and bubbles can contaminate much of the data. A further drawback is the limited duration of deployments, which is constrained by storage capacity.

Another mobile platform that has been developed by oceanographers in recent decades is the autonomous underwater glider (Rudnick et al., 2004). Gliders generate propulsion by changing their buoyancy and using wings to convert some of this vertical motion into forward movement. They consequently have a 'sawtooth' dive profile, and are able to travel slowly but efficiently, with deployment endurance of up to several hundred days (Rudnick et al., 2004). Several studies have successfully used gliders as PAM platforms (e.g. Rogers et al., 2004; Ferguson et al., 2010; Matsumoto et al., 2011; Klinck et al., 2012). Disadvantages of gliders include a small payload capacity, meaning sensors are limited by weight and battery power, and an inability to transmit signals into the atmosphere for real-time monitoring as some surface-operating devices are able to (e.g. PAMBuoy, 2013). One solution to the payload limitation has been to develop an autonomous sailboat (Klinck et al., 2009). The 'Roboat' is powered by batteries and solar panels, and can support a greater payload than submarine gliders. Acoustic data is recorded using a towed array.

Finally, an innovative mobile platform has been developed for the study of ambient noise in the deep ocean. 'Deep Sound' is an untethered glass sphere which descends from the surface under gravity to a predetermined depth, at which it releases a weight and returns to the surface under buoyancy (Barclay et al., 2009). The device has been used to study depth profiles of ambient noise at depths of up to 6 km in Pacific Ocean trenches, including the depth dependence of noise from wind (Barclay and Buckingham, 2013a) and rain (Barclay and Buckingham, 2013b).

2.4.2 Signal processing

Retrieving the pressure signal

The first step in analysing sound levels is to compute the acoustic pressure signal recorded by the hydrophone from the digitized data output of the PAM system. This is achieved through a two-stage process:

i. Conversion of the digitized data to a voltage signal.

ii. Conversion of this voltage signal to the pressure signal recorded by the hydrophone.

The steps required vary with the hardware used, and may involve computations in the frequency domain. Here, both frequency-dependent and frequency-independent calibration procedures are described.

Typically, PAM systems output data as WAV (Waveform audio format) files, though other file formats are also used (Sousa-Lima et al., 2013). WAV-formatted data are normalised to a ± 1 amplitude range, and knowledge of the corresponding voltage range of the analogue-to-digital converter (ADC) is necessary to retrieve the voltage signal. Denoting the WAV-formatted signal x_{WAV}, the corresponding voltage signal is

$$x_V = V_{\text{peak}} x_{\text{WAV}} \tag{2.5}$$

where V_{peak} is the zero-to-peak voltage range of the ADC.

This approach bypasses the bit-amplitude of the digital data (Fig. 2.10), which it may be important to calculate, for instance if the hydrophone sensitivity is given in μPa/bit. To compute this intermediate stage, the WAV signal is first converted to bits:

$$x_{\text{bits}} = 2^{N-1} x_{\text{WAV}} \tag{2.6}$$

where N is the bit-resolution of the ADC (typically 16 or 24 bits).

The voltage signal can then be computed as in Eq. 2.5:

$$x_V = \frac{V_{\text{peak}} x_{\text{bits}}}{2^{N-1}} = V_{\text{peak}} x_{\text{WAV}} \tag{2.7}$$

To convert the voltage signal to acoustic pressure, any pre-amplification of the voltage signal must be reversed and the pressure is then obtained using the hydrophone sensitivity, which describes the voltage generated by the hydrophone per μPa of acoustic pressure. If the frequency response of the hydrophone and any preamplification can be considered flat in the frequency range of interest, then a frequency-independent correction factor can be applied in both cases. For example, for a PAM system with a preamplifier gain $g = 12$ dB and a hy-

drophone sensitivity m_h = -165 dB re 1 V/μPa, the unamplified voltage signal, $x_{V\mathrm{u}}$, is given by

$$x_{V\mathrm{u}} = \frac{x_V}{10^{\frac{g}{20}}} \tag{2.8}$$

where the denominator is the preamplifier gain converted from dB to a linear multiplier. The acoustic pressure (in μPa) is then

$$x_{\mu\mathrm{Pa}} = \frac{x_{V\mathrm{u}}}{10^{\frac{m_h}{20}}} \tag{2.9}$$

where the denominator is the hydrophone sensitivity in linear units (V/μPa).

If the frequency response of either the hydrophone or the pre-amplifier varies significantly within the frequency range of interest, then a frequency-dependent correction should be applied. The operations in Eq. 2.8 and Eq. 2.9 are effected using a frequency-dependent preamplifier gain and a hydrophone sensitivity curve, respectively. These corrections are carried out in the frequency domain, i.e. after a discrete Fourier transform (DFT) has been applied to the signal. In practice, these frequency-dependent steps are integrated with the subsequent stage: calculation of the power spectral density (PSD), detailed below.

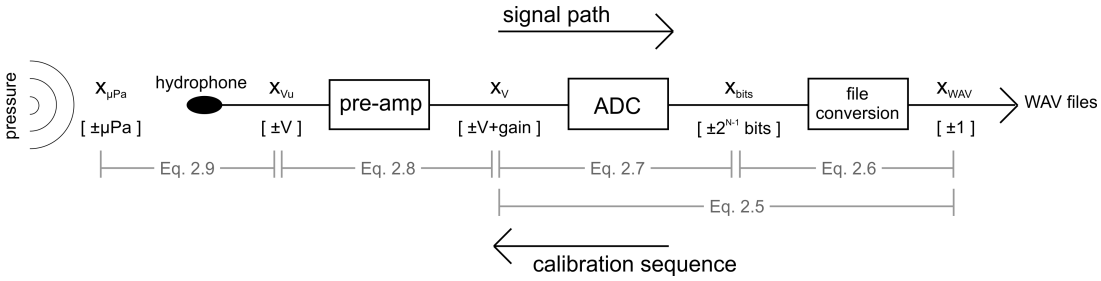

Figure 2.10: Signal path and calibration sequence for a typical passive acoustic monitoring system. Values in square brackets indicate signal units at each processing stage.

Computing power spectral density

To assess the frequency characteristics of the sound pressure signal, $x_{\mu\mathrm{Pa}}$, the signal is transposed into the frequency domain using a DFT. The time-series signal is segmented, multiplied by a window function, and then the DFT is applied to each time segment. This yields a frequency spectrum for each segment, which can be plotted as a spectrogram (sometimes termed periodogram), showing the variation in frequency content through time. For many

bioacoustics applications, such as detection and classification of marine mammal vocalisations, the absolute amplitude of the signal is not important, and spectrograms are computed in arbitrary units (relative dB). Here, it is assumed that absolute sound levels are required, and a derivation is provided of power spectral density (PSD), which can be considered a calibrated spectrogram.

	$w[n]$	σ	B
Rectangular (Dirichlet)	1	1	1
Hann	$0.5-0.5\cos\left(\frac{2\pi n}{N}\right)$	0.5	1.5
Hamming	$0.54-0.46\cos\left(\frac{2\pi n}{N}\right)$	0.54	1.36
Exact Blackman	$0.42-0.5\cos\left(\frac{2\pi n}{N}\right)+0.08\cos\left(\frac{4\pi n}{N}\right)$	0.42	1.73

Table 2.1: Selected window functions (w) for data segments of N samples, and their respective coherent gain factors (σ) and noise power bandwidths (B; Harris, 1978).

In transforming the time-series signal into the frequency domain using the DFT, there is an inherent trade-off between the precision with which individual frequency components can be resolved (spectral resolution) and the amount of spectral content which spreads erroneously into adjacent frequencies (spectral leakage). This, in turn, affects the amplitude accuracy of individual frequencies (Kay and Marple, 1981). The balance of this trade-off can be tailored by applying a window function to the time series before the DFT, prioritizing higher spectral resolution, lower spectral leakage, or greater amplitude accuracy. If no window function is applied, the window is effectively a rectangular (Dirichlet) window (Table 2.1). For analysis of signals whose content is as yet unknown, the Hann window is generally an appropriate choice (Cerna and Harvey, 2000). For a detailed discussion of windows for DFT analysis, see the review by Harris (1978).

To calculate the PSD, the sound pressure signal, $x_{\mu\mathrm{Pa}}$, is divided into segments, each containing N samples. Each segment is then multiplied by a window function, w, such that the mth segment is given by

$$x^{(m)}[n]=\frac{w[n]}{\sigma}x[n+(1-r)mN] \tag{2.10}$$

where $0\leq n\leq N-1$ (Marple, 1987), r is the window overlap expressed as a decimal (i.e. 0.75 for 75% overlap), and σ is the coherent gain factor of the window function (Cerna and Harvey, 2000). Using an overlap ensures that data near the boundary between time segments are represented, particularly if a window function which tapers to zero at its extremities is applied. A 50% overlap is typically sufficient for this purpose; higher overlaps are often used

to smooth spectrograms in the time domain.

The DFT of the mth time segment is given by

$$X^{(m)}(f) = \sum_{n=0}^{N-1} x^{(m)}[n] \exp\left(\frac{-j2\pi f n}{N}\right) \tag{2.11}$$

If N is a power of 2, the DFT can be computed more rapidly. Such DFTs are known as Fast Fourier Transforms (FFTs), though the term is often used for DFTs of any sample length. Common choices for N include 512- and 1024-point FFTs in the bioacoustics literature, though advances in computational capabilities mean the relative inefficiency of non-binary N is often no longer an obstacle.

For real signals, the DFT is symmetrical around the Nyquist frequency, $F_s/2$, where F_s is the sampling frequency. The frequencies above $F_s/2$ can therefore be discarded and the remaining values of the frequency bins doubled, yielding the single-sided power spectrum

$$P^{(m)}(f') = 2\left|\frac{X^{(m)}(f')}{N}\right|^2 \tag{2.12}$$

where $f' \leq F_s/2$.

The power spectrum periodogram, PP, is then a matrix comprising the single-sided power spectra of each of the data segments

$$PP(f', m) = 10\log_{10}\left(P^{(m)}(f')\right) \tag{2.13}$$

It is important to note that the number of bins in the DFT affects the absolute level of the power spectrum. If the DFT is shorter (i.e. if N is less), the frequency bins are wider, meaning more energy is included in each. To facilitate the comparison of different spectra, spectral analysis is often performed using a standardized time segment length of one second ($N = F_s$), which yields a frequency bin width of 1 Hz. This is known as the power spectral density (PSD). Other standardized spectra include fractional octave bands (typically 1/3-octave, but also 1/12 and whole octave) which consist of frequency bands of equal width in logarithmic space, defined for standardized frequencies (ANSI, 2009).

For many applications, and particularly when plotting long time-series spectra, a 1-s temporal

resolution may produce an unmanageable volume of data. This can be remedied by averaging the periodogram to a lower time resolution, which smooths the data. This approach is generally more computationally efficient than carrying out the original analysis with longer time segments (Welch, 1967). The standard method is known as the Welch method (sometimes referred to as the Bartlett method, which is actually a simpler version that does not include overlapping windows). The reduced time resolution periodogram, PP_W, of a full-resolution periodogram of (time) length M is given by

$$PP_W(f',q) = 10\log_{10}\left(\frac{R}{M}\sum_{m=(q-1)R+1}^{m=qR} P^{(m)}(f')\right) \tag{2.14}$$

where R is the downscaling factor, $Q = M/R$ is the number of averaged time segments produced, and $1 \leq q \leq Q$. Each segment of the reduced time resolution periodogram thus consists of the mean of Q full-resolution segments averaged in linear space.

Broadband SPL

Broadband SPL is the decibel level of the sum of the mean squared pressure over a given frequency range; in other words, it reduces the noise level to a single number. This simplicity can be problematic, however, since although it is among the most quoted metrics, broadband SPL is often reported without indicating the frequency range covered in the analysis, confounding interpretation of the results, and its single-dimensionality can disguise problems with system calibration that would be apparent in spectral representations. In practice, investigators reporting 'broadband SPL' have often neglected to consider the frequency-dependent characteristics of the recording system. To ensure the validity of broadband SPL measurements, the same care should be taken in correcting for frequency-dependent hydrophone sensitivity and gain as detailed above for PSD measurements.

Historically, sound was recorded using analogue equipment, and broadband SPL (as well as 1/3 octave bands, etc.) were measured by applying analogue filters to the signal. In the digital era, it is expedient to calculate the broadband SPL through the summation of frequency bins in the PSD. The mth measurement of the SPL, in dB re 1 μPa^2, is given by

$$\mathrm{SPL}(m) = 10\log_{10}\left(\frac{\sum_{f'=f_{\mathrm{low}}}^{f'=f_{\mathrm{high}}} \frac{P^{(m)}(f')}{B}}{p_{\mathrm{ref}}^2}\right) \tag{2.15}$$

where f_{low} and f_{high} are the lower and upper bounds of the frequency range under consideration, which should be specified when reporting broadband SPL, and p_{ref} is a reference pressure of 1 μPa. B is the noise power bandwidth of the window function, which corrects for inflation caused by spectral leakage, normalising the frequency bin values to those obtained with a rectangular (Dirichlet) window

$$B = \frac{1}{N} \sum_{n=0}^{N-1} \left(\frac{w[n]}{\sigma} \right)^2 \tag{2.16}$$

Note that the noise power bandwidth is only applied when making a summation of DFT frequency bins (e.g. for 1/3-octave bands or a broadband level), and not when analysing the amplitudes of individual frequency bins in the PSD (e.g. tonal signals).

2.4.3 Characterising acoustic habitats

Impulsive sound

'Impulsive' or 'pulse' sound can be described as sound which cannot be considered continuous over a given temporal extent. To characterise anthropogenic underwater noise, a distinction is conventionally drawn between *pulse* (and typically repetitive) sources such as seismic airguns and pile driving (see Section 2.2.4, p18) and *continuous* sources such as shipping and drilling (Southall et al., 2007). Many active sonar systems do not fit neatly into either category, since they typically emit sweeps of tonal (i.e. continuous) sound, but their onset and termination can be abrupt and sound projection is often on a repetitive on/off cycle. Pulse sounds also occur naturally, and include biotic sources such as snapping shrimp (Versluis et al., 2000), and abiotic sources such as glacier calving events (Pettit, 2012; Tegowski et al., 2012) and thunder (Dubrovskiy and Kosterin, 1993).

The discontinuous nature of pulse sound means that metrics based on average pressure, such as SPL, vary depending on the duration of the time window over which the metric is integrated (Madsen, 2005). To standardise time windows around pulses, some practitioners have used a 90% energy envelope [Fig. 2.11(c)], whereby the SPL is determined for the time window between 5% and 95% of the cumulative energy of the pulse (e.g. Blackwell et al., 2004). However, the key measures linked to auditory damage in mammalian ears are peak pressure amplitude and the sound exposure level (SEL; also termed energy flux density), and Madsen (2005) has demonstrated that signals with widely differing SELs can have similar SPLs. Consequently, SPL is now more widely regarded as an inappropriate measure of pulse sounds, and

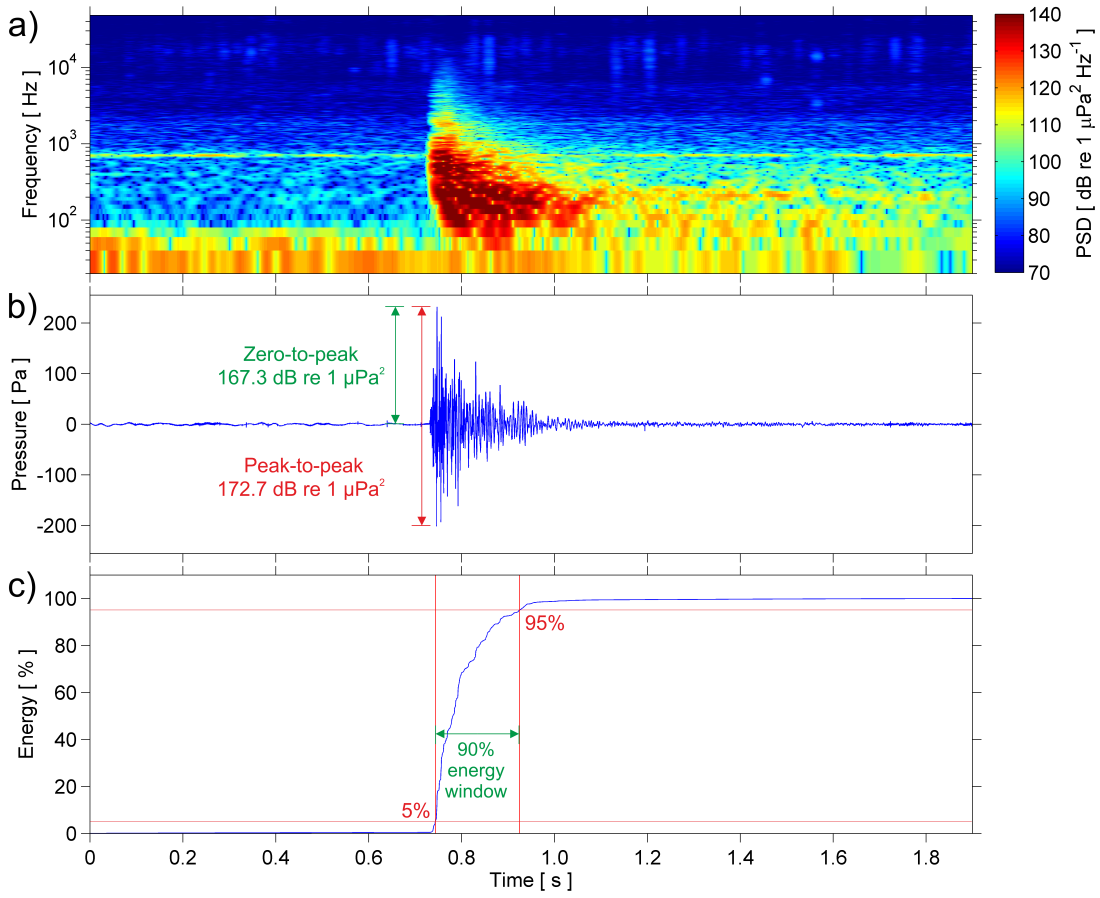

Figure 2.11: Seismic airgun array recorded at ∼6 km distance in Mayumba National Park, Gabon, October 30 2012. Sampling frequency: 96 kHz. (a) Power spectral density: 0.05-s Hann window, 99% overlap. (b) Pressure waveform illustrating peak-to-peak and zero-to-peak metrics. (c) Cumulative energy of pulse showing 90% energy envelope.

peak-to-peak (Eq. 2.17), zero-to-peak (Eq. 2.18) and SEL (Eq. 2.19; expressed in dB re 1 μPa^2 s, sometimes using the 90% energy envelope) are reported instead [see Fig 2.11(b)–(c)]. To accurately measure these characteristics of the pressure waveform, the recording system should be designed such that peak frequencies of the signal fall within the flat frequency response of the hydrophone and other hardware.

$$\mathrm{SPL}_{\mathrm{p-p}} = 10\log_{10}\left(\frac{\left(max(x_{\mu\mathrm{Pa}}) + \left|min(x_{\mu\mathrm{Pa}})\right|\right)^2}{p_{\mathrm{ref}}^2}\right) \tag{2.17}$$

$$\mathrm{SPL}_{0-\mathrm{p}} = 10\log_{10}\left(\frac{max(x^2_{\mu\mathrm{Pa}})}{p^2_{\mathrm{ref}}}\right) \tag{2.18}$$

$$\mathrm{SEL} = 10\log_{10}\left(\frac{\sum_{m=1}^{M}\sum_{f'=f_{\mathrm{low}}}^{f_{\mathrm{high}}} P^{(m)}(f')}{p^2_{\mathrm{ref}} \cdot 1s}\right) \tag{2.19}$$

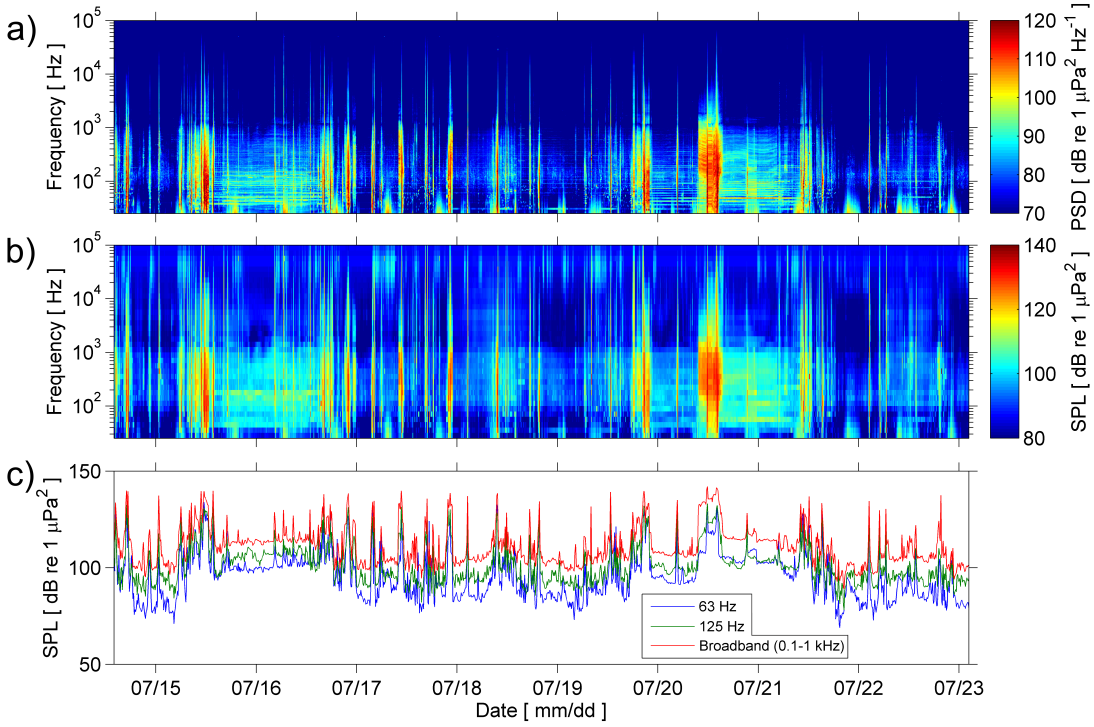

Figure 2.12: Time series analyses of a 9-day deployment in The Sutors, Moray Firth, Scotland, in July 2012. (a) PSD (b) 1/3-octave band spectrum (c) 63- and 125-Hz 1/3-octave bands and broadband (0.1–1 kHz) SPL.

Time series

Waveform representation [Fig. 2.11(b)] can be useful for characterising the amplitude of discrete signals, but to represent spectral characteristics and the evolution of nominally continuous sound through time, the PSD and broadband or 1/3 octave SPLs are more appropriate (see Section 2.4.2, p27, for derivations). Fig. 2.12 shows a time series for a 9-day deployment at The Sutors in the inner Moray Firth in July 2012 (see Section 4.2, p72, for details). The 1-Hz resolution of the PSD [Fig. 2.12(a)] gives detail of the tonal characteristics of vessels transiting the study site, while the 1/3 octave spectrogram [Fig. 2.12(b)] gives a lower reso-

lution on the frequency axis, with the advantage of higher noise levels at higher frequencies relative to the PSD, which makes presentation of high and low frequencies on the same figure easier. The broadband SPL, in this case for the range 0.1–1 kHz [Fig. 2.12(c)], is also often plotted as a time series, as are individual 1/3 octave band levels, such as the 63- and 125-Hz bands specified for the MSFD [Fig. 2.12(c)].

Summary statistics

While spectrograms are valuable tools to study the temporal and frequency evolution of sound, many applications benefit from a statistical analysis of noise levels to summarise the characteristics of the noise field. This is especially the case for comparison of noise levels from different sites or over different time periods. Among these techniques are average spectra [Fig. 2.13(a)] – be they PSDs, whole-octave, 1/3-octave or 1/12-octave bands. Note that band levels differ from the PSD since in linear frequency space the bands widen as frequency increases, meaning more energy is integrated. The PSD, by contrast, has a consistent 1-Hz bin width. Percentiles are also commonly used to indicate variability [Fig. 2.13(b)], though they do have some limitations (see Section 3.2, p46). Variability of band levels may also be presented as 'box and whisker' plots [Fig. 2.13(c)]. To summarise the average daily variability for long-term data, daily averaged 1/3-octave spectra can be used [e.g. median levels; Fig. 2.13(d)].

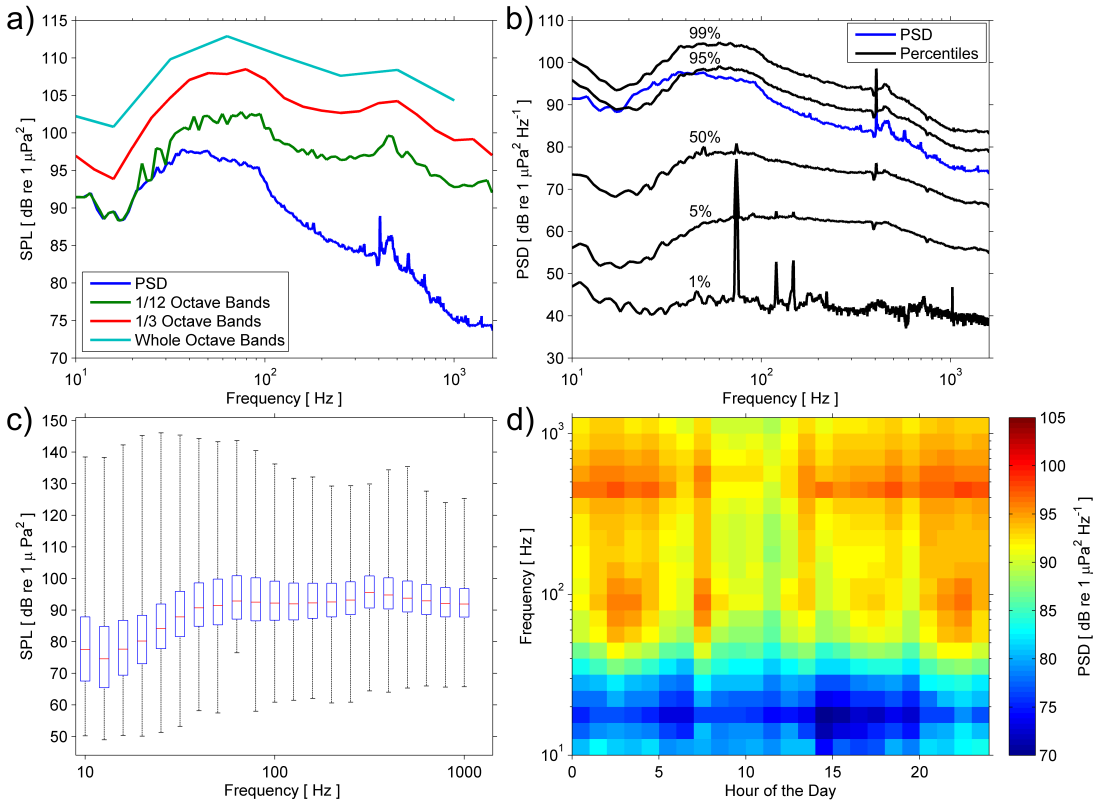

Figure 2.13: Summary representations of acoustic data recorded on the VENUS network in the Strait of Georgia, British Columbia, Canada, from Dec 2011 to Jul 2012. (a) Linear mean PSD and fractional octave bands (b) Linear mean PSD and percentiles (c) Box and whisker plot of 1/3-octave bands – mid-line is median, edges of boxes are first and third quartiles, whiskers are minima and maxima (d) Median 1/3-octave level for each hour of the day.

Chapter 3

Advancement of Analysis Methods

This chapter consists of two manuscripts published in *JASA Express Letters* which resulted from collaborations initiated during the PhD with Ocean Networks Canada (ONC; based at the University of Victoria) and the University of Aberdeen. The first (Section 3.1; Merchant

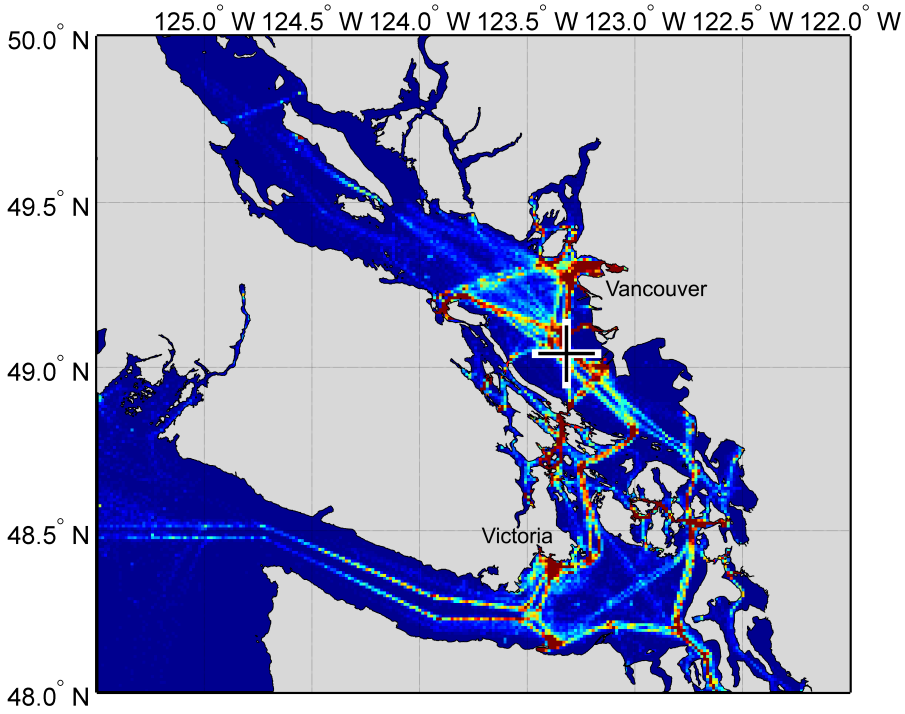

Figure 3.1: Map of the Strait of Georgia, British Columbia, Canada, showing the location of the VENUS hydrophone (black cross) used in this chapter. The colour scale indicates the density of shipping in the Strait based on AIS data for May 2012 (1 × 1-km grid).

et al., 2012a) addresses the use of different averaging metrics for the assessment of shipping noise using ∼4 months of continuous hydrophone recordings made on the VENUS cabled observatory in the Strait of Georgia, British Columbia, operated by ONC. In the second paper (Section 3.2; Merchant et al., 2013), a new analysis method for large PAM datasets is presented, and its utility is demonstrated using a longer sample of VENUS data (recorded over ∼7 months), as well as data from two deployments of autonomous PAM units in the Moray Firth, Scotland. These papers are unabridged from their published versions, though some footnotes have been added for clarity. Furthermore, a map of the VENUS site (Fig. 3.1) is provided here (there was not space for this in the original manuscripts), and a map of the Moray Firth location can be found in Section 4.2.2, p75.

3.1 Averaging Underwater Noise Levels for Environmental Assessment of Shipping

Rising underwater noise levels from shipping have raised concerns regarding chronic impacts to marine fauna. However, there is a lack of consensus over how to average local shipping noise levels for environmental impact assessment. This paper addresses this issue using 110 days of continuous data recorded in the Strait of Georgia, Canada. Probability densities of $\sim 10^7$ 1-s samples in selected 1/3 octave bands were approximately stationary across one-month subsamples. Median and mode levels varied with averaging time. Mean sound pressure levels averaged in linear space, though susceptible to strong bias from outliers, are most relevant to existing impact assessment metrics.

3.1.1 Introduction

Underwater sound pressure levels (SPLs) in areas of local shipping activity are highly variable due to vessel passages, and probability distributions of shipping noise are generally non-Gaussian (Brockett et al., 1987). Consequently, average SPLs depend on the averaging method employed. Although average SPLs of shipping noise are commonly reported in assessments of acoustic impact on marine life, there is a lack of consensus over which average is most appropriate: examples in the literature include the median (McQuinn et al., 2011), (linear space) mean (Hatch et al., 2008) and mode (Parks et al., 2009).

As environmental policy responds to advances in research into the effects of anthropogenic noise on marine fauna, there is a growing need for scientific consensus and clarity in the

reporting of underwater noise assessment metrics. One example is the European Marine Strategy Framework Directive (MSFD; European Commission, 2008), which aims to describe low-frequency ambient noise trends using average 1/3 octave band levels (Tasker et al., 2010), the first quantitative policy initiative of its kind. Subsequent work (Van der Graaf et al., 2012) has recommended the use of the (linear) mean SPL for the implementation of this legislation, solely on the basis that it is more robust to variations in averaging time than the median (though no evidence was presented for this assertion). We believe this case highlights the need for an evidence-based examination of this issue.

This paper assesses the case for the above averaging methods as applied to noise from heavy commercial shipping traffic. Data amounting to 110 days of continuous recording were acquired over a 137-day period in the Strait of Georgia, Canada, a major commercial shipping route. The underlying SPL distributions are analyzed at 1-s resolution, and each metric is empirically assessed for varying averaging times and in the presence of outliers. The relative merits of each method are then discussed with regard to standardization and relevance to the assessment of long-term impacts on marine life.

3.1.2 Data acquisition and analysis

Measurements were made from a cabled seafloor observatory in the Strait of Georgia, British Columbia, operated by Ocean Networks Canada (ONC). The observation station is located at 49° 02.5309′ N, 123° 19.0520′ W in waters ∼170 m deep, on the main shipping route south from the Port of Vancouver*. Data were recorded using an Instrument Concepts icListen-LF smart hydrophone system† comprising a GeoSpectrum M24 hydrophone and integrated electronics to transmit the digitized signal via Ethernet to shore. The instrument is deployed on the VENUS network (VENUS, 2013) as part of a technology demonstration run by ONC's Center for Enterprise and Engagement (ONCCEE). An end-to-end calibration of the system was performed by ONCCEE, using a custom-built pistonphone for the range 0.1–100 Hz. For the range 300–1600 Hz, the calibration was carried out using a reference hydrophone on a test rig in the Saanich Inlet at a depth of 100 m in waters ∼200 m deep. Both results agreed with the manufacturer's declared sensitivity. Data were sampled at 4 kHz and 24 bits, recording continuously in 5-minute segments.

All recordings made between 14 Dec 2011 and 30 April 2012 were downloaded from the VENUS server, and consisted of 31,908 WAV-formatted files totaling 107 GB. 196 files were

*See Fig. 3.1 for map.
†The hydrophone was 1.2 m above the seabed.

discarded due to anomalous metadata (which rendered the files unreadable at the correct sampling frequency) or file length (which would result in inconsistent averaging times in the subsequent analysis). Further data were absent due to downtime during administrative tasks and redactions made by the Royal Canadian Navy, which terminates the data stream intermittently to protect sensitive information. The overall coverage of the time series was 80%.

Data were processed in MATLAB (v. 2011b) using custom-written scripts. The power spectral density (PSD) was calculated in 1-s non-overlapping segments using a Hann window. Two files were produced for each 5-minute measurement: one containing 1/3 octave levels maintaining 1-s time resolution and another with the linearly averaged power spectrum (1-Hz resolution) of the entire 5-minute file. These were then concatenated to form master files for subsequent analysis. Probability distributions (PDs) of octave-separated 1/3 octave band levels were estimated using the kernel smoothing density estimate function 'ksdensity'[‡] in MATLAB using 0.1-dB bins.

Sound pressure level (SPL) is the mean squared sound pressure, p^2_{rms}, expressed in decibels:

$$\text{SPL} = 10\log_{10}\left(\frac{p^2_{\text{rms}}}{p^2_{\text{ref}}}\right) \tag{3.1}$$

where p_{ref} is a reference pressure of 1 μPa and SPL has units of dB re 1 μPa^2. Average SPLs were computed using the median, SPL_{Md}, the mode, SPL_{Mo}, and the linear-space mean, $\overline{\text{SPL}}_{\text{lin}}$. SPL_{Md} was computed in linear space. SPL_{Mo} was calculated as the maximum of the PD estimate. For N samples of p^2_{rms}, $\overline{\text{SPL}}_{\text{lin}}$ is given by

$$\overline{\text{SPL}}_{\text{lin}} = 10\log_{10}\left(\frac{\frac{1}{N}\sum_{i=1}^{N} p^2_{rms,i}}{p^2_{\text{ref}}}\right) \tag{3.2}$$

where $p^2_{rms,i}$ is the i^{th} value of the mean squared pressure. The dB-domain mean, $\overline{\text{SPL}}_{\text{dB}}$, was also included for completeness:

$$\overline{\text{SPL}}_{\text{dB}} = \frac{1}{N}\sum_{i=1}^{N} 10\log_{10}\left(\frac{p^2_{rms,i}}{p^2_{\text{ref}}}\right) \tag{3.3}$$

[‡]See http://www.mathworks.co.uk/help/stats/ksdensity.html for details.

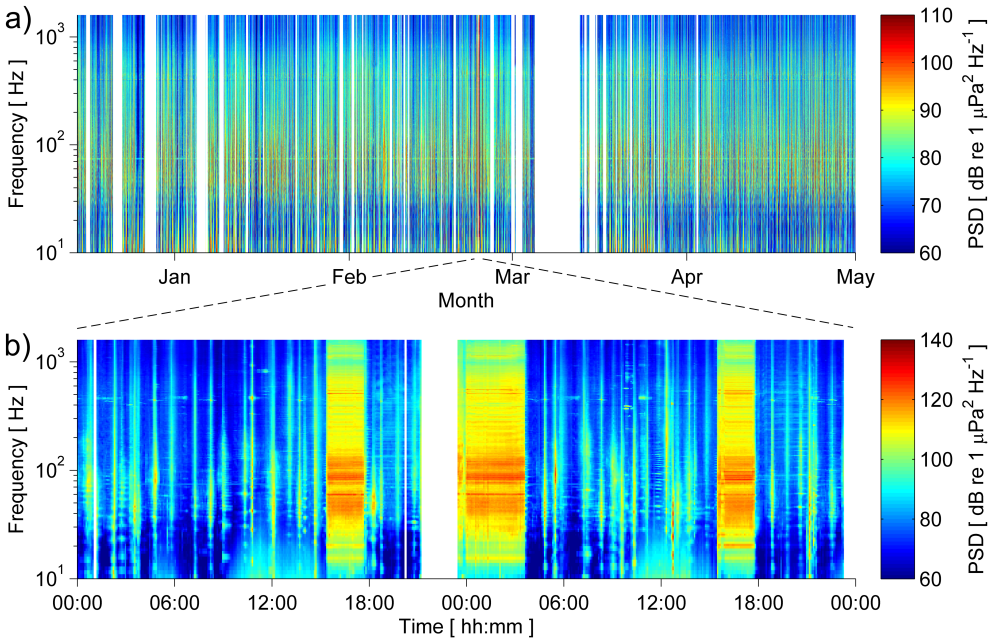

Figure 3.2: Power spectral densities over the range 10–1600 Hz using 5-minute averages. (a) Complete dataset: 14 December 2011 to 30 April 2012 (b) Exceptional ship signature: 23–24 February 2012. Note the difference in dynamic range between (a) and (b).

To examine the effect of varying averaging time, the temporal resolution of the 1/3 octave spectra was reduced from 1 s using the standard Welch (1967) method (i.e. using the mean of each frequency band in linear space) for averaging times of up to $\sim 10^7$ s. To limit the influence of transients in the spectrum, Parks et al. (2009) proposed an alternative to the Welch method using the median instead of the mean, and subsequently to use the mode of these median values as the average level. This approach was also implemented for comparison to the standard mode. In the discussion below, 'integration time' refers to the time over which p^2_{rms} was calculated (1 s), and 'averaging time' is the length of the averaged power spectrum windows (from 1 to $\sim 10^7$ s).

3.1.3 Distribution of shipping noise levels

The spectrogram for the analysis period consisted of frequent ship passages with frequency content concentrated in the range 30–500 Hz, and maximal between around 60 and 100 Hz [Fig 3.2(a)]. Two discrete spectral components were also apparent: one at 74 Hz and another at 400 Hz. The latter is believed to originate at an industrial terminal near the site, while the

former is likely to be system noise from a fan on adjacent equipment at the deployment site. The 1/3 octave bands chosen for analysis did not include these frequencies.

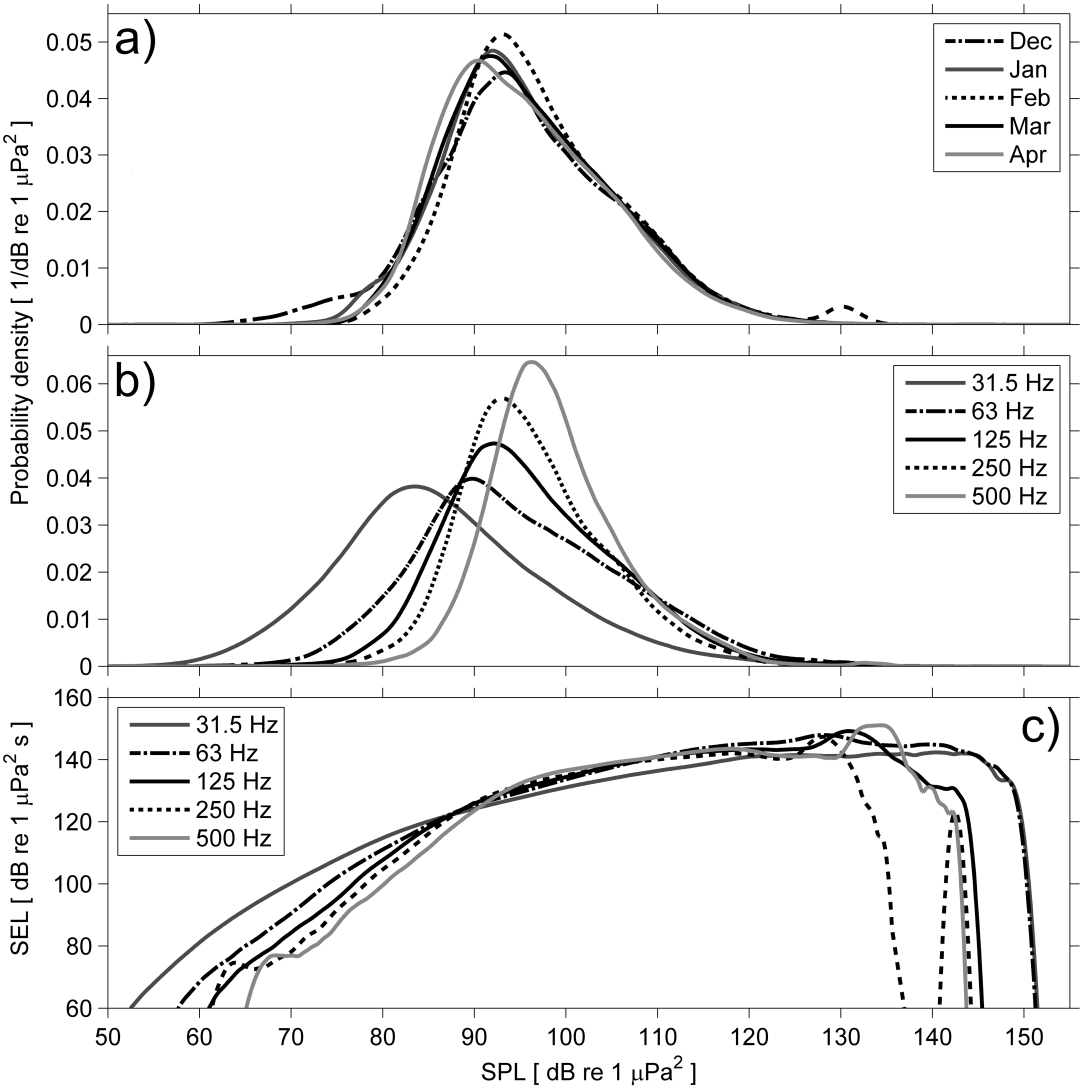

Figure 3.3: (a) Estimated probability densities (PDs) for each month in the 125-Hz band. Bin width: 0.1 dB, integration time: 1 s. (b) PDs of octave-separated 1/3 octave bands over observed frequency range of shipping noise. (c) 24-h SEL[¶] calculated from PDs in (b).

Monthly probability densities were plotted to examine stationarity over the period. The 125-Hz band, representative of the other octave-separated frequencies, is shown in Fig. 3.3(a). All months exhibited a similar density curve, agreeing more closely at higher SPLs. The greater occurrence of low SPLs in December and January is attributable to periods of exceptionally

[¶]This is the SEL calculated for each 0.1 dB bin of SPL, normalised to a 24-h period.

low shipping noise around December 25–26, January 1–2 and January 15, evident in Fig. 3.2(a). The peak at 130 dB re 1 μPa^2 in February [Fig. 3.3(a)] was due to the signature of the CCGS John P. Tully (on a VENUS maintenance cruise) between February 23 and February 24 [Fig. 3.2(b)]. Overall, probability densities of octave-separated 1/3 octave bands in the range 30–500 Hz appeared right-skewed [i.e. non-Gaussian; Fig. 3.3(b)]. The mode increased and variance decreased with increasing frequency across this range. Fig. 3.3(c) shows the distribution of sound exposure level (SEL) over the SPL densities in Fig. 3.3(b), computed for a period of 24 hours. SEL is a cumulative exposure metric defined as the integral of squared instantaneous sound pressure, $p^2(t)$, with respect to time, which can be expressed as a sum of non-overlapping 1-s samples of p^2_{rms}:

$$\mathrm{SEL} = 10\log_{10}\left(\frac{\int_0^T p^2(t)dt}{p^2_{\mathrm{ref}}\cdot s}\right) = 10\log_{10}\left(\frac{\sum_{i=1}^{T} p^2_{rms,i}}{p^2_{\mathrm{ref}}\cdot s}\right) \tag{3.4}$$

where T is the exposure period in seconds, s is a reference time of 1 s and SEL has units of dB re 1 μPa^2 s. The peaks in SEL in the SPL range 125–135 dB re 1 μPa^2 [Fig. 3.3(c)] were attributable to the ship signature mentioned above.

3.1.4 Approaches to averaging

The case for reporting $\mathrm{SPL}_{\mathrm{Md}}$ – as advocated, for example, by McQuinn et al. (2011) – is that it is more representative of SPLs commonly received by marine fauna (since it is generally closer to the peak of the SPL probability distribution than $\overline{\mathrm{SPL}}_{\mathrm{lin}}$). This argument was extended to its logical conclusion by Parks et al. (2009), who reported the most probable level, $\mathrm{SPL}_{\mathrm{Mo}}$ [using a non-standard method (see Section 3.1.2)]. While it may often be useful to report the most representative noise level, for the assessment of cumulative, long-term noise exposure, there is a strong case that (frequency-weighted) SEL is a more appropriate metric for marine mammals (Southall et al., 2007; Ellison et al., 2012) and may be an appropriate metric for fish (Popper and Hastings, 2009b). $\mathrm{SPL}_{\mathrm{Md}}$ and $\mathrm{SPL}_{\mathrm{Mo}}$ are insensitive to SEL, which is largely determined by higher SPLs (Fig. 3.3(c); see also Merchant et al., 2012b). In this regard, $\overline{\mathrm{SPL}}_{\mathrm{lin}}$ has the advantage of being directly related to SEL:

$$\mathrm{SEL} = \overline{\mathrm{SPL}}_{lin} + 10\log_{10}T \tag{3.5}$$

where T is the exposure period in seconds. Furthermore, in aerial acoustics $\overline{\mathrm{SPL}}_{\mathrm{lin}}$ is already an established metric for traffic noise assessment in the form of the equivalent continuous noise level, L_{eq}, which is A-weighted for human hearing and defined for specified time periods (e.g. 8 hours, 24 hours; Harris, 1991).

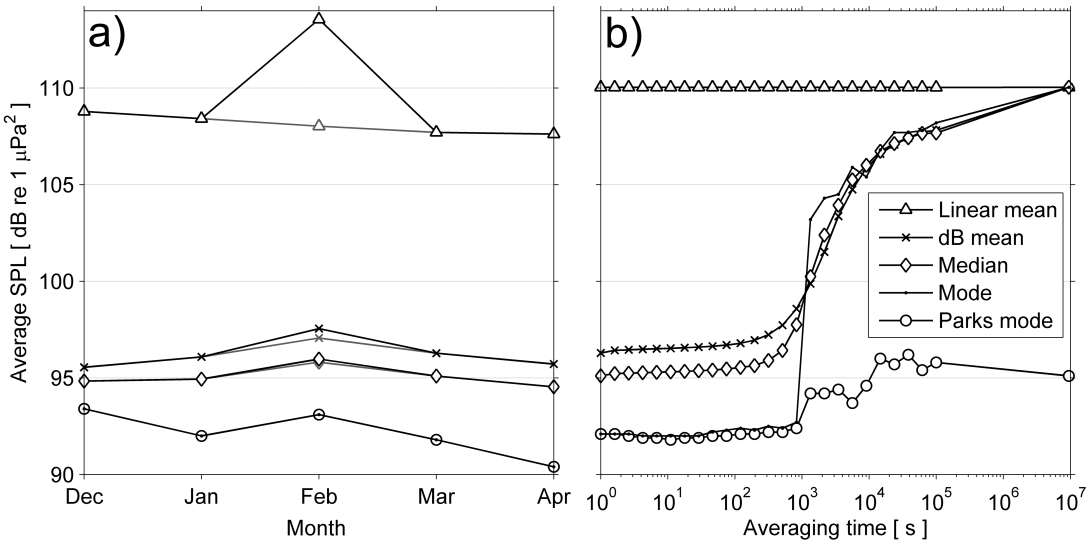

Figure 3.4: (a) Average SPLs in 125 Hz band for each month; averages with February ship signature [see Fig. 3.2(b)] omitted are plotted in gray. Integration time: 1 s. (b) Total average SPL for 125 Hz band vs. averaging time. 'Parks mode' refers to the averaging method in Parks et al. (2009)

The downside of the sensitivity of $\overline{\mathrm{SPL}}_{\mathrm{lin}}$ to higher SPLs is that it is susceptible to upward bias by loud events which may be anomalous or otherwise unrepresentative (Parks et al., 2009; McQuinn et al., 2011). This phenomenon is clearly demonstrated in Fig. 3.4(a), where $\overline{\mathrm{SPL}}_{\mathrm{lin}}$ for February was raised by 5.5 dB due to exceptionally high SPLs from a single vessel for only a few hours. If such biases are detected, potentially subjective judgments have to be made over how representative specific features of the data are for the habitat under consideration. Fig. 3.4(a) also shows that $\mathrm{SPL}_{\mathrm{Md}}$ was not immune to the influence of the ship signature, though at 0.2 dB its effect was greatly diminished. Any effect on $\mathrm{SPL}_{\mathrm{Mo}}$ was below the 0.1-dB bin resolution.

Since SPL is itself defined by p^2_{rms}, the aggregate mean, $\overline{\mathrm{SPL}}_{\mathrm{lin}}$, was unaffected by changes in averaging time [Fig. 3.4(b)]. As suggested by Van der Graaf et al. (2012), $\mathrm{SPL}_{\mathrm{Md}}$ varied with averaging time, increasing slightly ($\sim$0.5 dB) from 1 to 100 s, and rising more steeply above $\sim$400 s. In general, this variation will depend on the overall distribution of SPL. $\mathrm{SPL}_{\mathrm{Mo}}$ exhibited a sharp step at $\sim 10^3$ s: this resulted from bimodality in the SPL probability distribution as it progressed from background-dominated short averaging times to longer averaging times

dominated by ship passages. These results imply that if SPL_{Md} or SPL_{Mo} are to be used as indicators of shipping noise levels, the averaging time should be standardized and sufficiently short that p^2_{rms} can be considered continuous in each time window.

The alternative SPL_{Mo} proposed by Parks et al. (2009) varied less with averaging time than SPL_{Mo} [Fig. 3.4(b)], though the increased variability with increasing averaging time highlights the instability of the mode for small populations. Given the robustness of the mode to outliers [Fig. 3.4(a)], this approach appears to present a more reliable averaging method for large numbers of samples where it is preferable to compute the most probable SPL, or where extraneous transients bias SPL upwards.

Although it may be useful to report more than one averaging metric in shipping noise assessment, we suggest that in circumstances where one value must be chosen, $\overline{SPL}_{lin}$ presents the strongest case, given its relation to SEL, its robustness to varying averaging times, and its established use in aerial acoustics. While it is clear that brief, high-amplitude events can result in misleading bias when computing $\overline{SPL}_{lin}$, if a combination of analyses is employed, as presented here, the influence of such events can be identified, characterized and, if appropriate, removed.

Acknowledgements

We wish to thank Richard Dewey and Jeff Bosma for their contributions to the field work and for helpful comments on the manuscript, and Ross Chapman for valuable discussions. We also thank three anonymous reviewers whose constructive comments improved the manuscript. NDM is funded by an EPSRC Doctoral Training Award (#EP/P505399/1).

3.2 Spectral Probability Density as a Tool for Ambient Noise Analysis

This paper presents the empirical probability density of the power spectral density as a tool to assess the field performance of passive acoustic monitoring systems and the statistical distribution of underwater noise levels across the frequency spectrum. Using example datasets, it is shown that this method can reveal limitations such as persistent tonal components and insufficient dynamic range, which may be undetected by conventional techniques. The method is then combined with spectral averages and percentiles, which illustrates how the underlying

noise level distributions influence these metrics. This combined approach is proposed as a standard, integrative presentation of ambient noise spectra.

3.2.1 Introduction

Passive acoustic monitoring (PAM) of underwater ambient noise is the primary investigative tool in the growing research areas of acoustic habitat characterization and anthropogenic noise monitoring. Conventional methods of presenting ambient acoustic data include the power spectral density (PSD; e.g. Merchant et al., 2012a) to show temporal variation, and two-dimensional spectral averages (e.g. Wysocki et al., 2006) or percentiles (e.g. Curtis et al., 1999) to summarize frequency content. However, these standard techniques cannot reveal multimodality or outlying data, and may conceal contamination by system noise and inadequate dynamic range in the recording system.

An alternative to two-dimensional spectra has been developed for baseline monitoring and system diagnostics of seismic sensor networks, which presents the empirical probability densities of frequency bands computed from the PSD (McNamara and Buland, 2004). A less developed version of this method was previously presented in an underwater acoustics context by Parks et al. (2009). The technique (McNamara and Buland, 2004) presents the full range of observations in the form of normalized histograms, revealing modal behavior, outliers, and limiting features such as persistent tonal components and the system noise floor. Here, we adapt the method to include finer frequency resolution, maintaining the 1-Hz intervals of the PSD.

This more statistical approach requires large sample sizes, which are becoming the norm as advances in PAM technology make long-term deployments and large datasets feasible. Many emerging applications of long-term acoustic monitoring could benefit from this analysis, such as *in situ* performance assessment of cabled PAM observatories [e.g. NEPTUNE Canada (NEPTUNE, 2013), VENUS (VENUS, 2013), and the LIDO network (André et al., 2011b)], long-term noise monitoring for statutory regulation (e.g. the European Marine Strategy Framework Directive; Van der Graaf et al., 2012), and, more generally, data analysis and system diagnostics of autonomous and shipside PAM devices.

We combine the method, hereafter termed spectral probability density (SPD), with conventional percentiles and spectral averages, demonstrating the utility of this integrative approach through example datasets from an autonomous PAM device and a cabled undersea observatory. We propose that the SPD be considered alongside established analysis techniques for the assessment of ambient noise data.

3.2.2 Data acquisition and analysis

Data were recorded in two locations: the Moray Firth, Scotland, UK, and the Strait of Georgia, British Columbia, Canada. The Moray Firth data consisted of two deployments of a Wildlife Acoustics SM2M Ultrasonic autonomous PAM device in The Sutors[‖] (57°41.1402′ N, 3°59.8914′ W), firstly between 13 June and 7 July 2012, and then (with an upgraded circuit board) from 7–27 September 2012. Data were calibrated according to the manufacturer's specifications, which agreed with a separate pistonphone calibration to within ±1 dB over the frequency range 25–315 Hz. Recordings were made on a duty cycle of 1 minute every 10 minutes, sampling at 384 kHz/16 bits.

The Strait of Georgia data were acquired from the VENUS network, a cabled seafloor observatory[**] operated by ONC, using an Ocean Sonics icListen-LF smart hydrophone (0.1–1600 Hz). The system calibration and data acquisition were as described in previous work (Merchant et al., 2012a), but the data covered a longer period, from 14 December 2011 to 1 August 2012. A total of 57,957 5-minute recordings, sampled at 4 kHz and 24 bits and totaling 191 GB, were downloaded from the VENUS server. Due to anomalous metadata or file length, 268 files were discarded. Further data were absent due to downtime during administrative tasks and intermittent redactions made to protect sensitive information. The overall time series coverage was 85%.

The SPD is calculated from the PSD as normalized histograms of the decibel levels in each frequency bin. To calculate the PSD, the complete dataset of S samples of the instantaneous pressure $p(t)$ is divided into M segments, each containing N samples. The data segments are multiplied by a window function w, such that the mth non-overlapping segment is given by

$$p^{(m)}[n] = \frac{w[n]}{\sigma} p[n + mN] \tag{3.6}$$

where $0 \leq n \leq N-1$ and $0 \leq m \leq M-1$ (Marple, 1987), and σ is the coherent gain factor of the window function (Cerna and Harvey, 2000). The discrete Fourier transform (DFT) of the mth segment is then given by

$$P^{(m)}(f) = \sum_{n=0}^{N-1} p^{(m)}[n] \exp\left(\frac{-j2\pi f n}{N}\right) \tag{3.7}$$

[‖]See Fig. 4.8, p75, for map.
[**]See Fig. 3.1 for map.

For real signals, the DFT is symmetrical around the Nyquist frequency, $F_s/2$, and the single-sided pressure amplitude spectrum is

$$P_{ss}^{(m)}(f') = \frac{\sqrt{2}}{N} \cdot P^{(m)}(f') \tag{3.8}$$

where $1 \leq f' \leq N/2 - 1$. The power spectral density of the mth data segment is then

$$PSD^{(m)}(f') = \frac{1}{B} \left| P_{ss}^{(m)}(f') \right|^2 \tag{3.9}$$

where B is the noise power bandwidth of the window function, which normalizes the frequency bin values to those obtained with a bin width of 1 Hz and a rectangular (Dirichlet) window

$$B = \frac{1}{N} \sum_{n=0}^{N-1} \left(\frac{w[n]}{\sigma} \right)^2 \tag{3.10}$$

The PSD periodogram is then an $N/2 - 1$ by M matrix comprising the PSDs of each of the M data segments

$$PSD(f', m) = 10 \log_{10} \left(PSD^{(m)}(f') \right) \tag{3.11}$$

The SPD of frequency bin f' is given by the empirical probability density

$$SPD(f') = \frac{1}{Mh} H\left(PSD(f', m), h \right) \tag{3.12}$$

where $H(PSD(f', m), h)$ denotes the histogram of M values of the PSD at frequency f' with a histogram bin width of h dB re 1 μPa^2 Hz^{-1}. The histograms are then combined to form a matrix across all frequencies.

In the analyses presented in this paper, a Hann window ($\sigma = 0.5$, $B = 1.5$) of duration 1 s was used, and the temporal resolution of the periodograms was downsampled to 60 s using the standard Welch method (Welch, 1967). The histogram bin width, h, was 0.1 dB re 1 μPa^2 Hz^{-1}.

3.2.3 System and data diagnostics

The SPD can show whether the dynamic range of the recording system is appropriate to field conditions: in Fig. 3.5(a) and Fig. 3.5(b) the primary mode (maximal probability density) converges with the lowest recorded noise levels at ∼10 kHz, and the noise floor appears artificially flat, remaining at ∼47 dB re 1 μPa^2 Hz^{-1} above ∼1.5 kHz. This indicates that the data are constrained by the sensitivity of the instrument, and that additional gain or other system modifications would be needed to measure low noise levels in this frequency range. According to the canonical ambient noise curves produced by Wenz (1962), such a noise floor prevents measurement of the lowest sea states above ∼1.5 kHz. Conversely, Fig. 3.5(c) demonstrates that the VENUS data were not limited by the dynamic range of the instrument.

If ambient noise spectra are to be presented in 1/3 octave bands, any anomalous spikes in the narrowband spectrum should be characterized as these will dominate their respective 1/3 octave bands. Such tonal components are evident in Fig. 3.5(a) (as a series of harmonic spikes above 1 kHz, believed to be system self-noise) and Fig. 3.5(c) (at 74 Hz, believed to be system noise from an adjacent instrument; Merchant et al., 2012a). While tonals may appear in percentile plots (overlain on the SPD in Fig. 3.5) and the PSD, the SPD can show whether they are persistent throughout the deployment, as in Fig. 3.5(c) where this was clear from the lack of data points below the tonal spike at 74 Hz. By contrast, the tonal components between 0.1–1 kHz in Fig. 3.5(b) originated from persistent but variable low-level industrial noise, possibly from an oil rig or the nearby shipyard. The reduction in tonal system noise between the Moray Firth deployments [Fig. 3.5(a) and Fig. 3.5(b)] was due to an upgraded circuit board.

The dynamic ranges of PSD plots are often chosen to highlight specific spectral features, which may result in masking of low-level tonal components if the floor of the color scale is too high. The PSDs in Fig. 3.6, for example, exclude data below 70 dB re 1 μPa^2 Hz^{-1}, which Fig. 3.5 shows is a substantial proportion. Potential masking of persistent low-amplitude tonals is precluded by performing an SPD analysis, since the full dynamic range is presented. Combining this with spectral percentiles (as in Fig. 3.5) ensures that high-frequency tonal spikes, which may be too narrow to be evident on SPD or PSD plots, are not overlooked.

3.2.4 Ambient noise characterization

As well as evaluating data quality, the SPD can also help to characterize ambient noise levels. For example, the first Moray Firth deployment featured a one-week period of consistently

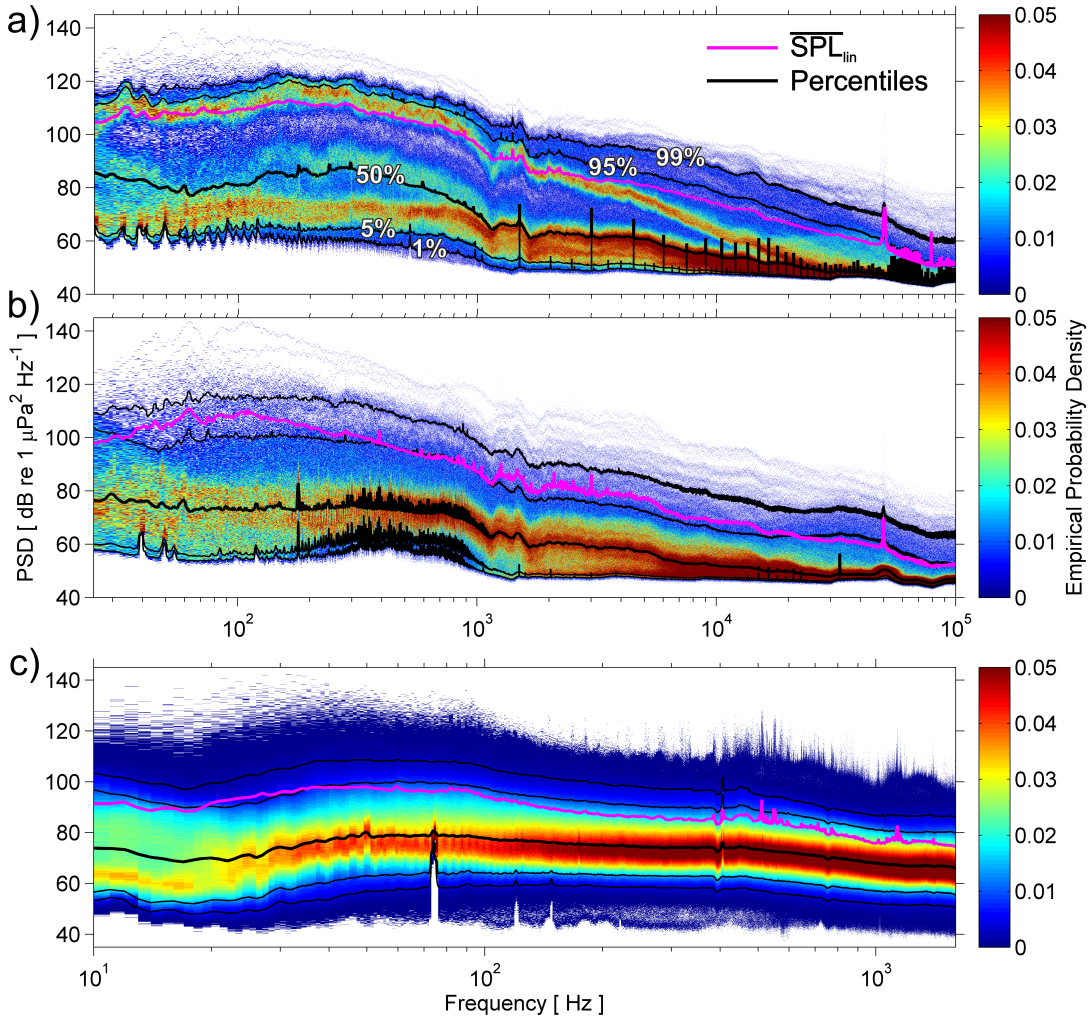

Figure 3.5: Spectral probability densities of Moray Firth deployments over the range 25 Hz–100 kHz: (a) 13 June to 7 July 2012 (b) 7–27 September 2012. (c) VENUS deployment over range 10–1600 Hz from 14 December 2011 to 1 August 2012. Note the different frequency range in (c).

high noise levels as an oil rig was towed into the area by two vessels operating with dynamic positioning (see Fig. 3.6(a) from June 16 onwards). The received vessel noise was concentrated below 1 kHz, and exhibited a tide-dependent Lloyd's mirror effect. In the SPD [Fig. 3.5(a)], this sustained period of vessel noise appears as a secondary modal ridge[††] ∼40 dB greater than the primary mode in the range 0.1–1 kHz. In contrast, this underlying bimodality is concealed by the linear mean, $\overline{SPL}_{lin}$, and percentiles, which could be misleading if used as the sole method of analysis.

[††]i.e. the mode which is 110 dB re 1 μPa^2 Hz^{-1} at 100 Hz and converges with the primary mode at 20 kHz.

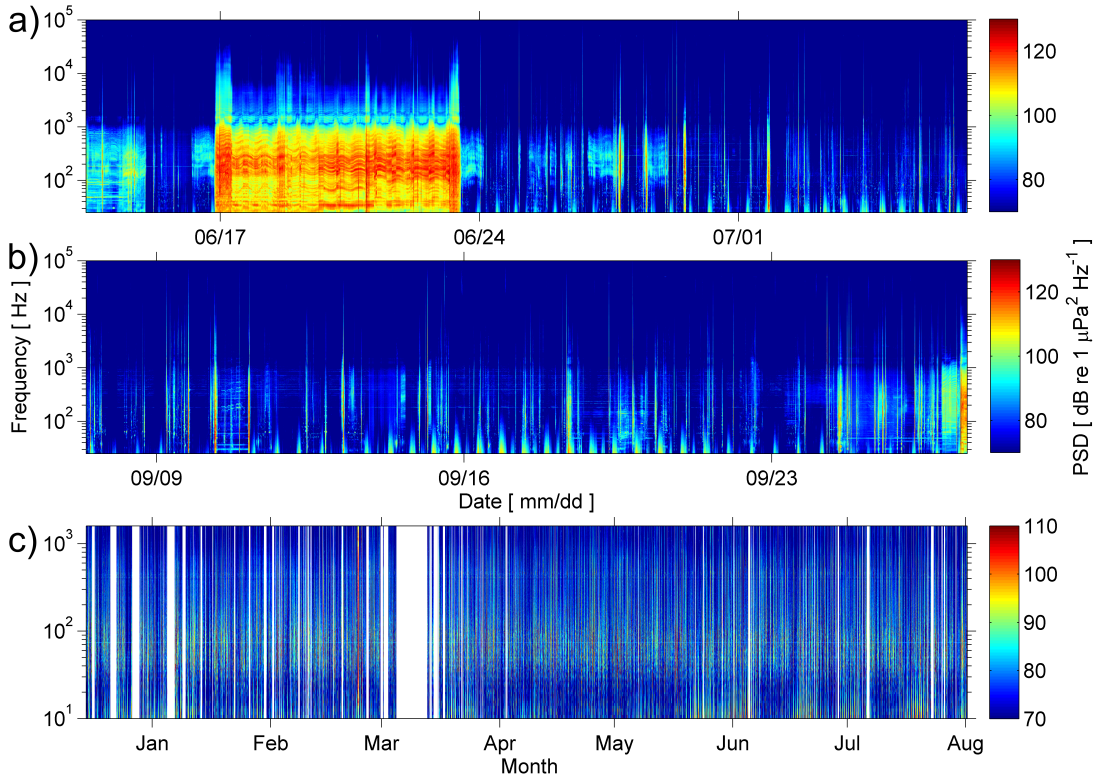

Figure 3.6: Power spectral densities of Moray Firth deployments over the range 25 Hz–100 kHz: (a) 13 June to 7 July 2012 (b) 7–27 September 2012. (c) VENUS deployment over range 10–1600 Hz from 14 December 2011 to 1 August 2012.

While it is often necessary to condense data into average noise levels (e.g. for comparison with other studies or to record temporal trends), different averaging metrics can produce widely differing average levels, which may result in misinterpretation of noise data (Merchant et al., 2012a). One way to assess the behavior of averages is to present them in the context of the distributions they represent. This can be performed across the frequency spectrum using the SPD: Fig. 3.5 shows that the shape of $\overline{\mathrm{SPL}}_{\mathrm{lin}}$ broadly follows the profile of the maximal recorded levels, while the median more closely reflects the mode, as shown by the maximal probability density.

A further application is the characterization of outliers and their influence on noise level metrics. In Fig. 3.5, $\overline{\mathrm{SPL}}_{\mathrm{lin}}$ is consistently below the 95th percentile except where maximal outliers are particularly deviant. Both Moray Firth deployments [Fig. 3.5(a) and Fig. 3.5(b)] featured tonal outliers at 50 kHz caused by shipborne depth sounders operating at this frequency. The broadband outliers in Fig. 3.5(b) were due to a rig being towed past the deployment site on 27 September, evident in Fig. 3.6(b), and those in Fig. 3.5(c) were partic-

ularly loud vessel passages, including the sustained presence of a VENUS maintenance vessel for several hours (Merchant et al., 2012a) visible on February 23–24 in Fig. 3.6(c). This illustrates how loud events influence $\overline{\mathrm{SPL}}_{\mathrm{lin}}$, and suggests that the relationship between $\overline{\mathrm{SPL}}_{\mathrm{lin}}$ and the 95th percentile could be used as an indicator of outlier influence.

3.2.5 Conclusion

With an expanding range of PAM systems on the market and increased exploitation of ambient noise monitoring for various research applications, there is a growing need to be able to assess whether an instrument's dynamic range and gain settings are appropriate to field conditions, and whether data are suitable for their intended purpose. We have demonstrated that the SPD can fulfill this role, complementing the calibration of PAM systems by assessing performance in the field.

We have also shown that the SPD contextualizes conventional spectral averages and percentiles by revealing the underlying noise level distribution. This can alert investigators to the influence of outliers and the presence of phenomena such as multimodality which are not shown by conventional techniques. Combining conventional methods with the SPD in this way enables a more complete understanding of ambient noise data, and should, we believe, be considered as a standard analysis technique for ambient noise monitoring.

Acknowledgements

We thank Richard Dewey and Jeff Bosma for their contributions to the VENUS field work, and Philippe Blondel for helpful comments on the manuscript. Funding for data collection in the Moray Firth was provided by Moray Offshore Renewables Ltd and Beatrice Offshore Wind Ltd. We thank Baker Consultants and Moray First Marine for their assistance with device calibration and deployment, respectively. N.D.M. is funded by an EPSRC Doctoral Training Award (No. EP/P505399/1).

Chapter 4

Incorporating Automatic Identification System (AIS) Data

This chapter comprises two manuscripts published in *Marine Pollution Bulletin*. The first paper (Section 4.1; Merchant et al., 2012b) resulted from a collaboration initiated during the PhD with the University of Exeter, and makes use of PAM data recorded for the purpose of baseline monitoring at a WEC test facility in Falmouth Bay, UK. This data is combined with ship-tracking data to identify which vessels are generating noise peaks, and a new method is developed to evaluate noise exposure from these vessel passages. The second paper (Section 4.2; Merchant et al., 2014) resulted from a separate collaboration with the University of Aberdeen, and used data recorded in the Moray Firth, Scotland. This study site is a marine protected area (MPA) for bottlenose dolphins and an important habitat for other marine mammal species, both of which may be affected by shipping noise in the area. The work formed part of a project to monitor baseline levels of anthropogenic noise ahead of expected increases in shipping traffic related to offshore windfarm construction outside the study area. The paper builds on the methods developed in the previous paper through the use of shore-based time-lapse cameras at two monitoring sites, and by assessing the noise exposure contributions of tracked and untracked vessels.

4.1 Assessing Sound Exposure from Shipping in Coastal Waters Using a Single Hydrophone and Automatic Identification System (AIS) Data

Underwater noise from shipping is a growing presence throughout the world's oceans, and may be subjecting marine fauna to chronic noise exposure with potentially severe long-term consequences. The coincidence of dense shipping activity and sensitive marine ecosystems in coastal environments is of particular concern, and noise assessment methodologies which describe the high temporal variability of sound exposure in these areas are needed. We present a method of characterising sound exposure from shipping using continuous passive acoustic monitoring combined with Automatic Identification System (AIS) shipping data. The method is applied to data recorded in Falmouth Bay, UK. Absolute and relative levels of intermittent ship noise contributions to the 24-h sound exposure level are determined using an adaptive threshold, and the spatial distribution of potential ship sources is then analysed using AIS data. This technique can be used to prioritise shipping noise mitigation strategies in coastal marine environments.

4.1.1 Introduction

Anthropogenic underwater noise can have deleterious effects on a variety of marine organisms, including mammals (Richardson et al., 1995; Nowacek et al., 2007), fish (Popper and Hastings, 2009a; Slabbekoorn et al., 2010) and cephalopods (André et al., 2011b). High-intensity, short-term events such as seismic surveys, pile driving operations and military sonar activities have been the focus of considerable attention due to their potential to cause physical injury and temporary or permanent loss of hearing sensitivity in marine mammals (e.g. Evans and England, 2001; Lucke et al., 2009; Bailey et al., 2010). Less intense sources can also elicit behavioural responses: boat noise, for example, has induced avoidance reactions in several cetacean species (Richardson and Würsig, 1997).

However, there is also growing recognition of the potential for long-term exposure to anthropogenic noise to induce chronic effects in marine species (Tyack, 2008; Slabbekoorn et al., 2010). These effects may occur at levels below those necessary to induce short-term behavioural responses, and through mechanisms which are more difficult to observe. They include masking of biologically significant sounds (Clark et al., 2009; Popper and Hastings, 2009a), chronic stress (Wright et al., 2007b; Rolland et al., 2012), subtle long-term behavioural responses (Picciulin et al., 2010) and shifts in attention (Purser and Radford, 2011). *In situ*

measurements of long-term exposure to anthropogenic noise both in absolute terms and relative to background levels are needed to inform further investigation in this area (Ellison et al., 2012).

Noise from shipping is pervasive throughout the marine environment, especially at low (<300 Hz) frequencies (Richardson et al., 1995; Chapman and Price, 2011), and is therefore a key concern regarding the effects of chronic noise exposure on marine species (Slabbekoorn et al., 2010). Deep water observations have shown that ambient noise levels have been rising since at least the 1960s due to increases in shipping traffic and tonnage (Andrew et al., 2002; Chapman and Price, 2011). Ambient noise levels in shallower coastal waters are more difficult to characterise as they exhibit much higher spatiotemporal variability (Urick, 1983). This is partly due to the greater dependence of acoustic propagation on local environmental factors such as the sound speed profile and seabed composition (Jensen et al., 2011). Significantly, variability is also caused by a higher concentration of shipping, industrial activity, and biological noise sources: it is this combination of potentially conflicting acoustic interests that necessitates the development of noise assessment methodologies applicable to coastal environments. To be meaningful, these methodologies must incorporate metrics relevant to the assessment of impacts on marine life.

For non-pulse sounds such as ship noise, sound exposure level (SEL) has been suggested as a suitable noise assessment metric for marine mammals (Southall et al., 2007) and fish (Popper and Hastings, 2009b). SEL is a cumulative measure of the acoustic energy of a sound throughout its temporal extent. Since coastal shipping noise is both persistent and dynamic (due to the presence of nearby vessels and more distant shipping), reliable measurement of sound exposure requires continuous monitoring. Previously, the large volumes of data accrued by such monitoring have rendered it impractical. However, advances in passive acoustic monitoring (PAM) technology and data processing capabilities are making measurement and analysis of continuous, long-term deployments feasible.

Hatch et al. (2008) made an extensive study of the Stellwagen Bank National Marine Sanctuary using 9 autonomous PAM devices over a 27-day period. The acoustic data were combined with Automatic Identification System (AIS) vessel tracking data, enabling analysis of the relationship between vessel movements and ambient noise levels. The purpose of the present study is to explore the efficacy of a similar approach using a single PAM device to assess long-term sound exposure from shipping. This would have clear benefits over a more complex experimental apparatus (ease of deployment, cost reduction, quantity of data) and could make more sophisticated analysis techniques accessible to a broader range of investigators.

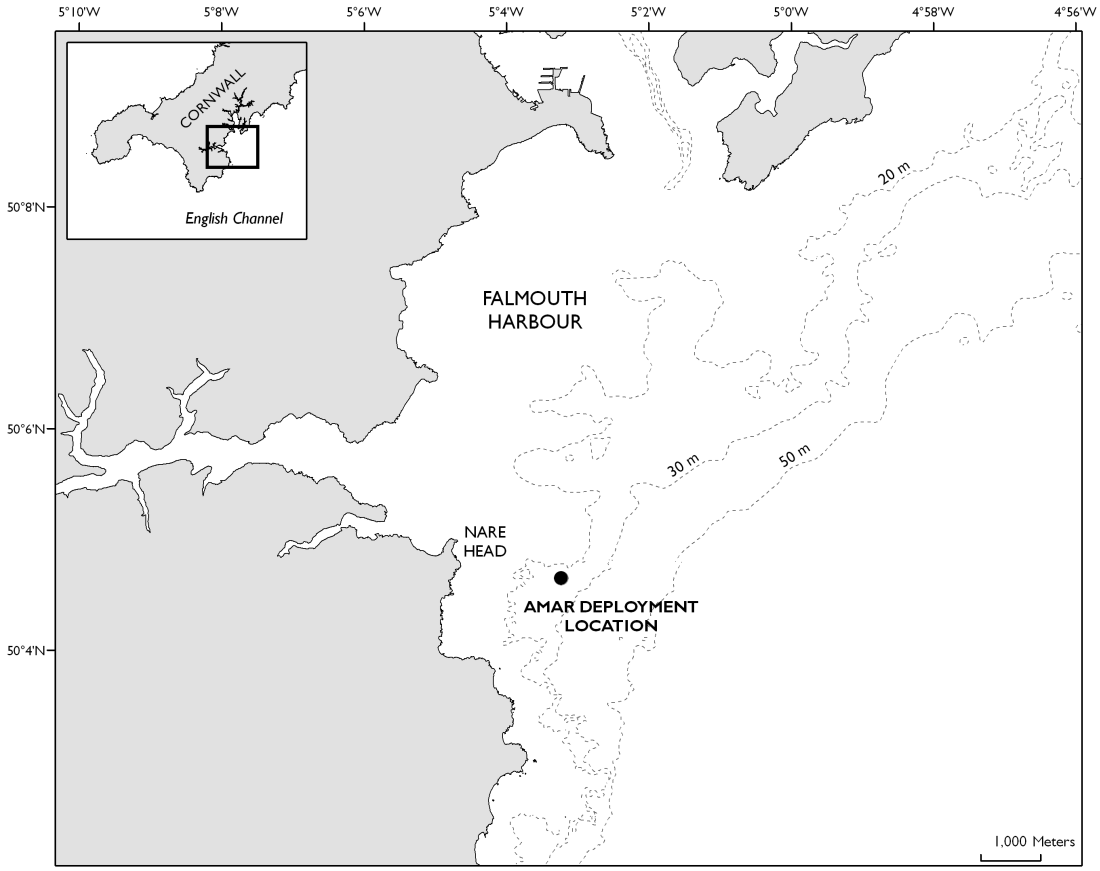

Figure 4.1: Deployment location: Falmouth Bay, UK.

4.1.2 Materials and methods

Deployment Location

Falmouth Bay (Fig. 4.1) is a large and deep natural harbour at the western entrance to the English Channel. The Channel is one of the busiest seaways in the world with around 45,000 ship transits annually (McQuinn et al., 2011). Traffic within the Bay consists of commercial shipping into Falmouth Harbour to the north, recreational boating, and activity related to bunkering (refuelling) of large vessels. The Bay is located just outside the western boundary of the North Sea Sulphur Emission Control Area (SECA), which came into effect in August 2007 (European Commission, 2005). This led to an increase in demand for low sulphur fuel at Falmouth, such that by 2008 commercial shipping traffic in the Bay had doubled (Dinwoodie et al., 2012). The latest published figures, from 2009, show total annual ship arrivals to Falmouth of 1,309 (Department for Transport, 2010).

Acoustic Data

An Autonomous Multichannel Acoustic Recorder (AMAR; Jasco Applied Sciences Ltd) was deployed in the Bay for 20 days between July 24 and August 13, 2010. It was positioned on a seabed of sand to muddy sand, 1.8 km offshore from Nare Head in waters ∼30 m deep. The AMAR was mounted on a custom-fabricated frame* containing an acoustically triggered pop-up buoy system, and was programmed to record continuously in 30-minute blocks, sampling at 16 kHz, using a GeoSpectrum M8E-132 hydrophone (effective bandwidth 5 Hz to 150 kHz). The frequency bandwidth of the recordings was therefore 5 Hz – 8 kHz.

Acoustic data were calibrated via the hydrophone sensitivity (-165 dB re 1 V μPa^{-1}) and the AMAR pre-amplifier gain (0 dB), then processed using custom-written MATLAB scripts. The power spectral density (PSD) was calculated using a 1-s Hann window with 50% overlap for each 30-minute measurement. 172 short (<1 s) bursts of system noise with exceptionally high amplitudes below 10 Hz were detected. These were purged using a frequency-sensitive noise gate. To reduce storage space, the mean PSD was then calculated in 60-s windows. The files were then concatenated to form a master file. This was used as the source file for the subsequent calculations of SPL and SEL (see below).

A 9 day period from 16:30 on July 24 to 16:30 on August 2 was selected for analysis. The remaining data were discarded since the signature of a single vessel dominated the acoustic spectrum from around 17:00 on August 2 onward, precluding analysis of surrounding shipping. The vessel was identified from AIS data as a 55-m tug within ∼1 km of the deployment site throughout the period from August 2 to (at least) August 13. Its presence may have been related to bunkering or other industrial activities in the Bay. This feature was considered anomalous and of limited relevance to other coastal areas.

Ancillary data

The Automatic Identification System (AIS) is a vessel-tracking system which operates on VHF radio bandwidth and can be detected by land-based receivers. AIS transceivers are compulsory for vessels exceeding 300 GT (gross tonnes) according to the International Convention for the Safety of Life at Sea (SOLAS) (IMO, 2000). AIS data for the duration of the deployment period were provided by a Web-based ship-tracking network (http://www.shipais.com/). This covered the area 48.0–51.0°N / 1.0–7.0°W, and included good coverage of Falmouth Bay and the surrounding area (see below). Hourly wind speed and rainfall data from the Culdrose weather station, 14 km to the west of the deployment location, were provided by the UK Met Office.

*The hydrophone was ∼1 m above the seabed.

Calculation of sound pressure level and sound exposure level

Sound pressure level (SPL) is the mean square pressure expressed in decibels relative to a reference pressure. The mean square pressure, Q, is given by

$$Q = \frac{1}{T}\int_0^T q^2(t)dt \tag{4.1}$$

where T is the integration time (the time over which the mean is calculated), and $q(t)$ is the instantaneous acoustic pressure at time t (Ainslie, 2009). The SPL is then

$$\text{SPL} = 10\log_{10}\left(\frac{Q}{p_{\text{ref}}^2}\right) \tag{4.2}$$

In underwater acoustics, p_{ref} is a reference pressure of 1 μPa at a distance of 1 m. The units of SPL are then dB re 1 μPa^2. Note that some authors express SPL in dB re 1 μPa; the levels are numerically equivalent (Ainslie, 2011).

An integration time of 300 s was used to calculate the SPL over a frequency bandwidth of 0.01–1 kHz. This bandwidth covers the nominal frequency range of commercial shipping noise (Tasker et al., 2010), and allowed comparison of recorded levels with relevant studies (e.g. Hatch et al., 2008; McKenna et al., 2012). The integration time was chosen such that the SPL varied over a similar timescale to the transmission rate of the AIS data (typically around 600 s). Reducing the time resolution of the acoustic data from 60 s to 300 s also reduced the temporal variability of the signal (smoothing). Consequently, ship passages were more likely to appear as unique local maxima in the SPL, rather than multiple maxima in the case of finer temporal resolution. This made it easier to identify ship passages from maxima in the SPL (see below).

The sound exposure level (SEL) is a cumulative measure of acoustic energy which allows the energy radiated by sounds of differing duration to be compared. It is a summation of multiple mean square pressures (consecutive or not) expressed in dB re 1 μPa^2 s:

$$\text{SEL} = 10\log_{10}\left(\frac{\int Q(t')dt'}{p_{\text{ref}}^2}\right) \tag{4.3}$$

where Q is the mean square pressure at time t', and p_{ref} is as above. The SEL for each 24-h period was calculated using an integration time of 300 s over the nominal frequency bandwidth of shipping (0.01–1 kHz) and the full recorded bandwidth (5Hz – 8kHz). The latter band-

width was included to assess the effect of higher frequency components on sound exposure levels.

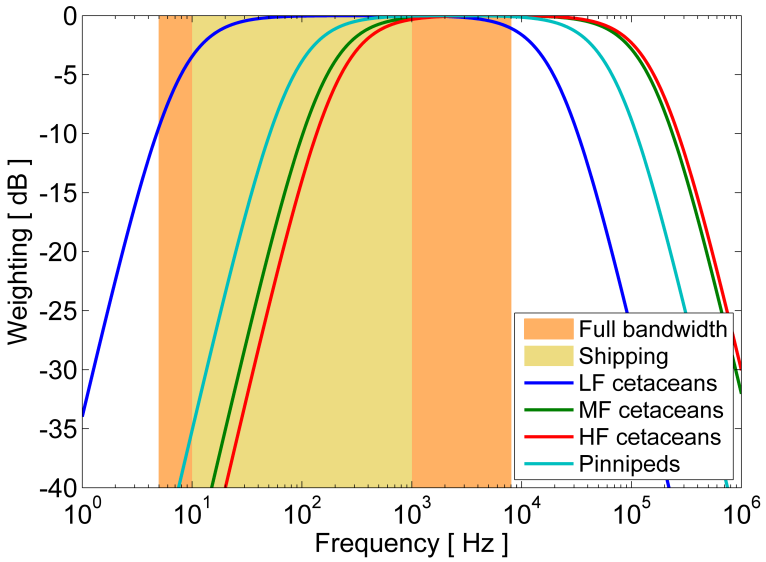

Figure 4.2: M-weightings for low-, medium- and high-frequency cetaceans and pinnipeds (in water) (Southall et al., 2007). The shaded areas indicate the frequency bandwidth of the recordings ('Full Bandwidth'; 5 Hz – 8 kHz) and the nominal frequency bandwidth of shipping noise ('Shipping'; 10 Hz – 1 kHz) used in this study for the calculation of SPL and SEL.

M-weightings

The M-weighted SEL for each 24-h period was also calculated. M-weightings are frequency weightings that can be applied to the SEL to adjust for the likely hearing sensitivity of marine mammals to high-amplitude acoustic sources (Southall et al., 2007). They are analogous to C-weightings used in terrestrial noise impact assessment for humans, and give an indication of the relative impact of noise sources on four broad functional hearing groups of marine mammals. The application of M-weightings to lower amplitude, chronic sources of noise is questionable since it is likely they overestimate the sensitivity of hearing (McQuinn et al., 2011). In this study, they are used as a notional indication of the relative impact of shipping noise on different marine mammal groups.

The M-weighting group most receptive to the nominal frequency range of shipping noise (0.01–1 kHz) is low-frequency cetaceans (baleen whales), followed by pinnipeds, mid- and high-frequency cetaceans (Fig. 4.2). Boats can emit significant levels of underwater noise above 1 kHz, particularly small vessels with outboard motors (Au and Green, 2000; McQuinn et al., 2011). To assess the contribution of these higher frequency components, the M-weighted levels over the full recorded bandwidth (5 Hz – 8 kHz) were also calculated.

Separation of intermittent ship noise from background

Intermittent ship noise was identified using an adaptive threshold. The threshold adapts to long-term variations in the broadband SPL while distinguishing short-term, relatively high-amplitude events. This enables the relative level of shipping noise exposure above the background to be determined. This was considered preferable to a fixed threshold, which would be insensitive to the temporal variability of ambient (background) noise and would have to be adjusted for different study areas due to the spatial heterogeneity of ambient noise. Another consideration is that ambient noise characteristics affect the degree of auditory masking (Clark et al., 2009) and are likely to influence behavioural responses to anthropogenic noise (Southall et al., 2007). The relative level of anthropogenic noise exposure is therefore a key metric in acoustic impact assessment (Ellison et al., 2012).

The adaptive threshold works on the assumption that the minimum recorded SPL over a given period is representative of the background noise level within that period. This period is the background window duration, W, which is chosen to be long enough that each window has data free from the noise source, and short enough to adapt to more gradual variations in ambient noise level. A tolerance above the minimum SPL, the threshold ceiling, C [dB], is then defined. As for W, C may be tailored for the application. The time-dependent adaptive threshold level, ATL(t), for a time-dependent SPL, SPL(t), is then:

$$\mathrm{ATL}(t) = \min\left[\mathrm{SPL}(t)\right]_{t-W/2}^{t+W/2} + C \tag{4.4}$$

where ATL(t) has units of dB re 1 μPa^2. In other words, ATL(t) is C decibels above the minimum recorded SPL within a rolling time window of duration W centred on time t.

In this study, W was set to 3 hours and C to 6 dB (i.e. double the minimum level). This value of W was necessary because of sustained periods of local shipping noise with durations approaching 3 hours. C was selected by experimentation and for simplicity: it was found to effectively distinguish background and intermittent contributions to the 24-h SEL (see below).

Data above the threshold were classed 'intermittent', data below the threshold 'background'. Maxima in the intermittent SPL data were detected for subsequent comparison to AIS data (see below). The intermittent and background SELs were then calculated for each 24-h period. An estimate of the SEL in the absence of intermittent data was also made. This was calculated by substituting the intermittent data with the median background level computed with a rolling 3-h window.

Spatial distribution of peak-generating ships

To assess the spatial distribution of ships generating intermittent peaks in the SPL, a graphical user interface (GUI) was designed in MATLAB. The GUI allows the operator to analyse each peak in the intermittent SPL with reference to figures displaying the tracks of AIS transmissions, the calibrated spectrogram, and the broadband SPL for a two-hour window centred on the SPL peak.

Firstly, the distance of each AIS transmission from the deployment location was calculated from its latitude and longitude coordinates. Transmissions within 50 km were plotted against time, linking data points from the same vessel (identified in the AIS log by a unique Maritime Mobile Service Identity (MMSI) number). The closest points of approach (CPAs) of each vessel were then computed geometrically, assuming each vessel maintained a direct course and constant speed between AIS transmissions (the transmission rate is typically around 10 minutes, although this can vary).

For each peak in the intermittent SPL, CPAs within a 15-minute window centred on the peak (i.e. $\pm$7.5 minutes) were considered. This assumes that CPAs coincide with peak SPLs, allowing a tolerance of $\pm$1 SPL data point (each of which comprises 5 minutes). Since acoustic propagation loss generally increases with distance (Urick, 1983) and the horizontal directionality of radiated ship noise appears maximal at broadside aspect (Arveson and Vendittis, 2000; Trevorrow et al., 2008), this was considered a reasonable assumption.

Finally, the spectrogram was consulted to confirm whether SPL peaks were due to ship signatures and not, for example, wind noise. These are readily distinguished by the tonal components present in ship noise signatures. Each SPL peak was then categorised as being uniquely identified (one CPA), due to multiple possible sources (more than one CPA), or unidentified (no CPA). The coordinates of each uniquely identified CPA were then recorded.

4.1.3 Results

Ambient noise spectrum and weather data

The ambient noise field was punctuated by wide bands of intermittent noise, some of which spanned the entire frequency range (Fig. 4.3). These were attributable to shipping (see below). The spectral energy of intermittent noise events was concentrated in the frequency range 0.01–1 kHz, which supports the use of this nominal bandwidth for shipping noise assessment.

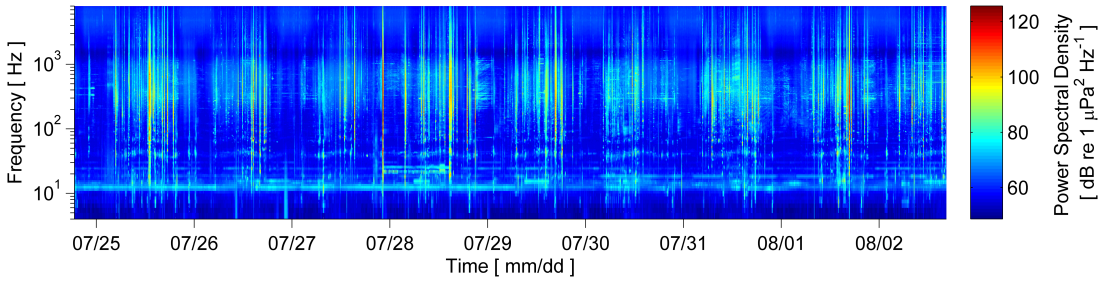

Figure 4.3: Power spectral density for 9 days of continuous monitoring. Frequency bandwidth 5 Hz – 8 kHz, integration time 300 s.

Mean hourly wind speeds at the Culdrose weather station ranged from 2 to 17 knots (1.0–8.7 m s^{-1}), with a maximum hourly increase of 6 knots (3.1 m s^{-1}). Wind speeds in this range have been associated with variations of up to around 20 dB in shallow water ambient noise levels (Urick, 1983). Spectra characteristic of wind noise did not feature in the frequency spectrum of the intermittent component, which was reviewed visually. This implies that either the wind-generated noise was below the adaptive threshold, meaning that the rate of increase in broadband (0.01–1 kHz) SPL due to wind did not exceed 6 dB per 1.5 hours (4 dB per hour), or that any rapid increases in wind speed were masked by local vessel activity. Rainfall was recorded at Culdrose in 12 hours of data over the 9 day period, with a maximum rate of 0.8 mm per hour. Since rain generates noise at frequencies above 1 kHz (Nystuen, 2001), it was not considered to contribute to the broadband (0.01–1 kHz) levels used for noise classification.

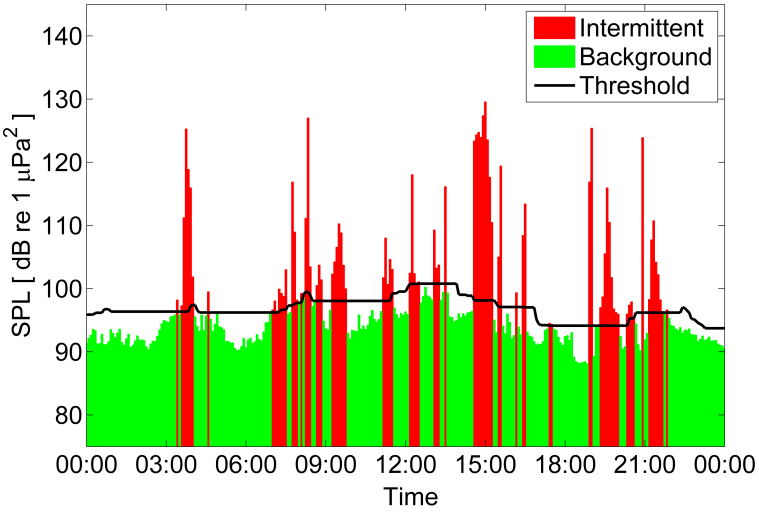

Figure 4.4: Broadband (0.01–1 kHz) SPL for a representative 24-h period (28 July) showing classification of 'intermittent' and 'background' data. Integration time: 300 s. The solid line is the adaptive threshold level.

Sound pressure levels

Overall, broadband (0.01–1 kHz) SPLs ranged from 86.1 to 148.6 dB re 1 μPa^2. The SPL was above the threshold level ('intermittent') 29% of the time, and below 71% ('background'). SPLs from a representative day are presented in Fig. 4.4.

The median threshold level was 96.2 dB re 1 μPa^2, with a range of 10.6 dB. Intermittent peaks in the SPL ranged from 92.8 to 148.6 dB re 1 μPa^2, and exceeded the threshold by a median of 6.4 dB. In total, there were 314 peaks in the intermittent SPL data (mean: 34.9 per day).

	Nominal shipping bandwidth (10 Hz – 1 kHz)		**Full bandwidth (5 Hz – 8 kHz)**	
	Median 24-h SEL (± range) (dB re 1 μPa^2 s)	Maximum 24-h SEL (dB re 1 μPa^2 s)	Median 24-h SEL (± range) (dB re 1 μPa^2 s)	Maximum 24-h SEL (dB re 1 μPa^2 s)
Unweighted				
24-h total	157.0 ± 19.1	173.9	158.3 ± 17.9	174.3
Intermittent	156.9 ± 19.4	173.9	157.9 ± 18.5	174.3
Background	141.1 ± 3.9	143.5	147.4 ± 1.8	148.5
24-h background	142.6 ± 3.4	145.0	149.1 ± 1.4	150.2
Low-frequency cetaceans				
24-h total	157.0 ± 19.1	173.9	158.2 ± 17.9	174.3
24-h background	142.5 ± 3.5	145.0	148.8 ± 1.5	150.0
Mid-frequency cetaceans				
24-h total	155.2 ± 18.7	171.7	156.9 ± 17.0	172.1
24-h background	141.6 ± 3.6	144.0	148.8 ± 1.3	149.8
High-frequency cetaceans				
24-h total	154.5 ± 18.5	170.8	156.3 ± 16.5	171.3
24-h background	141.2 ± 3.6	143.6	148.6 ± 1.3	149.6
Pinnipeds				
24-h total	156.3 ± 19.1	173.1	157.7 ± 17.6	173.5
24-h background	142.1 ± 3.6	144.6	149.0 ± 1.4	150.0

Table 4.1: Median and maximum 24-h SELs, calculated from 9 consecutive 24-h periods. '24-h background' is the estimated 24-h SEL in the absence of intermittent noise events.

Sound exposure levels

The broadband SEL for each 24-h period between 16:30 on July 24 and 16:30 on August 2 was calculated over the frequency ranges 0.01–1 kHz (nominal shipping bandwidth) and 5 Hz – 8 kHz (full bandwidth). The median and maximum SELs are presented in Table 4.1. Over both frequency ranges, the total SEL was dominated by the contribution of the

intermittent component. This was especially the case over the nominal shipping bandwidth, where the median total SEL was 14.4 dB greater than the estimated level in the absence of the intermittent events ('24-h background'). In the 24-h period with maximal total SEL (27–28 July), the intermittent component (27% of the time series in this period) raised the SEL in this frequency range by 28.9 dB above the 24-h background level.

The median 24-h SEL was concentrated above ~100 Hz, with a broad peak at 315 Hz [Fig. 4.5(a)]. The intermittent component was most dominant between around 30 and 2,000 Hz [Fig. 4.5(a)]. The variability of the intermittent data [Fig. 4.5(c)] appears to account for the variability of the total 24-h SEL [Fig. 4.5(b)] above ~30 Hz. In contrast, the 24-h SEL of the background component was comparatively stable at all frequencies [Fig. 4.5(d)].

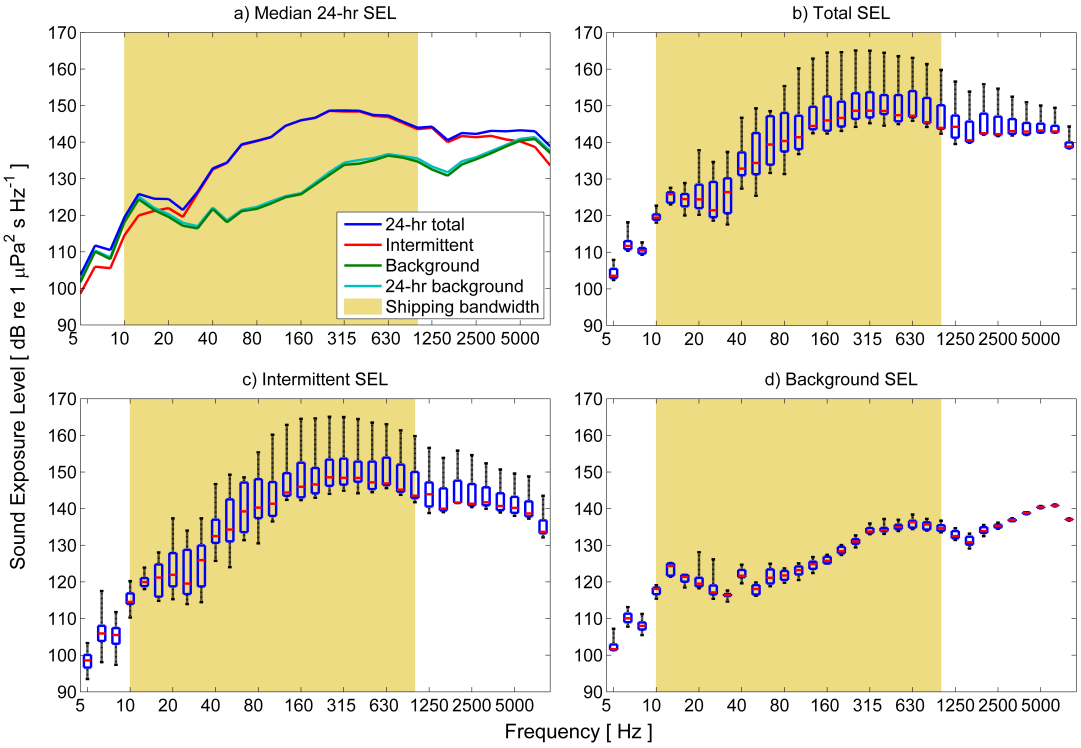

Figure 4.5: (a) Median 24-h SEL in third-octave bands, calculated from 9 consecutive 24-h periods. (b)–(d): total SEL and SEL due to intermittent and background components. The centre lines of the boxes denote the median and the box limits indicate the first quartile. The whiskers are the maximum and minimum values recorded. The shaded areas indicate the nominal bandwidth of shipping noise (0.01–1 kHz)

Above around 2 kHz, the median background levels rose [Fig. 4.5(d)]. Consequently, the background SELs across the two frequency bandwidths differed by ~5 dB (since only the full bandwidth SEL included this component; Table 4.1). This high frequency component

was the least variable part of the background sound exposure [Fig. 4.5(d)], and consisted of impulsive noise exhibiting a diurnal periodicity with maxima during the night (Merchant et al., 2011). It is probable that this noise was produced by snapping shrimp: these decapods generate characteristic impulses with peak frequencies in this range (Au and Banks, 1998; Radford et al., 2008). Two species of snapping shrimp have been documented in coastal waters to the east of the deployment site: *Alpheus glaber* near Plymouth (Holme, 1966) and *Alpheus macrocheles* further east around Weymouth (Holme, 1966; Hinz et al., 2011). There have also been unpublished reports of *Alpheus macrocheles* caught by fishermen in Falmouth Bay.

As expected, the M-weighting for low-frequency cetaceans yielded the highest SELs, followed by pinnipeds, mid- and high-frequency cetaceans (Table 4.1). The M-weighted SEL for low-frequency cetaceans was equivalent to the unweighted level: this weighting is flat in the range 0.1–1 kHz (Fig. 4.2) where the SEL was concentrated [Fig. 4.5(a)]. The M-weighted full-bandwidth total SELs were only marginally higher (1.2–1.8 dB) than for the nominal shipping bandwidth (Table 4.1), reflecting the concentration of shipping noise between 0.1 and 1 kHz in this study. In contrast, the full-bandwidth background SELs were 6.3–7.4 dB higher due to the high frequency contribution of impulsive noise.

In summary, the 24-h SEL comprised a stable background component (71% of the time series) and a more variable intermittent component (29%). The SEL of this intermittent component determined the magnitude and variability of the total SEL.

Spatial distribution of peak-generating ships

Peak-generating ships were identified manually using a GUI which displayed the AIS and acoustic data as shown in Fig. 4.6. Each of the peaks in the broadband SPL was categorised as uniquely identified, due to multiple ship sources, or unidentified, based on the number of CPAs within ±7.5 minutes of the peak. For example, in Fig. 4.6 the intermittent peak at 01:50 was classed as uniquely identified and attributed to the vessel 212032000. The previous peak at 01:30 was unidentified as there were no CPAs within its 15-minute window.

The AIS coverage of the Falmouth Bay area was not continuous throughout the deployment, and data were unavailable for 126 of the 314 peaks recorded. Of the remaining 188 peaks, 59 (31%) were classed as uniquely identified, 61 (32%) as due to multiple possible sources, and 68 (36%) as unidentified. Visual inspection of each plot suggested that 18 of the uniquely identified peaks could not unambiguously be attributed to individual CPAs, and were instead attributed to multiple ship sources. These 'false positives' were typically due to substantial shipping activity closer to the deployment than the identified vessel. A further 5 peaks having two CPAs in the 15-minute window were clearly attributable to one of the CPAs. All 5 cases

involved large (>77-m length) commercial vessels close to the deployment. Figures showing these 5 cases and 3 examples of false positives are presented in the supplementary material. The classification of peaks was then 46 (24%) uniquely identified, 74 (40%) due to multiple ship sources, and 68 (36%) unidentified.

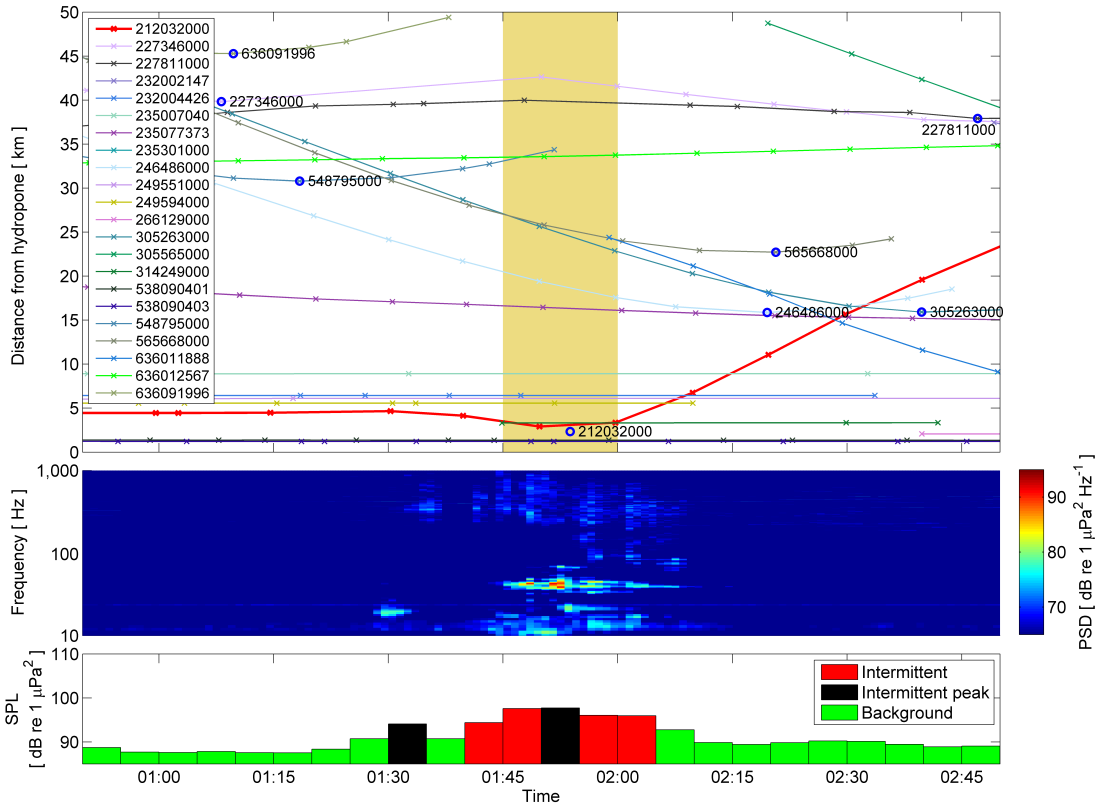

Figure 4.6: Example of ship identification using AIS data[‡]. *Top*: Range from hydrophone vs. time. Crosses denote individual AIS transmissions; lines connect transmissions from the same vessel; circles indicate closest points of approach, labelled with the MMSI number. Shaded area denotes 15-minute time window around SPL peak at 01:50; heavy line indicates track of vessel identified as source of peak. Note that the horizontal lines indicate AIS transmissions from stationary vessels. *Middle*: Power spectral density of concurrent acoustic data. *Bottom*: Broadband (0.01–1 kHz) SPL, showing 'background', 'intermittent', and 'intermittent' peaks.

Of the uniquely identified vessels, 24 were cargo ships, 13 were tankers and the remaining 9 consisted of 3 fishing boats, 2 military vessels, a research vessel, a pilot vessel, a recreational craft and an icebreaker. Peak broadband (0.01–1kHz) SPLs attributed to these vessels ranged from 92.8 to 148.6 dB re 1 μPa^2, with CPAs between 0.18 and 34.1 km from the hydrophone. Potential sources of the unidentified peaks include vessels less than 300 GT not transmit-

[‡]Vessel identified is 212032000, whose CPA coincides with the peak in broadband SPL. Note that the previous SPL peak coincides with the same vessel accelerating from rest.

ting AIS signals, ship noise unrelated to the passage of ships (engine activity, manoeuvring, bunkering operations, etc.), and vessels outside the 50 km range considered.

The coordinates of uniquely identified CPAs were distributed within Falmouth Bay and further south into the English Channel (Fig. 4.7). The largest cluster of CPAs to the east of the deployment corresponds to the paths of vessels entering and leaving Falmouth Harbour and the Bay. A second cluster ∼15 km south of the deployment site corresponds to paths of vessels navigating along the coast past the headland at Lizard Point. Small vessels were distributed within the Bay close to the deployment site, while the main shipping routes were populated by tankers and cargo ships. The tanker furthest west in the English Channel appears to have been falsely identified as the coast obscures the line of sight to the hydrophone. Error in the position of the CPA could also be the cause, since these were calculated assuming constant speed and direct trajectories between AIS transmissions.

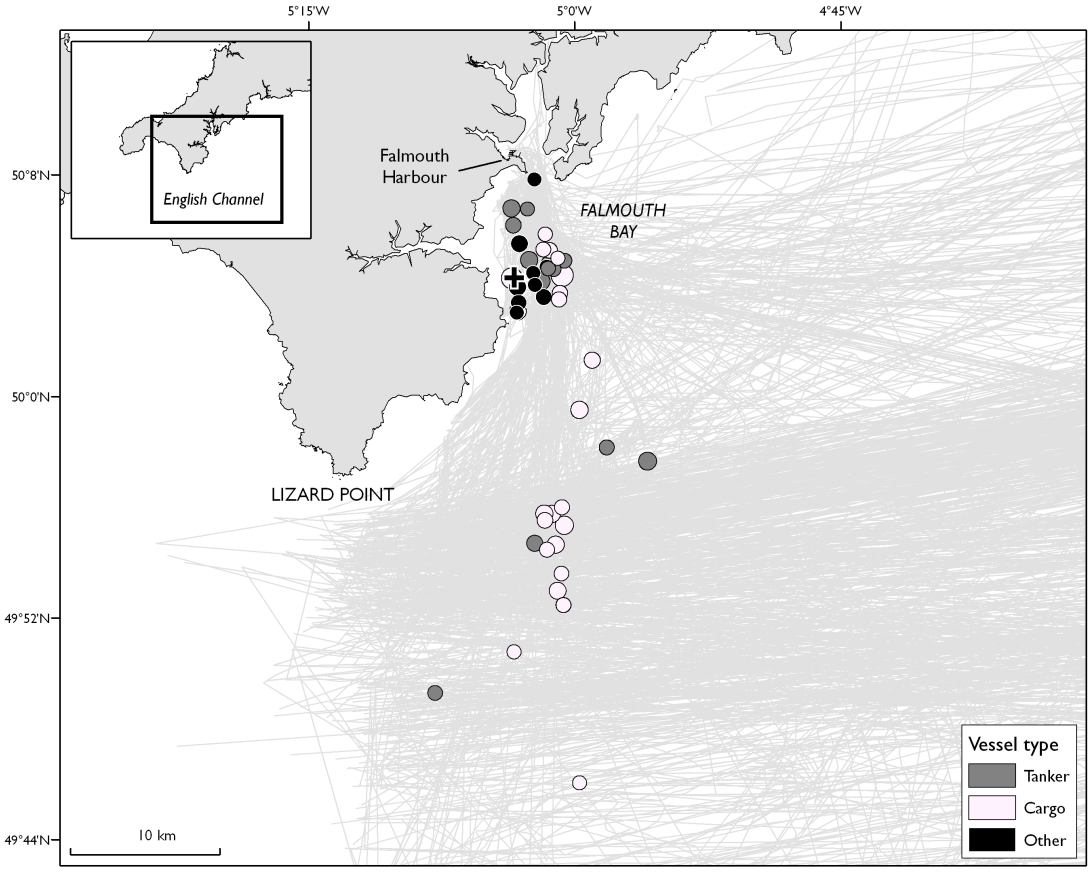

Figure 4.7: Positions of uniquely identified CPAs categorised by vessel type. The size of each circle corresponds to the magnitude of the associated SPL peak, ranging from 92.8 to 148.6 dB re 1 μPa^2. Cross denotes the location of the deployment. Lines indicate paths of AIS transmissions during the deployment period.

4.1.4 Discussion

The assessment of shipping noise in coastal waters is complicated by the presence of both intermittent noise from local vessel traffic and ambient noise from distant shipping. We have shown that these two components are clearly distinguished by the nature of their contribution to the 24-h SEL, and can be separated by applying an adaptive threshold to the sound pressure level. Intermittent ship noise produced a variable, high amplitude component [Fig. 4.5(c)] which determined the magnitude and variability of the total 24-h SEL [Fig. 4.5(b), Table 4.1]. A lower amplitude 'background' component remained stable over the 9 days analysed [Fig. 4.5(d)].

Analysing the sound exposure in this way makes it possible to assess both the absolute sound exposure at the deployment location and the contribution of intermittent shipping noise relative to background levels. In the nominal frequency range of shipping noise (0.01–1 kHz), we recorded a median 24-h SEL of 157.0 dB re 1 μPa^2 s compared to an estimated 142.6 dB re 1 μPa^2 s in the absence of intermittent shipping noise. Both elements are necessary to inform the investigation of chronic noise exposure on marine species (Ellison et al., 2012). Absolute SELs in representative marine habitats can be used in controlled studies of noise exposure (e.g. Codarin et al., 2009; Purser and Radford, 2011), while relative levels are needed to understand the relative impact of anthropogenic sources on the marine acoustic environment.

It is important to note that background levels are likely to be heightened by shipping noise below the level of the adaptive threshold applied to the SPL time series. The background level should therefore be understood as the estimated level in the absence of significant local shipping activity, not in the absence of shipping noise *per se*. In this study the 24-h SEL was determined by the intermittent component which constituted 29% of the time series. The intermittent component may be less dominant in coastal areas with a lower density of local shipping, and where there are fewer large commercial vessels.

By relating the acoustic data to the CPAs of AIS-transmitting vessels, it was possible to account for 64% of peaks in the intermittent SPL for which AIS data were available as being due to shipping. 24% of peaks appeared to be uniquely attributable to individual vessel passages. The spatial distribution of uniquely identified vessels (Fig. 4.7) indicates that the majority were large commercial vessels transiting either along the northern side of the English Channel or into Falmouth Bay. Although relatively few small vessels were identified, these may constitute only a small proportion of the small vessel fleet operating in the Bay, since AIS transceivers are only mandatory for vessels over 300 GT. The absence of these vessels from the AIS data may partially account for the 36% of peaks which remained unidentified.

Several factors limited the identification of ship sources of noise in the study area. Firstly, the density of shipping within a 50 km radius was high: multiple potential ship sources were identified for 40% of peaks, and manual oversight was necessary to detect ambiguous identifications, preventing automation of the technique. Secondly, it was clear that many vessels were mooring in Falmouth Bay, possibly for bunkering services. This meant it was often not possible to determine the CPA, and that ship noise not associated to CPAs such as manoeuvring, bunkering activity and idling was detected but could not be uniquely attributed to vessels by this method. Consequently, it is suggested that this method may be more successful in locations where most shipping traffic is transiting the deployment site, or where the density of shipping is lower.

One application of this approach could be for site-specific assessment of shipping noise in designated regions such as Marine Protected Areas (MPAs). There is evidence that current exclusion zones in MPAs deemed acoustically sensitive may be insufficient (Agardy et al., 2007; Haren, 2007; Hatch and Fristrup, 2009), and several authors have recommended the use of buffer zones in addition to exclusion zones (Hatch et al., 2008; Codarin et al., 2009; Wright et al., 2011). Since many MPAs are located in coastal waters (Toropova et al., 2010), where land-based receivers can track AIS transmissions of vessels, this assessment technique could be used to measure the spatial distribution of significant ship noise sources. This would help to prioritise shipping noise mitigation strategies, such as ship-quieting, speed restrictions and rerouting of shipping lanes, leading to more informed environmental management of shipping noise pollution.

The shipping noise recorded in Falmouth Bay was predominantly within the nominal frequency range of shipping [0.01–1 kHz; Fig. 4.3, Fig. 4.5(c)], and the inclusion of higher frequencies (up to 8 kHz) resulted in total SELs only $\sim$1 dB higher (Table 4.1). However, the peak frequency of sound exposure from intermittent ship noise (315 Hz) was considerably higher than that of reported source spectra for large commercial vessels, which are typically around 100 Hz or below (Arveson and Vendittis, 2000; Wales and Heitmeyer, 2002; McKenna et al., 2012). Propagation of sound in shallow water is subject to high attenuation at both high and low frequencies (Jensen et al., 2011), and favourable propagation at mid-frequencies may partly explain the spectral composition of noise observed. A more significant factor is likely to be the composition of the shipping fleet contributing to underwater noise, which may have included more small vessels than were indicated by the AIS data.

Received SPLs of transiting vessels were comparable to previous studies. Peak SPLs of uniquely identified CPAs were between 92.8 and 148.6 dB re 1 μPa^2 for CPAs ranging from 0.18–34.1 km. McKenna et al. (2012) reported received levels of noise from 29 commercial ves-

sels of 106.0–117.9 dB re 1 μPa^2 for CPAs at distances of 2.6–3.5 km over a similar frequency range (0.02–1 kHz). Hatch et al. (2008) reported received levels ranging from 113–131 dB re 1 μPa^2 for CPAs between 0.4 and 3.4 km over a narrower frequency range (71–141 Hz). In both studies, the narrower range of received levels reflects the narrower range of CPAs.

The equivalence of the unweighted 24-h SEL and the M-weighted level for low-frequency cetaceans (Table 4.1) highlights the degree of overlap between likely baleen whale hearing ranges and the dominant frequencies of radiated ship noise. The received SPLs of vessels observed in Falmouth Bay (92.8–148.6 dB re 1 μPa^2) are within ranges at which baleen whales have been observed to exhibit behavioural responses, which are particularly acute above received SPLs of around 120 dB re 1 μPa^2 (Southall et al., 2007). Recent evidence points towards increased stress levels in right whales associated to shipping noise (Rolland et al., 2012), though the long-term consequences for baleen whales and other marine mammals of sustained exposure to shipping noise remain largely unknown.

The dominance of ship noise in the range 0.1–1 kHz also coincides with the frequencies of greatest hearing sensitivity for many fish species (Popper and Hastings, 2009a). The SPLs of ship passages observed in this frequency range (Fig. 4.3, Fig. 4.4) are at levels which may cause masking of communication in vocal fish species, as has been observed in several impact studies (e.g. Vasconcelos et al., 2007; Codarin et al., 2009). Exposure to ship noise may also have longer term effects associated to physiological stress responses (Wysocki et al., 2006) and reduced foraging efficiency (Purser and Radford, 2011).

In this study, the PAM device was mounted on the seafloor, which has potential drawbacks related to acoustic propagation. In shallow water, propagation is strongly affected by interactions with the seabed and varies with depth (Kuperman and Lynch, 2004). Consequently, the noise levels recorded by bottom-mounted PAM devices may differ from levels recorded elsewhere in the water column. The potential for these effects could be reduced by positioning the hydrophone in the water column suspended on a buoy.

There is increasing awareness of the potential for chronic exposure to shipping noise to have harmful impacts on marine ecosystems. Developing techniques to measure long-term sound exposure in coastal habitats is a necessary step towards understanding how these dynamic acoustic environments affect marine fauna. Our results suggest that by using continuous acoustic monitoring to determine the 24-h sound exposure level, the contribution of intermittent shipping to underwater noise levels can be assessed with greater clarity. Further work is needed to establish the efficacy of this approach in other coastal environments. The method we present of analysing the spatial distribution of ship contributions to noise exposure using

AIS data could be used to inform the prioritisation of mitigation strategies in acoustically sensitive areas.

Acknowledgements

NDM is funded by an EPSRC Doctoral Training Award (#EP/P505399/1). BJG and GHS are funded by NERC, PRIMaRE and the South West Regional Development Agency. We gratefully acknowledge I. McConnell for providing the AIS log, L. Johanning, D. Parish and D. Raymond for assisting with the deployment and for access to the deployment site, and Falmouth Harbour Commissioners for their continued support.

4.2 Monitoring Ship Noise to Assess the Impact of Coastal Developments on Marine Mammals

The potential impacts of underwater noise on marine mammals are widely recognised, but uncertainty over variability in baseline noise levels often constrains efforts to manage these impacts. This paper characterises natural and anthropogenic contributors to underwater noise at two sites in the Moray Firth Special Area of Conservation, an important marine mammal habitat that may be exposed to increased shipping activity from proposed offshore energy developments. We aimed to establish a pre-development baseline, and to develop ship noise monitoring methods using Automatic Identification System (AIS) and time-lapse video to record trends in noise levels and shipping activity. Our results detail the noise levels currently experienced by a locally protected bottlenose dolphin population, explore the relationship between broadband sound exposure levels and the indicators proposed in response to the EU Marine Strategy Framework Directive, and provide a ship noise assessment toolkit which can be applied in other coastal marine environments.

4.2.1 Introduction

Underwater noise levels in the open ocean have been rising for at least the last five decades due to increases in shipping (McDonald et al., 2006; Chapman and Price, 2011) correlated to global economic growth (Frisk, 2012). Closer to shore, escalations in human activity, including shipping, pile driving and seismic surveys, have transformed coastal marine soundscapes (Richardson et al., 1995; Hildebrand, 2009) with uncertain consequences for the ecosystems that inhabit them.

These large-scale changes in the acoustic environment are of particular concern for marine mammals (Tyack, 2008), which rely on sound as their primary sensory mode. There is growing evidence that marine mammals perceive anthropogenic noise sources as a form of risk, which is then integrated into their ecological landscape and affects their decision-making process (Tyack, 2008). Noise also has the potential to mask important acoustic cues in marine mammal habitats, such as echolocation and communication (Erbe, 2002; Jensen et al., 2009), and may disrupt their prey (Popper et al., 2003) affecting foraging. These anthropogenic pressures may lead to physiological stress (Wright et al., 2007a; Rolland et al., 2012), habitat degradation, and changes in behaviour (Nowacek et al., 2007) including evasive tactics (Williams et al., 2002; Christiansen et al., 2010) and heightened vocalisation rate (Buckstaff, 2004) or duration (Foote et al., 2004). The cumulative cost of these responses can alter the animals' activity budget (Lusseau, 2003) and energy balance, which may have downstream consequences for individual vital rates (e.g. survival or reproductive success) and, ultimately, population dynamics. Efforts are underway to develop a framework to predict such population consequences of acoustic disturbance (PCAD; National Research Council, 2005).

Detailed investigation of these chronic and cumulative effects will require longitudinal studies of ambient noise trends in marine habitats and concurrent assessment of marine mammal fitness and population levels. However, long-term ambient noise data (on the scale of several or more years) are limited to the Northeast Pacific (e.g. McDonald et al., 2006; Chapman and Price, 2011) and data for other ocean basins and coastal regions are few and comparatively brief (e.g. Moore et al., 2012; Širović et al., 2013). In the European Union (EU), a regulatory framework which seeks to rectify this knowledge deficit is currently developing guidelines for ambient noise monitoring (European Commission, 2008; Tasker et al., 2010; Van der Graaf et al., 2012). The Marine Strategy Framework Directive (MSFD) will ascertain baseline noise levels and track year-on-year trends with a view to defining and attaining 'Good Environmental Status' in EU territorial waters by 2020. There is no specific requirement for long-term monitoring of the acoustic impact of human activities on marine mammal populations, though a proposed register of high-amplitude impulsive noise (e.g. pile driving, seismic surveys) could act as a proxy indicator of high-amplitude acoustic disturbance (Van der Graaf et al., 2012). For ambient noise (including noise from shipping), current recommendations are to monitor two 1/3-octave frequency bands (63 and 125 Hz), targeting areas of intensive shipping activity (Van der Graaf et al., 2012). Consequently, many key marine mammal habitats may not be included in monitoring programs. While such habitats may sustain less pressure from anthropogenic noise, they may, nevertheless, be more vulnerable to increases in underwater noise levels (Heide-Jørgensen et al., 2013).

This study characterises baseline noise levels in the inner Moray Firth, a Special Area of Con-

servation (SAC) for a resident population of bottlenose dolphins (*Tursiops truncatus*), and an important habitat for several other marine mammal species. The Moray Firth also provides an important base for the development of oil and gas exploration in the North Sea, and there are now plans to develop this infrastructure to support Scotland's expanding offshore renewables industry (Scottish Government, 2011). These developments will increase recent levels of vessel traffic to fabrication yards and ports within the SAC such as those at Nigg and Invergordon (New et al., 2013) and at the Ardersier yard (Fig. 4.8). Establishing current baseline levels will enable future noise monitoring to quantify the acoustic consequences of this expected increase, supporting analyses of any associated effects on marine mammal populations. In characterising key contributors to underwater noise levels in the SAC, we also advance methods for ship noise monitoring by combining Automatic Identification System (AIS) ship-tracking data and shore-based time-lapse video footage, and explore whether underwater noise modelling based on AIS data could accurately predict noise levels in the SAC. These methods can be applied in other other coastal regions to evaluate the contribution of vessel noise to marine soundscapes. Finally, we explore whether noise levels in frequency bands proposed for the MSFD (63 and 125 Hz) are effective indicators of broadband noise exposure from shipping.

4.2.2 Methods

Study site

The inner Moray Firth was designated a Special Area of Conservation (SAC) for bottlenose dolphins under the European Habitats Directive (92/43/EEC), since at least part of the north-east Scotland population spends a considerable proportion of time in this area (Cheney et al., 2013). Long-term monitoring of the population's size suggests that it is stable or increasing (Cheney et al., 2013). Within the SAC, dolphins have been observed to use discrete foraging patches around the narrow mouths of coastal estuaries [Hastie et al., 2004; Bailey and Thompson, 2010; Pirotta et al., 2014)]. Other marine mammal species are also regularly sighted in the area: harbour seal (*Phoca vitulina*), harbour porpoise (*Phocoena phocoena*), grey seal (*Halichoerus grypus*), and, further offshore, minke whale (*Balaenoptera acutorostrata*) and other smaller delphinid species (Reid et al., 2003). In addition to the bottlenose dolphin SAC, six rivers around the Firth are SACs for Atlantic salmon (*Salmo salar*), while the Dornoch Firth is an SAC for harbour seals (Butler et al., 2008).

Two locations were selected for underwater noise monitoring: The Sutors (57° 41.15′ N, 3° 59.88′ W), at the entrance to the Cromarty Firth, and Chanonry (57° 35.12′ N, 4° 05.41′ W),

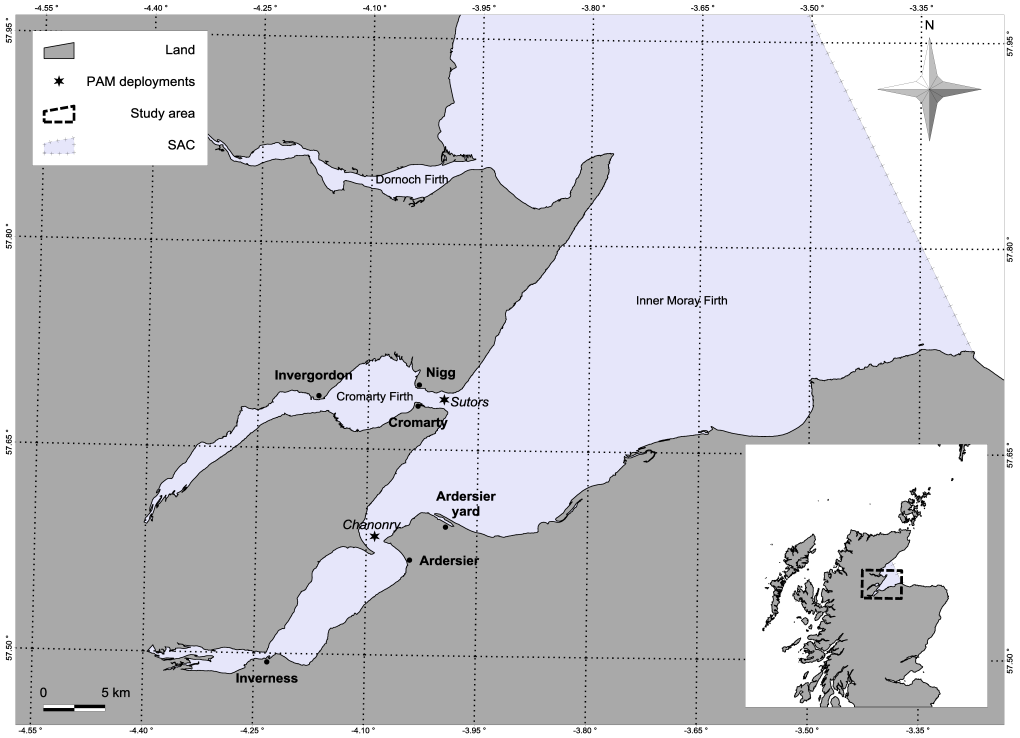

Figure 4.8: Map of study area. PAM units were deployed at The Sutors and Chanonry. Meteorological data for Chanonry were acquired from a weather station at Ardersier; time-lapse footage for The Sutors was recorded from Cromarty (see text).

to the southwest (Fig. 4.8). Both locations are deep narrow channels characterised by steep seabed gradients and strong tidal currents, heavily used by the dolphins for foraging [Hastie et al., 2004; Bailey and Thompson, 2010; Pirotta et al., 2014)]. The Sutors supports commercial ship traffic transiting in and out of the Cromarty Firth, while Chanonry is on the route to and from Inverness and to the west coast of Scotland via the Caledonian Canal (Fig. 4.9). Water depths at the deployment sites were 45 m (The Sutors) and 19 m (Chanonry). Proposed development of fabrication yards for offshore renewable energy at Nigg, Invergordon and Ardersier yard (Fig. 4.8) are expected to increase levels of ship traffic in the SAC.

Acoustic data

Several consecutive deployments of single PAM devices (Wildlife Acoustics SM2M Ultrasonic) were made at the two sites during summer 2012. The periods covered by the deployments are shown in Table 4.2. Gaps in the time series at The Sutors were caused by equipment malfunctions. Noise was monitored on a duty cycle of 1 minute every 10 minutes at a sampling rate of 384 kHz and 16 bits. This regime allowed for detection of ship passages with a

similar time resolution to the AIS data (∼10 minutes; see below) while also providing recordings of marine mammal sounds up to 192 kHz. Additionally, noise was recorded at 192 kHz, 16 bits during the remaining 9 minutes of the duty cycle. These data were only used for detailed analysis of illustrative events.

	Deployment	Start date	End date
The Sutors	1	13 Jun	07 Jul
	2	14 Jul	23 Jul
	3	07 Sep	27 Sep
Chanonry	1	20 Jul	10 Aug
	2	10 Aug	01 Sep

Table 4.2: Periods covered by successful PAM deployments at each site during summer 2012.

The PAM units were independently calibrated using a pistonphone in the frequency range 25–315 Hz. This calibration agreed with the manufacturer's declared sensitivity to within ±1 dB, and so the manufacturer's data were used for the entire frequency range (25 Hz – 192 kHz). Acoustic data were processed in MATLAB using custom-written scripts. The power spectral density was computed using a 1-s Hann window, and the spectra were then averaged to 60-s resolution using the standard Welch method (Welch, 1967), producing a single spectrum for each 1-minute recording. These were then concatenated to form a master file for subsequent analysis. Spectral analysis revealed low-amplitude tonal noise from the recording system at various frequencies above 1 kHz (Merchant et al., 2013). This system noise contaminated a small proportion of the frequency spectrum (<0.1%) and was omitted from the analysis. The analysis also showed that the noise floor of the PAM units was ∼47 dB re 1 μPa^2, exceeding background noise levels above ∼1.5 kHz. Although anthropogenic, biotic and abiotic sounds could still be detected and measured at these high frequencies, background noise levels above ∼1.5 kHz could not be determined.

Ancillary data

Automatic Identification System (AIS) ship-tracking data were provided by a Web-based ship-tracking network (http://www.shipais.com/) for the duration of the deployments (Fig. 4.9). Time-lapse footage was recorded at both sites using shore-based digital cameras (Brinno Gardenwatchcam™ GWC100) whose field of view included the PAM locations. One camera was positioned on the Lighthouse Field Station, Cromarty (The Sutors; 57° 40.98′ N, 4° 02.19′ W) and the other at Chanonry Point (57° 34.49′ N, 4° 05.70′ W; see Fig. 4.8).

Meteorological data were acquired for the Chanonry site from a weather station at Ardersier (∼4 km SE of deployment; Fig. 4.8) using the Weather Underground open-access database

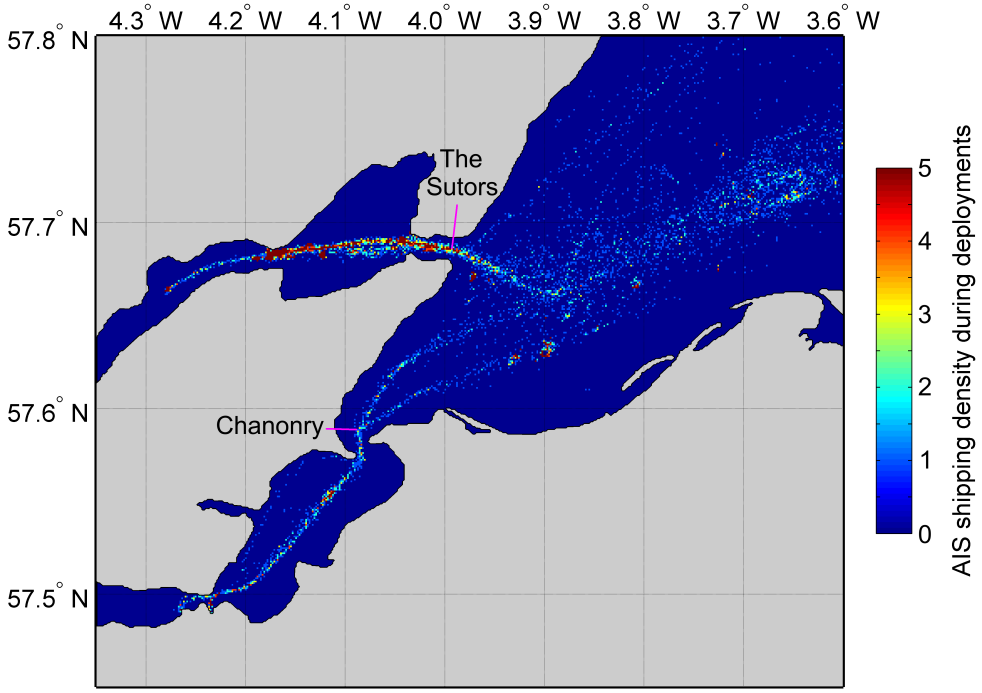

Figure 4.9: AIS shipping density in the inner Moray Firth for the duration of the deployments (13 June to 1 September 2012). Grid resolution: 0.1 km.

(http://www.wunderground.com/). The dataset included precipitation and wind speed measurements made at 5-min intervals. The POLPRED tidal computation package (provided by the National Oceanography Centre, Natural Environment Research Council, Liverpool, UK) was used to estimate tidal speeds and levels at 10-minute intervals (to match the acoustic data) in the nearest available regions to each site.

An autonomous underwater acoustic logger (C-POD, Chelonia Ltd., www.chelonia.co.uk) was independently deployed at each of the two sites as part of the bottlenose dolphin SAC monitoring programme (Cheney et al., 2013). C-PODs use digital waveform characterization to detect cetacean echolocation clicks. The time of detection is logged together with other click features, which are then used by the click-train classifier (within the dedicated analysis software) to identify bottlenose dolphin clicks. Here, the data from the C-PODs were used only to confirm dolphin occurrence at the two sites throughout the deployment periods. More detailed analysis is ongoing and will be reported elsewhere.

AIS data analysis

Peaks in the broadband noise level were attributed to AIS vessel movements using the tech-

nique developed by Merchant *et al*. (2012b). The method applies an adaptive threshold to the broadband noise level, which identifies brief, high amplitude events while adapting to longer-term variation in background noise levels. The adaptive threshold level (ATL) takes the form

$$\mathrm{ATL}(t) = \min\left[\mathrm{SPL}(t)\right]_{t-W/2}^{t+W/2} + C \tag{4.5}$$

where $\mathrm{SPL}(t)$ is the sound pressure level [dB re 1 μPa^2] at time t, W is the window duration [s] over which the minimum SPL is computed, and C is the threshold ceiling [dB], a specified tolerance above the minimum recorded SPL. In this study, a window duration of 3 hours and a threshold ceiling of 12 dB was used – a more conservative threshold than in previous work (3 hours, 6 dB; Merchant et al., 2012b) – in order to exclude persistent but variable low-level noise from the fabrication yard at Nigg (Fig. 4.8) which was not associated to vessel movements. A narrower frequency range (0.1–1 kHz, not 0.01–1 kHz) was also used to calculate the broadband noise level, since the spectrum below 100 Hz was contaminated by flow noise (see Section 3).

AIS analysis was only conducted for The Sutors, which had high (>80%) temporal coverage. Coverage at Chanonry was more sporadic, such that only a few illustrative examples could be produced. By comparing AIS vessel movements to the acoustic data, peaks in noise levels were classed as due to: (i) closest points of approach (CPAs) of vessel passages; (ii) due to other AIS vessel movements; (iii) unidentified. To compute the sound exposure attributable to each event, noise levels exceeding the adaptive threshold on either side of each peak were considered to form part of the same event.

4.2.3 Baseline noise levels

Chanonry

Ambient noise levels differed significantly between the two sites (Fig. 4.10). Compared to The Sutors [Fig. 4.10(b)], noise levels at Chanonry were relatively low, with only occasional vessel passages [Fig. 4.10(a)]. Variability in ambient noise levels at Chanonry was largely attributable to weather and tidal processes, as example data in Fig. 4.11 illustrate. Higher wind speeds were associated to broadband noise concentrated in the range 0.1–10 kHz [Fig. 4.11(a)–(b)], while a Spearman ranked correlation analysis [Fig. 4.11(d)] shows a broad peak with maximal correlation to wind speed at ∼500 Hz, consistent with the profile of wind

noise source levels (Wenz, 1962; Kewley, 1990). The influence of rain noise was less apparent, perhaps because of low rainfall levels during the deployment, though the peaks in rainfall rate appear to correspond to weak noise peaks at ∼20 kHz, which would agree with previous measurements (e.g. Ma and Nystuen, 2005).

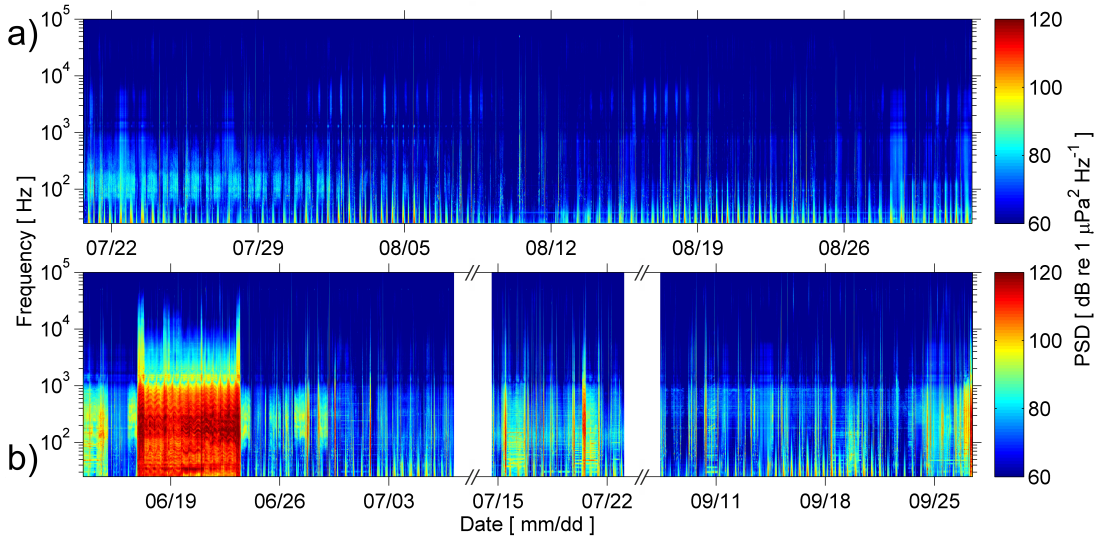

Figure 4.10: Ambient noise spectra: (a) Chanonry (b) The Sutors. Frequency range: 25 Hz–100 kHz; temporal resolution: 60 s.

Tide speed was correlated to noise levels at low and high frequencies [Fig. 4.11(d)]. The high (20–100 kHz) frequency component was attributable to sediment transport, which can generate broadband noise with peak frequencies dependent on grain size (Thorne, 1986; Bassett et al., 2013). Sublittoral surveys of the area show a seabed of medium sand, silt, shell and gravel in the vicinity of the deployment (Bailey and Thompson, 2010), which approximately corresponds to laboratory measurements of ambient noise induced by this grain size (Thorne, 1986). The low frequency component was caused by turbulence around the hydrophone in the tidal flow (Strasberg, 1979) known as flow noise, which is pseudo-noise (i.e. due to the presence of the recording apparatus) and not a component of the acoustic environment. Comparison of the tide speed [Fig. 4.11(c)] with the periodic low-frequency noise peaks in Fig. 4.11(a) shows that flow noise was markedly higher during the flood tide, possibly owing to fine-scale variations in tidal flow or the orientation of the PAM device in the water column. There was also a correlation to tide level at ∼6 kHz [Fig. 4.11(d)]. This may have been caused by wave action on the shingle beach near the deployment: at higher tides, waves can reach further up the beach face and displace more shingle, and the composition of shingle and incline also vary up the beach face.

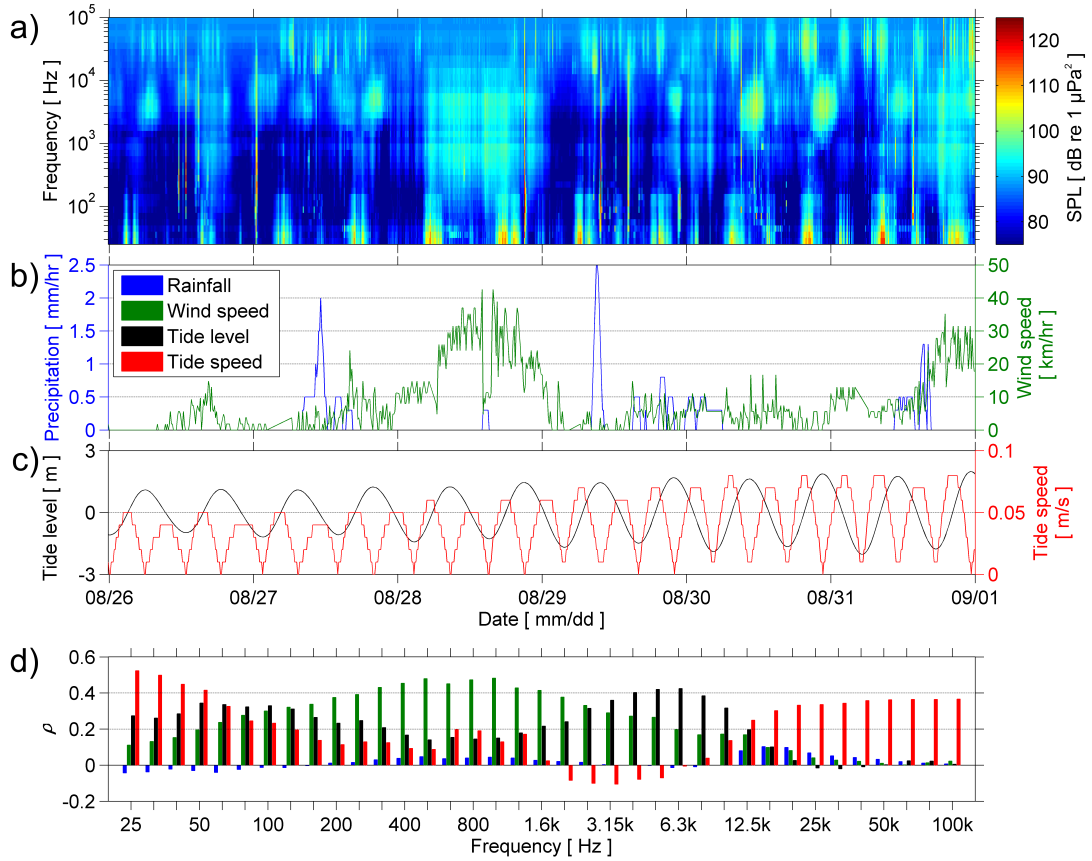

Figure 4.11: Effect of weather and tides on ambient noise in Chanonry. (a) 1/3 octave band spectrum from 26–31 August, 60-s resolution; (b) Rainfall and mean wind speed recorded at Ardersier; (c) Tide level and speed predicted by POLPRED model (d) Spearman ranked correlation coefficient of each process across frequency range for entire dataset.

The Sutors

Noise levels at The Sutors [Fig. 4.10(b)] were highly variable in the range 25 Hz–1 kHz, and the spectrum featured more frequent vessel passages (these appear as narrow, high-amplitude vertical lines with peaks typically between 0.1 and 1 kHz) than Chanonry [Fig. 4.10(a)]. There were also two instances of rigs being moored within or towed past The Sutors: firstly between 16–23 June, and the second at the end of the final deployment on 27 September [Fig. 4.10(b)]. The vessels towing and positioning the rigs [using dynamic positioning (DP)] produced sustained, high-amplitude broadband noise concentrated below ∼1 kHz.

The stronger influence of anthropogenic activity at The Sutors is also evident in the diurnal variability of noise levels recorded [Fig. 4.12(a)]. While the median noise levels at Chanonry were only weakly diurnal, the Sutors data show a marked rise in the range 0.1–1 kHz during

the day, corresponding to increased vessel noise. Mean levels [Fig. 4.12(b)] are largely determined by the loudest events (Merchant et al., 2012a), in this case particularly loud vessel passages, which were both louder [Fig. 4.12(b)] and more variable [Fig. 4.12(c)] at The Sutors. The week-long presence of rig-towing vessels evident in Fig. 4.10(a) was omitted from The Sutors data as this high-amplitude event entirely dominated the mean levels for The Sutors in Fig. 4.12(b). Note that the median levels [Fig. 4.12(a)] are likely to be raised by the noise floor of the PAM device above ~10 kHz (Merchant et al., 2013), and do not represent absolute values.

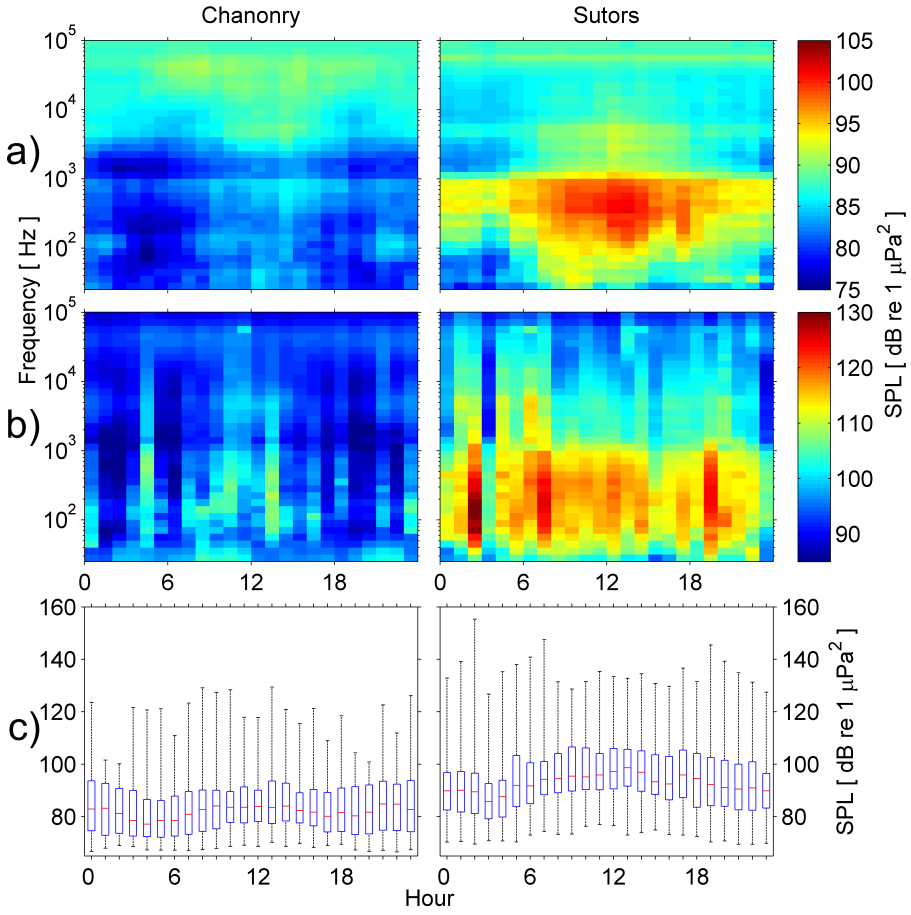

Figure 4.12: Hourly variability in noise levels at both sites in 1/3 octave bands. Left column: Chanonry; Right column: The Sutors. a) Median b) RMS Mean c) Broadband (0.1–1 kHz) level.

Bottlenose dolphin occurrence and vocalisations

The analysis of C-POD data confirmed that the two sites were heavily used by bottlenose dolphins throughout the deployment periods. The animals were present in both locations

every day (with the exception of 28 August in Chanonry) with varying intensity. The mean number of hours per day in which dolphins were detected was 8.3 (standard deviation = 4.8; range = 1–18) in The Sutors and 7.3 (standard deviation = 3.0; range = 0–15) in Chanonry.

Bottlenose dolphin vocalisations were also recorded on the PAM units [Fig. 4.13(a)]. There was considerable overlap between the frequency and amplitude ranges of vocalisations and ship noise observed, indicating the potential for communication masking. Sample spectra from Chanonry of a passing oil tanker [Fig. 4.13(b)] and bottlenose dolphin sounds [Fig. 4.13(a)] clearly illustrate that observed vocalisations in the range ~0.4–10 kHz coincide in the frequency domain with ship noise levels of higher amplitude during the vessel passage. Although underwater noise radiated by the vessel in Fig. 4.13(b) extends as high as the 50 kHz echosounder, masking at high frequencies is likely to be localised due to the increasing absorption of sound by water as frequency increases. This is apparent in the form of the acoustic signature: the highest frequencies are only visible at the closest point of approach (CPA), while low-frequency tonals are evident more than 30 min before the vessel transits past the hydrophone, when AIS data indicates it was 9 km away. Note also the upsurge in broadband (rather than tonal) noise following the CPA, as cavitation noise from the propeller becomes more prominent in the wake of the vessel. These effects can be observed more intuitively in the time-lapse footage (paired with acoustic and AIS data) documenting this passage included in the Supplementary Material.

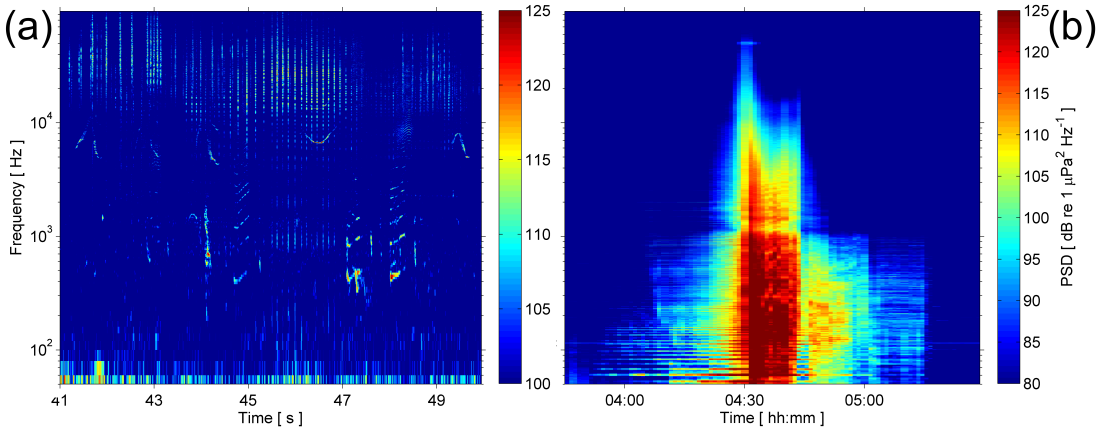

Figure 4.13: Sample spectra recorded at Chanonry. (a) Vocalisations and echolocation clicks of bottlenose dolphins on 12 Aug at 17:50. Spectra have the same frequency range but (a) has a finer amplitude range; (b) Oil tanker with closest point of approach (CPA) at 04:30 on 18 Aug.

Whether masking occurs and whether this has a significant impact will be context-dependent (Ellison et al., 2012) and will vary with the extent to which the signal-to-noise ratio of bio-

logically significant sounds is diminished by the presence of vessel noise (Clark et al., 2009), as well as the physiological and behavioural condition of the animals. Estimates of effective communication range (active space) for bottlenose dolphins in the Moray Firth range from 14 to 25 km at frequencies 3.5 to 10 kHz, depending on sea state (Janik, 2000). More detailed analysis would be required to model the extent to which vessel passages reduce this active space (e.g. Hatch et al., 2012).

4.2.4 Monitoring future ship noise trends

AIS analysis

Analysis of the AIS vessel movements in relation to peaks recorded in broadband (0.1–1 kHz) noise levels at The Sutors site identified 62% of peaks as due to AIS vessel movements, with 38% unidentified. This was a similar ratio to that reported by Merchant et al. (2012b), who observed a ratio of 64% identified to 36% unidentified in Falmouth Bay, UK. The 62% of peaks identified was composed of 52% attributed to vessel CPAs, with the remaining 10% due to other vessel movements such as acceleration from or deceleration to stationary positions. Fig. 4.14 shows an example ship identification of a 125-m vessel at its CPA; examples illustrating identification of a decelerating AIS vessel and an unidentified non-AIS vessel captured on time-lapse footage (see Section 4.2) are provided in the Supplementary Material.

Modelling underwater noise levels using AIS data has been proposed as a way to map noise exposure from shipping to enable targeted mitigation measures (Erbe et al., 2012). However, the efficacy of such an approach will depend on the proportion of anthropogenic noise exposure accounted for by vessels with operating AIS transmitters. Vessels below the current 300 GT gross tonnage threshold (IMO, 2000) not carrying AIS transceivers may also contribute significantly to noise exposure in some areas, and other sources of anthropogenic noise such as seismic surveys and pile driving may occasionally be more significant, though their spatiotemporal extent is generally more limited.

To investigate the feasibility of AIS noise modelling in the Moray Firth, the sound exposure attributable to AIS-identified and unidentified noise periods for each day of uninterrupted AIS coverage was calculated for The Sutors. These periods were computed as the cumulative sound exposure from the period surrounding a noise peak during which the noise level was above the adaptive threshold. So for example, the 'above threshold' and 'peak above threshold' data in Fig. 4.14(e) were counted towards the cumulative sound exposure of the AIS-identified component for that day.

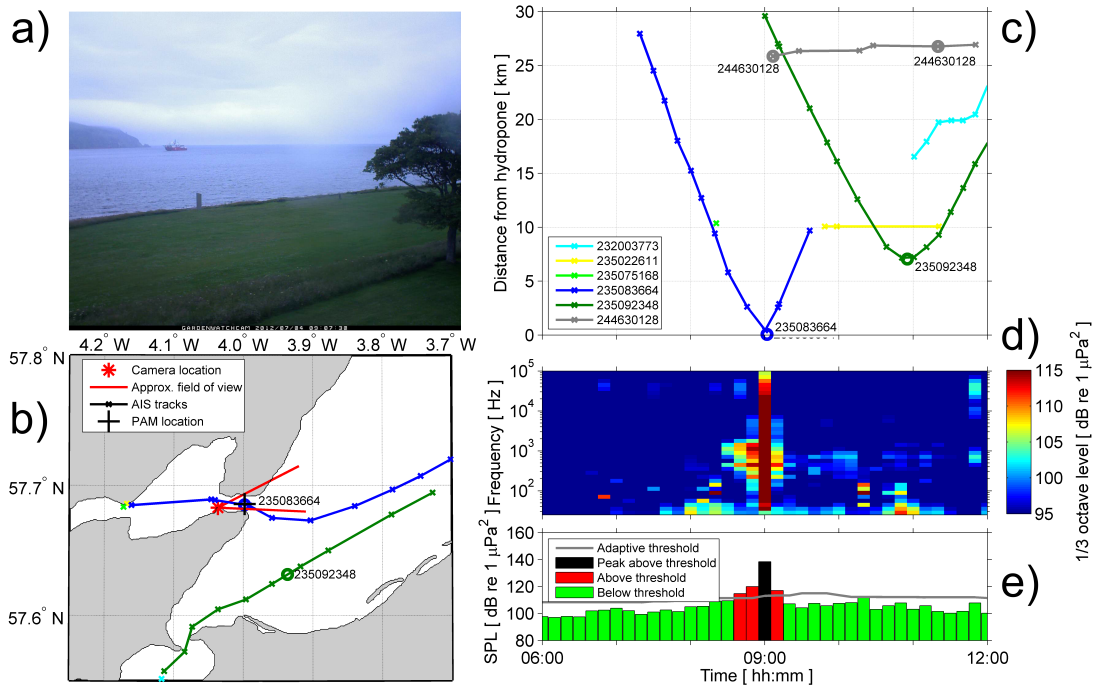

Figure 4.14: AIS analysis example with time-lapse footage. (a) Still of time lapse footage showing vessel whose CPA occurred at 09:00 on July 4; (b) Map of AIS movements in 6-hour period centred on CPA. Black cross denotes location of PAM unit in The Sutors, circles indicate CPAs labelled with Maritime Mobile Service Identity (MMSI) number; (c) Range of AIS transmissions from PAM unit versus time; (d) 1/3 octave spectrum of concurrent acoustic data; (e) Broadband level in frequency range 0.1–1 kHz, showing peak identification using adaptive threshold.

The 24-h sound exposure level (SEL) of each component (total SEL, AIS-identified SEL, and SEL from unidentified peaks) is presented in Fig. 4.15(a) for the range 0.1–1 kHz. Note that SEL is a logarithmic measure, so the sum of the component parts of the total SEL does approximate the whole, but in linear space. During the presence of the rig-towing vessels operating with DP from June 16–23 [see Fig. 4.10(b)] the noise level was consistently high, such that only two peaks were recorded by the adaptive threshold (both of which were AIS-identified vessels). As the rig-towing vessels were using AIS, their presence would be included in an AIS noise model, though their source levels are likely to be significantly elevated by the use of DP, which may not be accounted for by a generic ship source level database.

For all but four of the remaining days with uninterrupted AIS coverage, the AIS-identified peaks generated the vast majority of sound exposure recorded in this range [Fig. 4.15(a)]. On two of the four days (24 Jun and 8 Sep), unidentified peaks produced marginally greater sound exposure than AIS-identified peaks. This may have been caused by the particularly

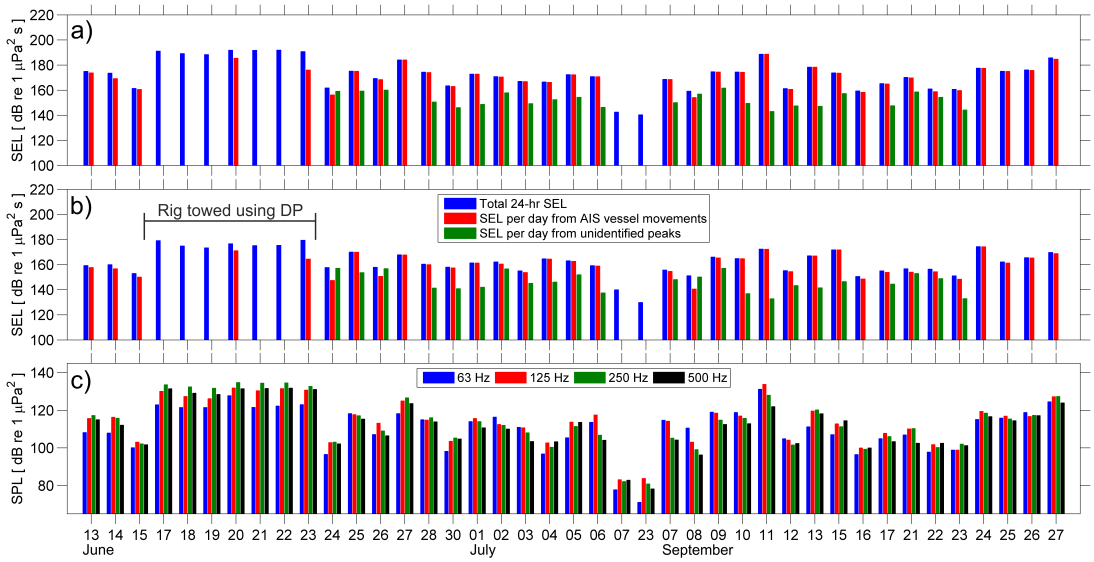

Figure 4.15: Broadband SEL per day for days with uninterrupted AIS coverage of The Sutors. (a) 0.1–1kHz (b) 1–10 kHz. Noise exceeding the adaptive threshold was attributed to AIS vessel movements or classed as unidentified. 'Rig towed using DP': this data did not exceed the adaptive threshold, but was attributable to AIS vessels (see text). (c) Mean SPL per day for four 1/3 octave frequency bands, including those proposed for use in the MSFD (63 and 125 Hz).

close presence of a non-AIS vessel in combination with only a small or relatively distant AIS-tracked vessel. On 7 July and 23 July, no peaks were recorded at all, and total sound exposure was ∼20 dB lower than the minimal levels recorded with detectable ship passages.

Since small vessels (which are not obliged to carry AIS transceivers) may emit noise with peak levels at up to several kHz (Kipple and Gabriele, 2003; Matzner et al., 2010), the 24-h SEL in the 1–10 kHz bandwidth was also computed to analyse whether higher frequencies were more dependent on unidentified peaks, which are likely to originate from small vessels [Fig. 4.15(b)]. This analysis retained the peak classification data used for the 0.1–1 kHz range. As expected, the recorded levels were consistently lower than at 0.1–1 kHz. Only one day (26 June) showed a significant difference, with unidentified sound exposure more dominant than in the lower frequency band. This demonstrates that sound exposure generated by AIS-carrying vessels at the study site was generally greater than that produced by non-AIS vessels for the range of both frequency bands (0.1–10 kHz). Consequently, a modelling approach based on vessel movements derived from AIS data should account for the majority of variability in noise exposure, provided the ship source levels input to the model are sufficiently accurate and acoustic propagation models are sufficiently predictive. Future work could explore whether this is achievable through implementation of such models and comparison

with recorded data.

Time-lapse footage

In addition to analysis of AIS movements, time-lapse footage was also reviewed to explore the potential for corroboration of AIS vessel identifications, detection of non-AIS vessels responsible for unidentified noise peaks, and characterisation of unusual acoustic events. The frame presented in Fig. 4.14(a) corresponds to the timing of the noise peak at around 09:00 presented in Fig. 4.14(c)–(e), and confirms the previous identification of this vessel from the CPA of its AIS track. An example in the Supplementary Material of a noise peak unidentified by AIS also shows a small vessel in the field of view of the time-lapse camera (although it is difficult to distinguish). Two examples of time-lapse footage paired with acoustic and AIS data are provided in the Supplementary Material as videos, which demonstrate the potential for this method to be used as a quick review tool of ship movements and underwater noise variability in coastal environments. They also provide an intuitive and informative educational tool to highlight the impact of ship noise on marine soundscapes and the potential for masking, behavioural and physiological impacts to marine fauna. As the examples provided illustrate, improving the visual and temporal resolution and the field of view would significantly enhance the power of this method for vessel monitoring and identification in coastal waters.

MSFD frequencies

The MSFD proposes to monitor underwater ambient noise in EU waters, using two 1/3-octave frequency bands (63 and 125 Hz) as indicators of shipping noise levels (European Commission, 2008; Van der Graaf et al., 2012). Ships also generate noise above these frequencies – as was observed in this study [Figs. 4.12(a), 4.13(b)] – though at higher frequencies sound is attenuated more rapidly by water and so is generally more localised. To assess whether higher frequency bands may be appropriate indicators for noise exposure from shipping, we compared mean noise levels in 1/3-octave frequency bands centred on 63, 125, 250 and 500 Hz [Fig. 4.15(c)] with daily broadband sound exposure levels in the range 0.05–1 kHz. This wider frequency band (0.05–1 kHz) approximately corresponds to the nominal range of shipping noise (0.01–10 kHz; Tasker et al., 2010). All four bands were highly correlated with noise exposure levels in the wider frequency band (Fig. 4.16), but this relationship was strongest at 125 Hz. The reduced correlation in the 63 Hz band may have been caused by noise related to tidal flows (Fig. 4.11) or low-frequency propagation effects characteristic of shallow water waveguides (Jensen et al., 2011). These effects may also limit the efficacy of the 63 Hz band as an indicator of anthropogenic noise in other shallow water, coastal sites.

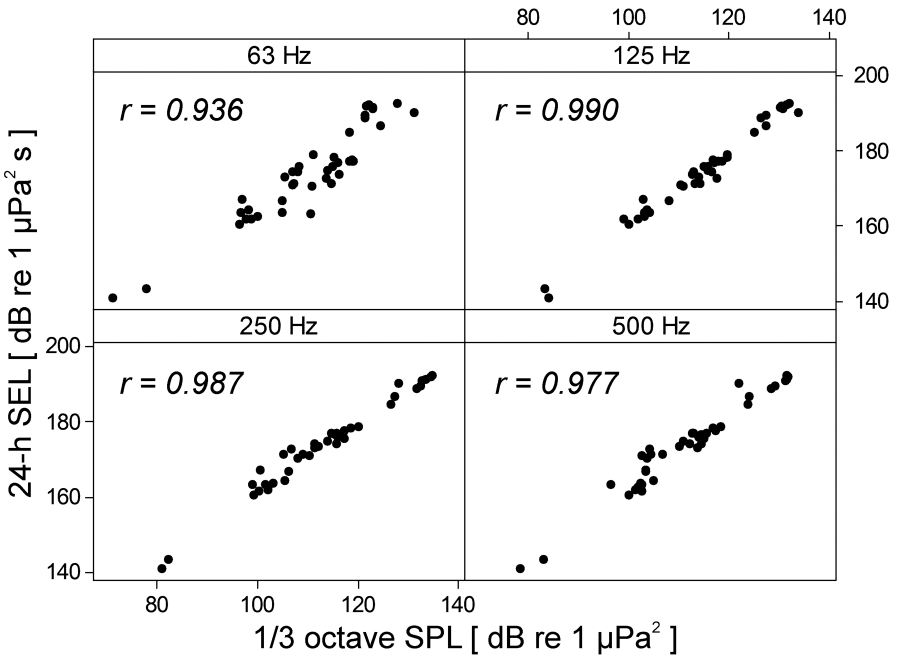

Figure 4.16: Relationships between broadband SEL (0.05–1 kHz) per day and mean SPL per day at The Sutors for four 1/3 octave frequency bands, including those proposed for use in the MSFD (63 and 125 Hz).

4.2.5 Discussion

The measurements of underwater noise at The Sutors and Chanonry establish baseline noise levels within the Moray Firth SAC during the summer field season, providing an important benchmark against which to quantify the acoustic impact of any future changes in shipping activity or other anthropogenic sources. The recordings revealed conspicuous differences in overall noise level and variability between the two sites (Fig. 4.10): shipping traffic and industrial activity related to the fabrication yard at Nigg and port activities at Invergordon (Fig. 4.8) were the dominant sources of noise at The Sutors, generating strongly diurnal variability in median levels [Fig. 4.12(a)]. In contrast, median noise levels at Chanonry were comparatively low [Fig. 4.12(a)], with only occasional vessel passages [Fig. 4.10(a)] and variability determined by weather and tidal processes (Fig. 4.11). Analysis of daily noise exposure at The Sutors highlighted the extent to which ship noise raises the total noise exposure above natural levels: on two days when no ship passages were detected, total daily noise exposure was ∼20 dB lower than normal in the 0.1–10 kHz range (Fig. 4.15).

Both sites used in this study are important foraging hotspots for the population of bottlenose dolphins in the inner Moray Firth [Hastie et al., 2004; Bailey and Thompson, 2010; Pirotta

et al., 2014)] and dolphins were confirmed to use them regularly throughout the deployment periods. Since the population appears to be stable or increasing (Cheney et al., 2013), the current noise levels we present are not expected to pose a threat to dolphin population levels. Nevertheless, the difference in baseline soundscape between the two foraging areas could influence how these sites may be affected by any future increases in shipping noise. While The Sutors is currently expected to experience greater increases in traffic associated with offshore energy developments, dolphins may already be accustomed to higher noise levels in this area. On the other hand, Chanonry is currently much quieter, meaning that a smaller increase in shipping noise could represent a greater degradation of habitat quality.

Analysis of noise levels at The Sutors in conjunction with AIS ship-tracking data demonstrated that the majority of total sound exposure at the site was attributable to vessels operating with AIS transceivers (Fig. 4.15). This indicates that modelling of cumulative noise exposure based on AIS-vessel movements as proposed by Erbe et al. (2012) should account for most of the noise exposure observed experimentally, provided other model parameters (ship source levels, acoustic propagation loss profiles) are sufficiently accurate. This result suggests that models based on planned increases in vessel movements in the Moray Firth (Lusseau et al., 2011; New et al., 2013) may be able to forecast associated increases in noise exposure, and is a promising indication that AIS-based noise mapping could be successfully applied to target ship noise mitigation efforts in other marine habitats. However, caution should be exercised in extrapolating from this result since in areas further from commercial shipping activity, the dominant source of ship noise may be smaller craft not operating with AIS transceivers.

This study also introduces the pairing of shore-based time-lapse footage with acoustic and AIS data as a tool for monitoring the influence of human activities on coastal marine soundscapes. The method enabled identification of abnormally loud events such as rigs being towed past the deployment site, and facilitated detection of non-AIS vessels responsible for noise peaks and corroboration of AIS-based vessel identification (Fig. 4.14). With improved resolution and field of view, time-lapse monitoring could facilitate more detailed characterisation of non-AIS vessels in coastal areas, enhancing understanding of the relative importance of small vessel traffic to marine noise pollution.

Comparison of spectra documenting bottlenose dolphin vocalisations and a ship passage at Chanonry (Fig. 4.13) highlights the potential for vocalisation masking by transiting vessels. Odontocetes use echolocation to navigate and to find and capture food (Au, 1993). Disruption to these activities caused by acoustic masking could thus affect energy acquisition and allocation, with long-term implications for vital rates (New et al., 2013). A noisier soundscape could also lead to degradation of the dolphin population's habitat (Tyack, 2008) such as

through effects on fish prey (Popper et al., 2003). Moreover, social interactions could be affected by vocalisation masking since sound is critical for communication among conspecifics. Future work could investigate the extent to which the effective communication range – which has been estimated for this population in the absence of vessels (Janik, 2000) – is reduced by the presence of vessel noise (Erbe, 2002; Hatch et al., 2012). A rise in noise from ship traffic could also induce anti-predatory behavioural responses (Tyack, 2008) and increase individual levels of chronic stress (Wright et al., 2007a). Research efforts should thus aim to characterise dolphin responses to ship noise in this area, and to understand whether increased ship traffic has the potential to alter the animals' activity budget.

The study also highlighted some important issues for the implementation of the European MSFD. Our measurements show that low-frequency flow noise may dominate in areas of high tidal flow, potentially contaminating noise levels at 63 and 125 Hz – frequencies at which the current legislation proposes to monitor ambient noise (European Commission, 2008; Van der Graaf et al., 2012). Flow noise is a form of pseudo-noise caused by turbulence around the hydrophone (Strasberg, 1979), and is not actually present in the environment. While noise from shipping was more dominant than flow noise at both sites (Fig. 4.12), flow noise exceeded non-anthropogenic noise levels below $\sim$160 Hz at the Chanonry site (Fig. 4.11), and so may influence measurements in areas of low shipping density. Since flow noise decreases with increasing frequency (Strasberg, 1979), higher frequency bands would be progressively less susceptible to flow noise contamination than those at 63 and 125 Hz.

Comparison of the proposed 1/3-octave frequency bands with those at 250 and 500 Hz (Fig. 4.16) indicates that the 250 Hz band may be as responsive to noise exposure from large vessels as the 125 Hz band, and may perform better than the 63 Hz band in shallow water. Although peak frequencies of commercial ship source levels are typically $<$100 Hz (e.g. Arveson and Vendittis, 2000; McKenna et al., 2012), low-frequency sound may be rapidly attenuated in shallow water depending on the water depth (Jensen et al., 2011), meaning received ship noise levels may have higher peak frequencies than in the open ocean. Inclusion of noise levels at frequencies greater than 125 Hz may therefore be particularly informative for MSFD noise monitoring in shallow waters.

A wider concern for the efficacy of the MSFD with regard to shipping noise is the proposed focus (Van der Graaf et al., 2012) of ambient noise monitoring on high shipping density areas. While it is important that the most acoustically polluted waters are represented in noise monitoring programs, it is arguably the case that habitats most at threat from anthropogenic pressure should be given greater weight. If noise levels in high shipping areas are to determine whether a member state of the European Union attains 'Good Environmental Status', there

is a risk that more significant changes to the marine acoustic environment in less polluted areas will be overlooked.

Acknowledgements

Funding for equipment and data collection was provided by Moray Offshore Renewables Ltd and Beatrice Offshore Wind Ltd. We thank Baker Consultants and Moray First Marine for their assistance with device calibration and deployment, respectively. The POLPRED tidal model was kindly provided by NERC National Oceanography Centre. We also thank Stephanie Moore for advice on sediment transport, and Ian McConnell of shipais.com for AIS data. N.D.M. was funded by an EPSRC Doctoral Training Award (No. EP/P505399/1). E.P. was funded by the MASTS pooling initiative (The Marine Alliance for Science and Technology for Scotland) and their support is gratefully acknowledged. MASTS is funded by the Scottish Funding Council (grant reference HR09011) and contributing institutions.

Chapter 5

Synthesis and Discussion

The main body of this thesis consists of four manuscripts presented in Chapters 3 and 4. This chapter draws out recurrent themes and reviews the key outcomes of this work. It is worth returning here to the objectives set out at the beginning of the project, as described in the Introduction (p3):

i. To examine and build upon methodologies for acoustic habitat monitoring in marine environments.
ii. To develop ways of measuring the contribution of ships to noise exposure in coastal habitats.
iii. To explore how these methods can inform emerging policy initiatives to monitor and regulate underwater noise from shipping.

Each of the following sections addresses one of these goals, and the final section then explores how these findings can inform future research in this area.

5.1 Ambient Noise Analysis Methods

The work presented in Chapter 3 contributes new insights into basic analysis techniques for passive acoustic monitoring of the marine environment. Until now, ambient noise data have been analysed and presented using spectral averages and percentiles, methods which have been in use since at least the 1960s (Wenz, 1962; Buck, 1966). In the fifty years since, the technology

to record and analyse ambient noise has greatly advanced, particularly with the advent of digital recording and autonomous PAM devices (Van Parijs et al., 2009; Sousa-Lima et al., 2013). This has enabled researchers to gather ever larger volumes of data over long time periods in a cost-effective way, giving correspondingly greater statistical power to these measurements. To exploit and elucidate this statistical power, it is necessary to go beyond simple summary statistics such as averages and percentiles – which conceal the quantity and nature of the data points which give rise to them – and to present the underlying distributions directly. This can be achieved using the spectral probability density, introduced in Section 3.2, p46, which presents the empirical probability density of each frequency band in the dataset.

As the examples in Fig. 3.5 show (p51), the SPD reveals modal behaviour, outliers, and exceedance of the dynamic range of the instrument. As well as enabling greater understanding of noise level distributions in large datasets, the SPD can show whether an instrument's dynamic range is appropriate to field conditions, and whether persistent tonal components, such as those from system self-noise, are present. This ability to detect potential shortcomings in PAM recording systems is particularly valuable as the number of these instruments on the market increases. Previously, autonomous PAM units were developed in-house by various research groups: examples include the Marine Acoustic Recording Unit (MARU, Cornell Bioacoustics Research Program), the Ecological Acoustic Recorder (EAR, University of Hawaii; Lammers et al., 2008), and the High-frequency Acoustic Recording Package (HARP, Scripps Institute of Oceanography; Wiggins and Hildebrand, 2007). More recently, many commercial operators have entered the market, including JASCO Research (Autonomous Multichannel Acoustic Recorder; AMAR) and Wildlife Acoustics (Song Meter 2 Marine; SM2M), and there are now over 30 different units available (Sousa-Lima et al., 2013). By carrying out a SPD analysis, investigators can assess the quality of data from PAM instruments, detecting system noise and insufficient dynamic range which may skew or contaminate measurements. A growing number of projects are employing large numbers of PAM units, often of different types, in large-scale monitoring programs. For example, the Baltic Sea Information on the Acoustic Soundscape (BIAS) project, an international collaboration between several Baltic states, will use 40 acoustic recorders of two different types to monitor noise levels in the Baltic Sea for one year (J. Tougaard, pers. comm., 2013). Ensuring data consistency over different monitoring locations and hardware platforms will be challenging, and could be made much simpler by using the SPD as an analysis tool.

Section 3.1 (p39) demonstrated that the integration or averaging time chosen affects the distribution of noise levels (and consequently the various averaging metrics). The distribution of noise levels in the SPD will similarly be affected by the averaging time, so to maintain consistency across different datasets, the same parameters should be used. What, then, is

an appropriate averaging time for SPD analysis? The analyses presented in Section 3.2 (p46) reduced the time resolution from a 1-s integration time to 60-s averages: this was for convenience as it saved computation time. The low ($<$ 1 dB) variation of the median and mode with averaging time in the VENUS dataset (Fig. 3.4, p45) between 1 and 60 s suggests that this loss of resolution would have little effect on the underlying distribution (at around 125 Hz). Nevertheless, it would be preferable to have a *de facto* standard averaging time for SPD analysis so that results will be generally comparable. In the context of marine acoustic habitats and impact assessment of anthropogenic noise, a reasoned approach might be to mimic the temporal sensitivity of the species under consideration by approximating its auditory integration time [Tougaard et al., (In Press)]. In many cases, however, acoustic monitoring will be undertaken with no particular species in mind, or with multiple, diverse species potentially affected. An alternative argument would be to select the most logical time period from the standpoint of standardisation, without consideration for biological relevance. Assuming the computation times required for large datasets are not prohibitive, an obvious choice would be a 1-s integration time without further reduction in time resolution: this integration time yields the standard 1-Hz frequency bins of the PSD (see Section 2.4.2, p29) and results in a fine time resolution, meaning the empirical PDs in the SPD are well populated with a large number of data points. This timescale is also not greatly dissimilar to auditory integration times observed at low frequencies in a bottlenose dolphin (0.1 s at 250 Hz; Johnson, 1968), and so may be appropriate for the monitoring of some marine mammal habitats.

The analysis of averaging metrics presented in Section 3.1 clearly illustrates how different metrics and averaging times can produce widely varying average SPLs, and provides empirical justification for the use of $\overline{\text{SPL}}_{\text{lin}}$ as the most appropriate metric for environmental assessment of shipping noise. $\overline{\text{SPL}}_{\text{lin}}$ is defined by the aggregate mean of the squared pressure, and so directly corresponds to the definition of SPL itself (Eq. 3.2, p41). This genealogy is apparent in the limiting case of the averaging time being equal to the total duration of the dataset, in which all of the (conventionally defined) averages converge on $\overline{\text{SPL}}_{\text{lin}}$ (Fig. 3.4(b), p45). In selecting a single average metric, $\overline{\text{SPL}}_{\text{lin}}$ is the most defensible choice, both in terms of standardisation – due to its invariance with averaging time – and assessment of potential impacts on marine life, owing to its relationship to sound exposure (Eq. 3.5, p44). A significant drawback of $\overline{\text{SPL}}_{\text{lin}}$, however, is its sensitivity to high noise levels. High-amplitude sound which may only represent a very small proportion of the time series can significantly skew average SPLs upwards (Fig. 3.4(a), p45). Consequently, using $\overline{\text{SPL}}_{\text{lin}}$ computed over long periods of time in the acoustically dynamic environments found in many coastal regions could be problematic, since exceptional high-amplitude events could strongly influence the overall average noise level recorded. Some have proposed using $\overline{\text{SPL}}_{\text{lin}}$ computed over as much as a year in

coastal waters (Erbe et al., 2012; Dekeling et al., 2013), but such levels could be skewed by loud events during only a small portion of the year. In the terrestrial realm, $\overline{\text{SPL}}_{\text{lin}}$ is often computed over a period of 24 hours (Harris, 1991), and there is perhaps merit in taking the lead of this long-established field, since using 24-h $\overline{\text{SPL}}_{\text{lin}}$ would reduce the risk of skewing by short-term events, and would give a higher time resolution, making it more relevant for impact assessment where the presence of marine species is often seasonal. By basing annual average noise levels on the distribution of 24-h $\overline{\text{SPL}}_{\text{lin}}$ – for example, the 5th percentile of this distribution – the influence of singular or exceptional events would be contained and limited to the days in which they occur, and the resultant metric would be more representative of typical noise levels and so more indicative of year-on-year trends.

5.2 Noise Exposure Assessment of Shipping

The second objective of the thesis was to develop new ways of assessing the contribution of ship passages to noise exposure in coastal habitats. The work addressing this aim is presented in Chapter 4, and evolved over the course of two studies conducted at sites in the western English Channel (Section 4.1, p55; Merchant et al., 2012b) and the inner Moray Firth (Section 4.2, p72; Merchant et al., 2014). The techniques developed constitute a three-stage progression from solely acoustical analysis to the integration of multiple data sources:

i. Separation of the broadband SPL time series using an adaptive threshold, resulting in ambient/background periods and intermittent events. Analysis of levels and variability of sound exposure from each component.
ii. Identification of peaks in the intermittent events and cross-referencing of each peak with AIS vessel movements to identify possible sources. Analysis of sound exposure from AIS and non-AIS passages, and potentially from different AIS vessel types.
iii. Integration of further data sources, such as time-lapse footage for corroboration of vessel identifications, and meteorological and tidal data to assess natural sources of variability in background noise levels.

Here, each component described above is reviewed with reference to current and emerging applications and alternative methodologies.

The adaptive threshold level, introduced in Section 4.1.2 (p61), provides a simple and intuitive way to parse the broadband SPL time series into background and intermittent components

whose sources can then be identified and characterised. The ATL adapts to gradual changes in the background noise level while distinguishing short-term increases. A relatively long averaging time of 300 s was used to smooth the amplitude profile of vessel passages, making the overall amplitude peak clearer to identify, and also to diminish the influence of short-term transient spikes in the data. Another potential hazard in applying an approach based solely on noise levels is that natural sound sources can be erroneously attributed to shipping. By limiting the frequency range considered to that dominated by shipping (0.01–1 kHz) and excluding low frequencies when these were observed to be contaminated by flow noise (see Section 4.2, where the broadband range was 0.1–1 kHz), the likelihood of erroneous detections from natural sources such as rain, flow noise, sediment transport, and high-frequency (>1 kHz) biological noise was reduced. However, the frequencies dominated by shipping coincide with wind-generated noise (Wenz, 1962), and so particular attention was paid to misidentification of this source. In both study areas, the contribution from wind-generated noise in the broadband frequency range chosen for ship noise did not exceed the ATL, suggesting that the rise time of the wind noise observed was sufficiently gradual within the 3-hour window (and using the 300-s averaging time) not to be misidentified as a ship passage. One difficulty which did occur was the converse of this problem: misidentification of nearby shipping as background noise. In both studies, the sustained presence of a ship (or ships) near the hydrophone over several days raised the ATL to the level of this persistent noise such that very few vessel passages were detected. In the first study, these data were discarded altogether, while in the second they were treated as an exceptional event. This is a drawback of the technique as it demands that these events be identified (e.g. with AIS or time-lapse footage) and considered separately from the rest of the data. However, these events may be peculiarities of the study sites chosen, both of which are termini for vessel traffic: Falmouth Bay is a hub for the bunkering of large vessels, while the area near The Sutors supports two shipyards which scrap and refit oil platforms. Study sites where shipping patterns are more transient are likely to be unaffected by this problem.

Once vessel passages have been separated from the background, the contribution they make to noise exposure at the site can be assessed. Both studies showed that the magnitude and variability of the 24-h sound exposure were due to the intermittent component, and in the Moray Firth study (Section 4.2, p72), the intermittent events caused by AIS-carrying vessels were shown to be the principal determinant of 24-h SEL. This result suggests that AIS-based modelling of noise levels could be predictive at this site, provided model parameters (e.g. ship source levels, propagation loss) are sufficiently accurate. The empirical approach taken allows the contribution of non-AIS vessels to be quantified and temporal patterns of noise exposure to be explored. Alternative approaches to ship noise assessment have relied on modelling via

AIS data without quantification of the non-AIS contribution. These include producing noise maps of long-term cumulative noise exposure (Erbe et al., 2012) or 'noise budgets' attributing some proportion of noise exposure to each vessel type (Bassett et al., 2012). The clear advantage of a modelling approach is the possibility of making predictions of noise levels beyond the locations of PAM devices, or potentially without making any acoustical measurements (e.g. Erbe et al., 2012; NOAA, 2012). However, without quantifying the contribution of non-AIS vessels to noise exposure, the validity of an AIS-based model cannot be established. An approach which combined the empirical evaluation of sound exposure from AIS and non-AIS vessels with extrapolation to spatiotemporal modelling of noise levels would therefore present a significant step forward for noise assessment of shipping.

A further impediment to AIS-based modelling of shipping noise levels is the variability in radiated noise levels from individual vessels depending on their operational condition. To date, modelling approaches rely on generic ship spectra as source inputs, but time-varying factors including ship speed and load condition are likely to affect radiated noise levels (McKenna et al., 2013), and vessels using dynamic positioning, such as those recorded positioning an oil rig at The Sutors (Section 4.2, p72), are likely to have differing noise characteristics to vessels transiting at cruising speed. Whether uncertainty in ship source levels is a significant constraint in AIS-based noise modelling (compared to uncertainty in propagation loss or levels of non-AIS shipping, for example) will become clearer as future work endeavours to ground-truth these models with acoustical measurements.

Incorporating shore-based time-lapse footage into the suite of data sources employed at the Moray Firth site introduced a novel dimension to ship noise monitoring in coastal waters. Although underwater video technology has long been used in scientific research (Shortis et al., 2007) including observations of responses of marine fauna to anthropogenic sound (Wardle et al., 2001), I am unaware of any studies linking footage of surface vessels to underwater recordings, nor to AIS ship-tracking data. The videos presented in the accompanying DVD bring together PAM recordings and analysis, animated maps of AIS vessel movements and shore-based time-lapse footage of surface activity. The influence of ship passages and weather on noise levels at the site is readily apparent, which makes these videos an effective way of conveying the potential impact of shipping noise on marine habitats to non-specialist audiences. Furthermore, the footage presents an opportunity to corroborate identifications of vessel passages made using acoustic and AIS data with visual observations. Though the resolution of the time-lapse camera limited the efficacy of these observations, and observations were occasionally occluded by weather conditions, the project was nevertheless a useful proof-of-concept for these techniques. The study locations at The Sutors and Chanonry were well suited to video capture since they each focus vessel traffic into a narrow 'bottleneck' near to

shore, meaning all vessel traffic could be captured using a single shore-based camera. This is not typical of many coastal environments, where shipping lanes may be spread too wide or too far from shore for such shore-based monitoring to be effective. Where there are nodes of shipping activity away from shore, buoys could potentially be used as an alternative visual monitoring platform. Additional challenges compared to shore-based monitoring would include variability in coverage and loss of visibility due to wave action, and the likely need for a panoramic field of view which would increase the data load. Given the availability of multi-sensor buoy-based platforms (including PAM, e.g. PAMBuoy, 2013), an integrated system equipped with PAM, an AIS receiver, and time-lapse camera could be deployed, though the data load would likely preclude wireless transmission, and the system would instead be archival.

5.3 Relevance to Environmental Policy

As well as contributing new methods and insights to the science of underwater noise monitoring, the work presented in this thesis also has applications to the development of policy initiatives to monitor and regulate underwater noise pollution from shipping. The most direct example is the section on averaging methods (Section 3.1, p39; Merchant et al., 2012a) which addressed the lack of consensus on the most appropriate metric to use when averaging ship noise levels. This issue has policy significance as the EU policy initiative (MSFD) proposes to use the trend in ambient noise levels averaged over one year as an indicator of 'Good Environmental Status'. The paper published in 2012 (Merchant et al., 2012b) provided an empirical evaluation of averaging methods using data from a coastal shipping lane – the kind of environment in which the MSFD proposes that noise monitoring is focused (Van der Graaf et al., 2012). Subsequent guidance issued by the technical subgroup responsible for MSFD noise monitoring (Dekeling et al., 2013) has drawn on the findings of this paper, as has similar work on averaging methods applied to deep-water environments (Van der Schaar et al., 2014).

The analysis technique from which the SPD was adapted was designed to assess the performance of seismological monitoring stations in a nationwide cabled network (McNamara and Buland, 2004). It is conceivable that future policy-led efforts to monitor regional trends in underwater noise levels will encompass analogous cabled observatories, such as RSN (Cowles et al., 2010), those operated by ONC (Martin Taylor, 2009), and others [see Favali et al. (In Press)], and are likely to entail deployment of autonomous PAM devices of various types. The SPD method introduced in Section 3.2 (p46) could therefore play a similar role in per-

formance assessment of the many PAM systems composing a regional noise monitoring network, acting as a system diagnostic tool as described previously (Section 3.2.3, p50). This would alert operators of sensor networks to potential problems with monitoring stations, and would enable comparison of the performance of diverse PAM systems.

A final policy-related application is the potential for the noise exposure monitoring methods developed in Chapter 4 to be applied to the ground-truthing of regional noise maps generated from shipping data. In the United States, much of the environmental policy relating to underwater noise has been driven by federal agencies which are mandated to protect marine mammal species under the Marine Mammal Protection Act, 1972. The National Oceanic and Atmospheric Administration (NOAA), the principal agency responsible, has developed modelling tools which overlay maps of projected noise levels from shipping with cetacean distributions in US territorial waters, identifying key areas of concern for the disturbance of cetaceans by shipping noise (NOAA, 2012). However, these noise maps are derived from models based on shipping data, and there is now a need to ground-truth such models to assess whether they can be predictive and to determine which variables are the most significant sources of error. One aspect of this could be to measure noise exposure at key locations using the methods presented in Chapter 4, which evaluate the variability of sound exposure at the site, including the contribution of AIS and non-AIS vessel passages. This agreement between measured and modelled levels could then be assessed, and the significance of vessels not accounted for in the shipping data could be better understood.

5.4 Future Work

The work presented here opens up several avenues of inquiry for further development of analysis methods. One current shortcoming of the method of linking AIS vessel movements with received noise levels is that the process is manual: peaks in the intermittent data are automatically identified, but then the interpretation of the AIS tracks for each peak is carried out by the operator. Automating this process would greatly enhance the method as it would save considerable time and would formalise the criteria for vessel identification. The difficulty in achieving this would be to incorporate both the range of the vessel and the temporal alignment of CPA and noise peak as factors determining whether a positive identification is made. Ideally, trial data from diverse sites, combined with manual oversight of automated detections, would be used to train the identification algorithm.

As discussed in Section 4.2 (p72), the resolution of the time-lapse camera was a constraining factor in the visual identification of vessels transiting through the study sites. The temporal

resolution and field of view were apparently sufficient to detect all large vessels transiting both sites, but higher image resolution would be needed to determine small vessel types and to distinguish identification numbers of large vessels. There are currently high-definition cameras on the market which would meet these requirements*, though the volume of data would be significantly higher. Greater temporal resolution and field of view could also be beneficial, though these would similarly increase the data load. A complementary approach could be to explore the use of other wavelengths for the detection of marine mammals and vessels. The potential for marine mammal detection using infrared wavelengths has been demonstrated by Cuyler et al. (1992), and infrared detection and identification of vessels has long been used in military applications (e.g. Lee et al., 1990).

Another possible area of investigation is the variability of the SPD with integration time. It was suggested in Section 5.1 that a 1-s averaging time would be the most justifiable standard time period for the calculation of SPD. However, it would still be useful to empirically evaluate the variation of SPD representations of acoustic data with averaging time to assess the influence this variable might have on results. This would give better understanding of how comparable SPD analyses might be if a different averaging time has been used.

*e.g. Brinno TLC200 Pro http://www.brinno.com/html/TLC200pro.html

Chapter 6

Conclusions

This thesis has developed a suite of analysis methods for the assessment of noise exposure from shipping in coastal environments. These include:

i. The introduction of the *adaptive threshold level* as a means to identify ship passages in time series of passive acoustic data.
ii. A method of linking movements of AIS-transmitting vessels to ship passages identified using the adaptive threshold.
iii. The introduction of shore-based time-lapse footage as a method of corroborating vessel identifications and identifying non-AIS vessels.
iv. The integration of these data sources into animated videos which intuitively convey the influence of natural and anthropogenic sources on coastal marine soundscapes.

These techniques may be taken separately or combined – as presented here – to further the understanding of noise exposure from shipping in other areas.

Contributions have also been made to more fundamental methods of underwater noise analysis. The *spectral probability density* is a new way of presenting ambient noise spectra which reveals the statistical distribution of noise levels across the frequency spectrum. The method is a substantial enhancement to established techniques, and could serve many applications, including performance assessment of PAM devices and contextualization of summary statistics. Empirical assessment of the behaviour of averaging metrics provided new insights into the suitability of these metrics for environmental assessment of shipping noise. $\overline{\mathrm{SPL}}_{\mathrm{lin}}$, the

mean SPL averaged in linear space, was found to be most appropriate both for standardisation and for relevance to potential impacts on marine fauna, though its sensitivity to exceptional high-amplitude events is a significant drawback.

Measurements made at The Sutors in the inner Moray Firth, Scotland, indicated that the magnitude of daily noise exposure was determined by the contribution of AIS-transmitting vessels. This result suggests that AIS-based modelling at the site could be predictive of noise levels, and demonstrates that the methods developed here could help to validate such models. The emerging policy initiatives in the EU and the US both rely heavily on spatial modelling of noise levels, and the techniques presented in this thesis could inform the ground-truthing of the preliminary models which have thus far been developed. Taken together with the more fundamental advances in analysis methods described above, these contributions help to strengthen the methodological basis for the management of underwater noise exposure from shipping.

References

Agardy, T., Aguilar, N., Cañadas, A., Engel, M., Frantzis, A., Hatch, L., Hoyt, E., Kaschner, K., LaBrecque, E., Martin, V., Notarbartolo di Sciara, G., Pavan, G., Servidio, A., Smith, B., Wang, J., Weilgart, L., Wintle, B., Wright, A., 2007. A global scientific workshop on spatio-temporal management of noise. Report of the Scientific Workshop. 44pp.

Aguilar de Soto, N., Delorme, N., Atkins, J., Howard, S., Williams, J., Johnson, M., 2013. Anthropogenic noise causes body malformations and delays development in marine larvae. Scientific Reports 3, 2831.

Aguilar de Soto, N., Madsen, P. T., Tyack, P., Arranz, P., Marrero, J., Fais, A., Revelli, E., Johnson, M., 2012. No shallow talk: Cryptic strategy in the vocal communication of Blainville's beaked whales. Marine Mammal Science 28 (2), E75–E92.

Aiken, R., 1985. Sound production by aquatic insects. Biological Reviews 60 (2), 163–211.

Ainslie, M. A., 2009. Principles of Sonar Performance Modelling. Springer-Praxis, UK.

Ainslie, M. A., 2011. Standard for measurement and monitoring of underwater noise, Part I: Physical quantities and their units. TNO-DV 2011 C235. Tech. rep., TNO, The Hague. 52pp.

Alsarayreh, T., Zedel, L., 2011. Quantifying snowfall rates using underwater sound. Atmosphere-Ocean 49 (2), 61–66.

Amoser, S., Wysocki, L. E., Ladich, F., 2004. Noise emission during the first powerboat race in an Alpine lake and potential impact on fish communities. Journal of the Acoustical Society of America 116 (6), 3789–3797.

André, M., Solé, M., Lenoir, M., Durfort, M., Quero, C., Mas, A., Lombarte, A., van der Schaar, M., López-Bejar, M., Morell, M., Zaugg, S., Houégnigan, L., 2011a. Low-frequency sounds induce acoustic trauma in cephalopods. Frontiers in Ecology and the Environment 9 (9), 489–493.

André, M., van der Schaar, M., Zaugg, S., Houégnigan, L., Sánchez, A. M., Castell, J. V., 2011b. Listening to the deep: Live monitoring of ocean noise and cetacean acoustic signals. Marine Pollution Bulletin 63 (1-4), 18–26.

Andrew, R. K., Howe, B. M., Mercer, J. A., Dzieciuch, M. A., 2002. Ocean ambient sound: Comparing the 1960s with the 1990s for a receiver off the California coast. Acoustics Research Letters Online 3 (2), 65–70.

ANSI, 2009. ANSI/ASA S1.11-2004 (R2009) Specification For Octave-band And Fractional-octave-band Analog And Digital Filters.

Arveson, P. T., Vendittis, D. J., 2000. Radiated noise characteristics of a modern cargo ship. Journal of the Acoustical Society of America 107 (1), 118–129.

Au, W. W., 1993. The Sonar of Dolphins. Springer, NY.

Au, W. W. L., Banks, K., 1998. The acoustics of the snapping shrimp *Synalpheus parneomeris* in Kaneohe Bay. Journal of the Acoustical Society of America 103 (1), 41–47.

Au, W. W. L., Green, M., 2000. Acoustic interaction of humpback whales and whale-watching boats. Marine Environmental Research 49 (5), 469–481.

Au, W. W. L., Hastings, M. C., 2008. Principles of Marine Bioacoustics. Springer, NY.

Au, W. W. L., Pack, A. A., Lammers, M. O., Herman, L. M., Deakos, M. H., Andrews, K., 2006. Acoustic properties of humpback whale songs. Journal of the Acoustical Society of America 120 (2), 1103–1110.

Bahtiarian, M., Fischer, R., 2006. Underwater radiated noise of the NOAA ship Oscar Dyson. Noise Control Engineering Journal 54 (4), 224–235.

Bailey, H., Senior, B., Simmons, D., Rusin, J., Picken, G., Thompson, P. M., 2010. Assessing underwater noise levels during pile-driving at an offshore windfarm and its potential effects on marine mammals. Marine Pollution Bulletin 60 (6), 888–897.

Bailey, H., Thompson, P., 2010. Effect of oceanographic features on fine-scale foraging movements of bottlenose dolphins. Marine Ecology Progress Series 418, 223–233.

Barclay, D. R., Buckingham, M. J., 2013a. Depth dependence of wind-driven, broadband ambient noise in the Philippine Sea. Journal of the Acoustical Society of America 133 (1), 62–71.

Barclay, D. R., Buckingham, M. J., 2013b. The depth-dependence of rain noise in the Philippine Sea. Journal of the Acoustical Society of America 133 (5), 2576–2585.

Barclay, D. R., Simonet, F., Buckingham, M. J., 2009. Deep Sound: A free-falling sensor platform for depth-profiling ambient noise in the deep ocean. Marine Technology Society Journal 43 (5), 144–150.

Bass, S. J., Hay, A. E., 1997. Ambient noise in the natural surf zone: Wave-breaking frequencies. IEEE Journal of Oceanic Engineering 22 (3), 411–424.

Bassett, C., Polagye, B., Holt, M., Thomson, J., 2012. A vessel noise budget for Admiralty Inlet, Puget Sound, Washington (USA). Journal of the Acoustical Society of America 132 (6), 3706–3719.

Bassett, C., Thomson, J., Polagye, B., 2013. Sediment-generated noise and bed stress in a tidal channel. Journal of Geophysical Research: Oceans 118 (4), 2249–2265.

Bassett, C., Thomson, J., Polagye, B., Rhinefrank, K., 2011. Underwater noise measurements of a 1/7th scale wave energy converter. In: Proceedings of MTS/IEEE OCEANS 2011.

Bejder, L., Samuels, A., Whitehead, H., Gales, N., Mann, J., Connor, R., Heithaus, M., Watson-Capps, J., Flaherty, C., Kruetzen, M., 2006. Decline in relative abundance of bottlenose dolphins exposed to long-term disturbance. Conservation Biology 20 (6), 1791–1798.

Blackwell, S. B., Greene, C. R., 2005. Underwater and in-air sounds from a small hovercraft. Journal of the Acoustical Society of America 118 (6), 3646–3652.

Blackwell, S. B., Lawson, J. W., Williams, M. T., 2004. Tolerance by ringed seals (*Phoca hispida*) to impact pipe-driving and construction sounds at an oil production island. Journal of the Acoustical Society of America 115, 2346.

Blondel, P., Murton, B. J., 1997. Handbook of seafloor sonar imagery. Wiley, Chichester, UK.

Brockett, P. L., Hinich, M., Wilson, G. R., 1987. Nonlinear and non-Gaussian ocean noise. Journal of the Acoustical Society of America 82 (4), 1386–1394.

Bruintjes, R., Radford, A. N., 2013. Context-dependent impacts of anthropogenic noise on individual and social behaviour in a cooperatively breeding fish. Animal Behaviour 85 (6), 1343–1349.

Buck, B. M., 1966. Arctic acoustic transmission loss and ambient noise. Tech. rep., DTIC Document AD0485552, http://www.dtic.mil/cgi-bin/GetTRDoc?Location=U2&doc=GetTRDoc.pdf&AD=AD0485552.

Buckstaff, K. C., 2004. Effects of watercraft noise on the acoustic behavior of bottlenose dolphins, *Tursiops truncatus*, in Sarasota Bay, Florida. Marine Mammal Science 20 (4), 709–725.

Butler, J. R., Middlemas, S. J., McKelvey, S. A., McMyn, I., Leyshon, B., Walker, I., Thompson, P. M., Boyd, I. L., Duck, C., Armstrong, J. D., 2008. The Moray Firth Seal Management Plan: An adaptive framework for balancing the conservation of seals, salmon, fisheries and wildlife tourism in the UK. Aquatic Conservation: Marine and Freshwater Ecosystems 18 (6), 1025–1038.

Caldwell, J., Dragoset, W., 2000. A brief overview of seismic air-gun arrays. The Leading Edge 19 (8), 898–902.

Castellote, M., Clark, C. W., Lammers, M. O., 2012. Acoustic and behavioural changes by fin whales (*Balaenoptera physalus*) in response to shipping and airgun noise. Biological Conservation 147 (1), 115–122.

Cerna, M., Harvey, A. F., 2000. The fundamentals of FFT-based signal analysis and measurements, Application Note 041. Tech. rep., National Instruments. http://www.ct.infn.it/∼microel/signal_analysis/signal2.pdf.

Chapman, N. R., Price, A., 2011. Low frequency deep ocean ambient noise trend in the Northeast Pacific Ocean. Journal of the Acoustical Society of America 129 (5), EL161–EL165.

Cheney, B., Thompson, P. M., Ingram, S. N., Hammond, P. S., Stevick, P. T., Durban, J. W., Culloch, R. M., Elwen, S. H., Mandleberg, L., Janik, V. M., Quick, N. J., Islas-Villanueva, V., Robinson, K. P., Costa, M., Eisfeld, S. M., Walters, A., Phillips, C., Weir, C. R., Evans, P. G. H., Anderwald, P., Reid, R. J., Reid, J. B., Wilson, B., 2013. Integrating multiple data sources to assess the distribution and abundance of bottlenose dolphins *Tursiops truncatus* in Scottish waters. Mammal Review 43 (1), 71–88.

Christiansen, F., Lusseau, D., Stensland, E., Berggren, P., 2010. Effects of tourist boats on the behaviour of Indo-Pacific bottlenose dolphins off the south coast of Zanzibar. Endangered Species Research 11 (1), 91–99.

Clark, C. W., 1990. Acoustic behavior of mysticete whales. In: Sensory abilities of cetaceans. Plenum Press, NY, pp. 571–583.

Clark, C. W., Ellison, W. T., Southall, B. L., Hatch, L., Van Parijs, S. M., Frankel, A., Ponirakis, D., 2009. Acoustic masking in marine ecosystems: Intuitions, analysis, and implication. Marine Ecology Progress Series 395, 201–222.

Codarin, A., Wysocki, L. E., Ladich, F., Picciulin, M., 2009. Effects of ambient and boat noise on hearing and communication in three fish species living in a marine protected area (Miramare, Italy). Marine Pollution Bulletin 58 (12), 1880–1887.

Collins, M. D., 1995. User's Guide for RAM Versions 1.0 and 1.0p. Naval Research Lab, Washington, DC.

Collins, M. J., 2011. Passive acoustic monitoring of weather patterns in the ocean. Ph.D. thesis, University of Bath.

Colosi, J. A., Baggeroer, A. B., Birdsall, T. G., Clark, C., Cornuelle, B. D., Costa, D., Dushaw, B. D., Dzieciuch, M. A., Forbes, A. M. G., Howe, B. M., Menemenlis, D., Mercer, J. A., Metzger, K., Munk, W., Spindel, R. C., Worcester, P. F., Wunsch, C., 1999. A review of recent results on ocean acoustic wave propagation in random media: Basin scales. IEEE Journal of Oceanic Engineering 24 (2), 138–155.

Constantine, R., Brunton, D. H., Dennis, T., 2004. Dolphin-watching tour boats change bottlenose dolphin (*Tursiops truncatus*) behaviour. Biological Conservation 117 (3), 299–307.

Cowles, T., Delaney, J., Orcutt, J., Weller, R., 2010. The Ocean Observatories Initiative: Sustained ocean observing across a range of spatial scales. Marine Technology Society Journal 44 (6), 54–64.

Curtis, K. R., Howe, B. M., Mercer, J. A., 1999. Low-frequency ambient sound in the North Pacific: Long time series observations. Journal of the Acoustical Society of America 106 (6), 3189–3200.

Cuyler, L., Wiulsrød, R., Øritsland, N., 1992. Thermal infrared radiation from free living whales. Marine Mammal Science 8 (2), 120–134.

De Robertis, A., Wilson, C. D., Furnish, S. R., Dahl, P. H., 2013. Underwater radiated noise measurements of a noise-reduced fisheries research vessel. ICES Journal of Marine Science: Journal du Conseil 70 (2), 480–484.

Deane, G. B., 2000. Long time-base observations of surf noise. Journal of the Acoustical Society of America 107 (2), 758–770.

Dekeling, R., Tasker, M., Ainslie, M., Andersson, M., André, M., Castellote, M., Borsani, J., Dalen, J., Folegot, T., Leaper, R., Liebschner, A., Pajala, J., Robinson, S., Sigray, P., Sutton, G., Thomsen, F., Van der Graaf, A., Werner, S., Wittekind, D., Young, J., 2013. Monitoring Guidance for Underwater Noise in European Seas – 2nd Report of the Technical Subgroup on Underwater noise (TSG Noise). Interim Guidance Report. Tech. rep.

Department for Transport, 2010. Transport Statistics Report: Maritime Statistics 2009. DfT, London, UK.

DeRuiter, S. L., Southall, B. L., Calambokidis, J., Zimmer, W. M., Sadykova, D., Falcone, E. A., Friedlaender, A. S., Joseph, J. E., Moretti, D., Schorr, G. S., 2013. First direct measurements of behavioural responses by Cuvier's beaked whales to mid-frequency active sonar. Biology Letters 9 (4), 20130223.

Dinwoodie, J., Tuck, S., Knowles, H., Benhin, J., Sansom, M., 2012. Sustainable development of maritime operations in ports. Business Strategy and the Environment 21 (2), 111–126.

Dubrovskiy, N., Kosterin, S., 1993. Noise in the ocean caused by lightning strokes. In: Natural Physical Sources of Underwater Sound. Springer, pp. 697–709.

Dudzinski, K. M., Brown, S. J., Lammers, M., Lucke, K., Mann, D. A., Simard, P., Wall, C. C., Rasmussen, M. H., Magnusdottir, E. E., Tougaard, J., Eriksen, N., 2011. Troubleshooting deployment and recovery options for various stationary passive acoustic monitoring devices in both shallow- and deep-water applications. Journal of the Acoustical Society of America 129 (1), 436–448.

Dunlop, R. A., Noad, M. J., Cato, D. H., Stokes, D., 2007. The social vocalization repertoire of east Australian migrating humpback whales (*Megaptera novaeangliae*). Journal of the Acoustical Society of America 122, 2893.

Dyer, I., 1973. Statistics of distant shipping noise. Journal of the Acoustical Society of America 53 (2), 564–570.

Ellison, W. T., Southall, B. L., Clark, C. W., Frankel, A. S., 2012. A new context-based approach to assess marine mammal behavioral responses to anthropogenic sounds. Conservation Biology 26 (1), 21–28.

Erbe, C., 2002. Underwater noise of whale-watching boats and potential effects on killer whales (*Orcinus orca*), based on an acoustic impact model. Marine Mammal Science 18 (2), 394–418.

Erbe, C., 2013. Underwater noise of small personal watercraft (jet skis). Journal of the Acoustical Society of America 133 (4), EL326–EL330.

Erbe, C., Farmer, D. M., 2000a. A software model to estimate zones of impact on marine mammals around anthropogenic noise. Journal of the Acoustical Society of America 108 (1), 1327–1331.

Erbe, C., Farmer, D. M., 2000b. Zones of impact around icebreakers affecting beluga whales in the Beaufort Sea. Journal of the Acoustical Society of America 108 (3), 1332–1340.

Erbe, C., MacGillivray, A., Williams, R., 2012. Mapping cumulative noise from shipping to inform marine spatial planning. Journal of the Acoustical Society of America 132 (5), EL423–EL428.

Etter, P. C., 1991. Underwater Acoustic Modeling: Principles, Techniques and Application.

Etter, P. C., 2009. Review of ocean-acoustic models. In: Proceedings of MTS/IEEE OCEANS 2009.

European Commission, 2005. Directive 2005/33/EC of the European Parliament and of the Council of 6 July 2005 amending Directive 1999/32/EC as regards the sulphur content of marine fuels. Official Journal of the European Union L191, 59-69.

European Commission, 2008. Directive 2008/56/EC of the European Parliament and of the Council of 17 June 2008, establishing a framework for community action in the field of marine environmental policy (Marine Strategy Framework Directive). Official Journal of the European Union L164, 19-40.

Evans, D. L., England, G. R. E., 2001. Joint interim report Bahamas marine mammal stranding event of 15-16 March 2000. Tech. rep., US Department of Commerce and Secretary of the Navy. 59pp.

Everest, F. A., Young, R. W., Johnson, M. W., 1948. Acoustical characteristics of noise produced by snapping shrimp. Journal of the Acoustical Society of America 20 (2), 137–142.

Favali, P., Beranzoli, L., Santis, A., (In Press). Seafloor Observatories: A New Vision of the Earth from the Abyss. Springer-Praxis, UK.

Ferguson, B. G., Lo, K. W., Rodgers, J. D., 2010. Sensing the underwater acoustic environment with a single hydrophone onboard an undersea glider. In: Proceedings of MTS/IEEE OCEANS 2010.

Fofonoff, N. P., Millard, R. C., 1983. Algorithms for computation of fundamental properties of seawater. UNESCO Tech. Papers in Marine Science 44, 53.

Foote, A. D., Osborne, R. W., Hoelzel, A. R., 2004. Whale-call response to masking boat noise. Nature 428 (6986), 910–910.

Frankel, A. S., Ellison, W. T., Buchanan, J., 2002. Application of the Acoustic Integration Model (AIM) to predict and minimize environmental impacts. In: Proceedings of MTS/IEEE OCEANS 2002. Vol. 3. pp. 1438–1443.

Frantzis, A., 1998. Does acoustic testing strand whales? Nature 392 (6671), 29–29.

Frisk, G., 2012. Noiseonomics: The relationship between ambient noise levels in the sea and global economic trends. Scientific Reports 2, 437.

Garrett, J. K., Witt, M. J., Johanning, L., (In Press). Underwater sound levels at a wave energy device testing facility in Falmouth Bay, UK. In: Effects of Noise on Aquatic Life II. Springer, NY.

Gershman, A. B., Nemeth, E., Bohme, J. F., 2000. Experimental performance of adaptive beamforming in a sonar environment with a towed array and moving interfering sources. IEEE Transactions on Signal Processing 48 (1), 246–250.

Gisiner, R., Harper, S., Livingston, E., Simmen, J., 2006. Effects of sound on the marine environment (ESME): An underwater noise risk model. IEEE Journal of Oceanic Engineering 31 (1), 4–7.

Goldbogen, J. A., Southall, B. L., DeRuiter, S. L., Calambokidis, J., Friedlaender, A. S., Hazen, E. L., Falcone, E. A., Schorr, G. S., Douglas, A., Moretti, D. J., 2013. Blue whales respond to simulated mid-frequency military sonar. Proceedings of the Royal Society B: Biological Sciences 280 (1765), 20130657.

Graham, A. L., Cooke, S. J., 2008. The effects of noise disturbance from various recreational boating activities common to inland waters on the cardiac physiology of a freshwater fish, the largemouth bass (*Micropterus salmoides*). Aquatic Conservation: Marine and Freshwater Ecosystems 18 (7), 1315–1324.

Greene, C. R., 1987. Characteristics of oil industry dredge and drilling sounds in the Beaufort Sea. Journal of the Acoustical Society of America 82 (4), 1315–1324.

Haikonen, K., Sundberg, J., Leijon, M., 2013. Characteristics of the operational noise from full scale wave energy converters in the Lysekil project: Estimation of potential environmental impacts. Energies 6 (5), 2562–2582.

Hamson, R. M., 1997. The modelling of ambient noise due to shipping and wind sources in complex environments. Applied Acoustics 51 (3), 251–287.

Handegard, N. O., Michalsen, K., Tjøstheim, D., 2003. Avoidance behaviour in cod (*Gadus morhua*) to a bottom-trawling vessel. Aquatic Living Resources 16 (3), 265–270.

Haren, A. M., 2007. Reducing noise pollution from commercial shipping in the Channel Islands National Marine Sanctuary: A case study in marine protected area management of underwater noise. Journal of International Wildlife Law and Policy 10 (2), 153–173.

Harris, C. M., 1991. Handbook of Acoustical Measurements and Noise Control, 3rd Edition. McGraw-Hill, NY.

Harris, F. J., 1978. On the use of windows for harmonic analysis with the discrete Fourier transform. Proceedings of the IEEE 66 (1), 51–83.

Hastie, G. D., Wilson, B., Wilson, L., Parsons, K., Thompson, P., 2004. Functional mechanisms underlying cetacean distribution patterns: Hotspots for bottlenose dolphins are linked to foraging. Marine Biology 144 (2), 397–403.

Hatch, L., Clark, C., Merrick, R., Van Parijs, S., Ponirakis, D., Schwehr, K., Thompson, M., Wiley, D., 2008. Characterizing the relative contributions of large vessels to total ocean noise fields: A case study using the Gerry E. Studds Stellwagen Bank National Marine Sanctuary. Environmental Management 42 (5), 735–752.

Hatch, L., Fristrup, K., 2009. No barrier at the boundaries: Implementing regional frameworks for noise management in protected natural areas. Marine Ecology Progress Series 395, 223–244.

Hatch, L. T., Clark, C. W., Van Parijs, S. M., Frankel, A. S., Ponirakis, D. W., 2012. Quantifying loss of acoustic communication space for right whales in and around a U.S. National Marine Sanctuary. Conservation Biology 26 (6), 983–994.

Heide-Jørgensen, M. P., Hansen, R. G., Westdal, K., Reeves, R. R., Mosbech, A., 2013. Narwhals and seismic exploration: Is seismic noise increasing the risk of ice entrapments? Biological Conservation 158, 50–54.

Hildebrand, J. A., 2009. Anthropogenic and natural sources of ambient noise in the ocean. Marine Ecology Progress Series 395, 5–20.

Hinz, H., Capasso, E., Lilley, M., Frost, M., Jenkins, S. R., 2011. Temporal differences across a bio-geographical boundary reveal slow response of sub-littoral benthos to climate change. Marine Ecology Progress Series 423, 69–82.

Holles, S., Simpson, S. D., Radford, A. N., Berten, L., Lecchini, D., 2013. Boat noise disrupts orientation behaviour in a coral reef fish. Marine Ecology Progress Series 485, 295–300.

Holme, N. A., 1966. The bottom fauna of the English Channel. Part II. Journal of the Marine Biological Association of the United Kingdom 46 (02), 401–493.

Horowitz, C., Jasny, M., 2007. Precautionary management of noise: Lessons from the US Marine Mammal Protection Act. Journal of International Wildlife Law and Policy 10 (3), 225–232.

Hotchkin, C., Parks, S., 2013. The Lombard effect and other noise-induced vocal modifications: Insight from mammalian communication systems. Biological Reviews 88 (4), 809–824.

Ichikawa, K., Tsutsumi, C., Arai, N., Akamatsu, T., Shinke, T., Hara, T., Adulyanukosol, K., 2006. Dugong (*Dugong dugon*) vocalization patterns recorded by automatic underwater sound monitoring systems. Journal of the Acoustical Society of America 119 (6), 3726–3733.

IMO, 2000. International convention for the Safety of Life at Sea (SOLAS), Chapter V Safety of Navigation, Regulation 19 (1st ed. 1974, amended Dec 2000).

Janik, V. M., 2000. Source levels and the estimated active space of bottlenose dolphin (*Tursiops truncatus*) whistles in the Moray Firth, Scotland. Journal of Comparative Physiology A 186 (7-8), 673–680.

Jensen, F. B., Kuperman, W. A., Porter, M. B., Schmidt, H., 2011. Computational Ocean Acoustics. Springer, NY.

Jensen, F. H., Bejder, L., Wahlberg, M., Soto, N. A., Johnson, M., Madsen, P. T., 2009. Vessel noise effects on delphinid communication. Marine Ecology Progress Series 395, 161–175.

Johnson, C. S., 1968. Relation between absolute threshold and duration-of-tone pulses in the bottlenosed porpoise. Journal of the Acoustical Society of America 43 (4), 757–763.

Johnson, M. P., Tyack, P. L., 2003. A digital acoustic recording tag for measuring the response of wild marine mammals to sound. IEEE Journal of Oceanic Engineering 28 (1), 3–12.

Johnson, M. W., Everest, F. A., Young, R. W., 1947. The role of snapping shrimp (*Crangon* and *Synalpheus*) in the production of underwater noise in the sea. Biological Bulletin 93 (2), 122–138.

Kay, S. M., Marple, S. L., J., 1981. Spectrum analysis - A modern perspective. Proceedings of the IEEE 69 (11), 1380–1419.

Kenny, A., Cato, I., Desprez, M., Fader, G., Schüttenhelm, R., Side, J., 2003. An overview of seabed-mapping technologies in the context of marine habitat classification. ICES Journal of Marine Science: Journal du Conseil 60 (2), 411–418.

Kewley, D. J., 1990. Low-frequency wind-generated ambient noise source levels. Journal of the Acoustical Society of America 88 (4), 1894–1902.

Kinsler, L. E., Frey, A. R., Coppens, A. B., Sanders, J. V., 1999. Fundamentals of Acoustics, 4th ed. Wiley, NJ.

Kipple, B., Gabriele, C., 2003. Glacier Bay Watercraft Noise. NSWC Technical Report NSWCCD-71-TR-2003/522.

Klinck, H., Mellinger, D. K., Klinck, K., Bogue, N. M., Luby, J. C., Jump, W. A., Shilling, G. B., Litchendorf, T., Wood, A. S., Schorr, G. S., Baird, R. W., 2012. Near-real-time acoustic monitoring of beaked whales and other cetaceans using a Seaglider®. Plos One 7 (5), e36128.

Klinck, H., Stelzer, K., Jafarmadar, K., Mellinger, D. K., 2009. AAS Endurance: An autonomous acoustic sailboat for marine mammal research. In: Proceedings of the International Robotic Sailing Conference (IRSC). pp. 43–48.

Knudsen, V. O., Alford, R. S., Emling, J. W., 1948. Underwater ambient noise. Journal of Marine Research 7 (3), 410–429.

Kuperman, W. A., Lynch, J. F., 2004. Shallow-water acoustics. Physics Today 57 (10), 55–61.

Lammers, M. O., Brainard, R. E., Au, W. W. L., Mooney, T. A., Wong, K. B., 2008. An ecological acoustic recorder (EAR) for long-term monitoring of biological and anthropogenic sounds on coral reefs and other marine habitats. Journal of the Acoustical Society of America 123 (3), 1720–1728.

Lee, H. J., Huang, L. F., Chen, Z., 1990. Multi-frame ship detection and tracking in an infrared image sequence. Pattern Recognition 23 (7), 785–798.

Leighton, T., 1994. The Acoustic Bubble. Academic Press, London, UK.

Lesage, V., Barrette, C., Kingsley, M. C. S., Sjare, B., 1999. The effect of vessel noise on the vocal behavior of belugas in the St. Lawrence River estuary, Canada. Marine Mammal Science 15 (1), 65–84.

Lloyd, T., Humphrey, V., Turnock, S., 2011. Noise modelling of tidal turbine arrays for environmental impact assessment. In: Proceedings of the 9th European Wave and Tidal Energy Conference (EWTEC).

Lucke, K., Siebert, U., Lepper, P. A., Blanchet, M. A., 2009. Temporary shift in masked hearing thresholds in a harbor porpoise (*Phocoena phocoena*) after exposure to seismic airgun stimuli. Journal of the Acoustical Society of America 125 (6), 4060–4070.

Lurton, X., 2010. An Introduction to Underwater Acoustics: Principles and Applications, 2nd ed. Springer-Praxis, UK.

Lusseau, D., 2003. Effects of tour boats on the behavior of bottlenose dolphins: Using Markov chains to model anthropogenic impacts. Conservation Biology 17 (6), 1785–1793.

Lusseau, D., 2005. Residency pattern of bottlenose dolphins *Tursiops spp.* in Milford Sound, New Zealand, is related to boat traffic. Marine Ecology Progress Series 295, 265–272.

Lusseau, D., New, L., Donovan, C., Cheney, B., Thompson, P., Hastie, G., Harwood, J., 2011. The development of a framework to understand and predict the population consequences of disturbances for the Moray Firth bottlenose dolphin population. Tech. rep., Scottish Natural Heritage. Commissioned Report No. 468, Scottish Natural Heritage, Perth UK.

Ma, B. B., Nystuen, J. A., 2005. Passive acoustic detection and measurement of rainfall at sea. Journal of Atmospheric and Oceanic Technology 22 (8), 1225–1248.

MacLennan, D. N., Simmonds, E. J., 1992. Fisheries Acoustics. Blackwell Science, Oxford, UK.

Madsen, P. T., 2005. Marine mammals and noise: Problems with root mean square sound pressure levels for transients. Journal of the Acoustical Society of America 117 (6), 3952–3957.

Madsen, P. T., Wahlberg, M., Tougaard, J., Lucke, K., Tyack, P., 2006. Wind turbine underwater noise and marine mammals: Implications of current knowledge and data needs. Marine Ecology Progress Series 309, 279–295.

Marple, S., 1987. Digital Spectral Analysis with Applications. Prentice Hall Inc, NJ.

Martin Taylor, S., 2009. Transformative ocean science through the VENUS and NEPTUNE Canada ocean observing systems. Nuclear Instruments and Methods in Physics Research Section A: Accelerators, Spectrometers, Detectors and Associated Equipment 602 (1), 63–67.

Matsumoto, H., Haxel, J. H., Dziak, R. P., Bohnenstiehl, D. R., Embley, R. W., 2011. Mapping the sound field of an erupting submarine volcano using an acoustic glider. Journal of the Acoustical Society of America 129 (3), EL94–EL99.

Matzner, S., Maxwell, A., Myers, J., Caviggia, K., Elster, J., Foley, M., Jones, M., Ogden, G., Sorensen, E., Zurk, L., Tagestad, J., Stephan, A., Peterson, M., Bradley, D., 2010. Small vessel contribution to underwater noise. In: Proceedings of MTS/IEEE OCEANS 2010.

McCauley, R. D., Fewtrell, J., Popper, A. N., 2003. High intensity anthropogenic sound damages fish ears. Journal of the Acoustical Society of America 113 (1), 638–642.

McDonald, M. A., Hildebrand, J. A., Mesnick, S., 2009. Worldwide decline in tonal frequencies of blue whale songs. Endangered Species Research 9 (1), 13–21.

McDonald, M. A., Hildebrand, J. A., Wiggins, S. M., 2006. Increases in deep ocean ambient noise in the Northeast Pacific west of San Nicolas Island, California. Journal of the Acoustical Society of America 120 (2), 711–718.

McKenna, M. F., Ross, D., Wiggins, S. M., Hildebrand, J. A., 2012. Underwater radiated noise from modern commercial ships. Journal of the Acoustical Society of America 131 (1), 92–103.

McKenna, M. F., Wiggins, S. M., Hildebrand, J. A., 2013. Relationship between container ship underwater noise levels and ship design, operational and oceanographic conditions. Scientific Reports 3, 1760.

McNamara, D. E., Buland, R. P., 2004. Ambient noise levels in the continental United States. Bulletin of the Seismological Society of America 94 (4), 1517–1527.

McQuinn, I. H., Lesage, V., Carrier, D., Larrivee, G., Samson, Y., Chartrand, S., Michaud, R., Theriault, J., 2011. A threatened beluga (Delphinapterus leucas) population in the traffic lane: Vessel-generated noise characteristics of the Saguenay-St. Lawrence Marine Park, Canada. Journal of the Acoustical Society of America 130 (6), 3661–3673.

Means, S. L., Heitmeyer, R. M., 2002. Surf-generated noise signatures: A comparison of plunging and spilling breakers. Journal of the Acoustical Society of America 112 (2), 481–488.

Medwin, H., 1975. Speed of sound in water: A simple equation for realistic parameters. Journal of the Acoustical Society of America 58 (6), 1318–1319.

Medwin, H., Clay, C. S., 1998. Fundamentals of Acoustical Oceanography. Academic Press, Boston, MA.

Mellen, R. H., 1952. The thermal-noise limit in the detection of underwater acoustic signals. Journal of the Acoustical Society of America 24 (5), 478–480.

Merchant, N. D., Barton, T. R., Thompson, P. M., Pirotta, E., Dakin, D. T., Dorocicz, J., 2013. Spectral probability density as a tool for ambient noise analysis. Journal of the Acoustical Society of America 133 (4), EL262–EL267.

Merchant, N. D., Blondel, P., Dakin, D. T., Dorocicz, J., 2012a. Averaging underwater noise levels for environmental assessment of shipping. Journal of the Acoustical Society of America 132 (4), EL343–EL349.

Merchant, N. D., Pirotta, E., Barton, T. R., Thompson, P., 2014. Monitoring ship noise to assess the impact of coastal developments on marine mammals. Marine Pollution Bulletin 78 (1-2), 85–95.

Merchant, N. D., Witt, M. J., Blondel, P., Godley, B. J., Smith, G. H., 2011. Ambient noise in the Western English Channel: Temporal variability due to shipping and biological sources. Proceedings of the Institute of Acoustics 33 (5), 27–29.

Merchant, N. D., Witt, M. J., Blondel, P., Godley, B. J., Smith, G. H., 2012b. Assessing sound exposure from shipping in coastal waters using a single hydrophone and Automatic Identification System (AIS) data. Marine Pollution Bulletin 64 (7), 1320–1329.

Mitson, R. B., 1995. Underwater Noise of Research Vessels, ICES Co-operative Research Report 209. Tech. Rep. 0906-060X.

Moore, S. E., Stafford, K. M., Melling, H., Berchok, C., Wiig, O., Kovacs, K. M., Lydersen, C., Richter-Menge, J., 2012. Comparing marine mammal acoustic habitats in Atlantic and Pacific sectors of the High Arctic: Year-long records from Fram Strait and the Chukchi Plateau. Polar Biology 35 (3), 475–480.

Mossbridge, J. A., Thomas, J. A., 1999. An acoustic niche for Antarctic killer whale and Leopard seal sounds. Marine Mammal Science 15 (4), 1351–1357.

Myrberg, A. A., 1990. The effects of man-made noise on the behavior of marine animals. Environment International 16 (4-6), 575–586.

Nachtigall, P. E., Mooney, T. A., Taylor, K. A., Yuen, M. M., 2007. Hearing and auditory evoked potential methods applied to odontocete cetaceans. Aquatic Mammals 33 (1), 6–13.

National Research Council, 2005. Marine Mammal Populations and Ocean Noise: Determining when Noise Causes Biologically Significant Effects. National Academy Press, Washington, DC.

NEPTUNE, 2013. http://www.neptune.uvic.ca/ (Last accessed 30 Sep 2013).

New, L. F., Harwood, J., Thomas, L., Donovan, C., Clark, J. S., Hastie, G., Thompson, P. M., Cheney, B., Scott-Hayward, L., Lusseau, D., 2013. Modelling the biological significance of behavioural change in coastal bottlenose dolphins in response to disturbance. Functional Ecology 27 (2), 314–322.

NOAA, 2012. Cetsound project: http://cetsound.noaa.gov/index.html (Last accessed 30 Sep 2013).

Norris, T. F., 1995. Effects of boat noise on the singing behavior of humpback whales (*Megaptera novaeangliae*). MSc thesis, San Jose State University.

Nowacek, D. P., Thorne, L. H., Johnston, D. W., Tyack, P. L., 2007. Responses of cetaceans to anthropogenic noise. Mammal Review 37 (2), 81–115.

Nowacek, S. M., Wells, R. S., Solow, A. R., 2001. Short-term effects of boat traffic on bottlenose dolphins, *Tursiops truncatus*, in Sarasota Bay, Florida. Marine Mammal Science 17 (4), 673–688.

Nystuen, J. A., 2001. Listening to raindrops from underwater: An acoustic disdrometer. Journal of Atmospheric and Oceanic Technology 18 (10), 1640–1657.

PAMBuoy, 2013. http://www.pambuoy.co.uk/ (Last accessed 30 Sep 2013).

Papastavrou, V., Smith, S. C., Whitehead, H., 1989. Diving behaviour of the sperm whale, *Physeter macrocephalus*, off the Galapagos Islands. Canadian Journal of Zoology 67 (4), 839–846.

Parks, S., Searby, A., Celerier, A., Johnson, M., Nowacek, D., Tyack, P., 2011a. Sound production behavior of individual North Atlantic right whales: Implications for passive acoustic monitoring. Endangered Species Research 15, 63–76.

Parks, S. E., Clark, C. W., Tyack, P. L., 2007. Short- and long-term changes in right whale calling behavior: The potential effects of noise on acoustic communication. Journal of the Acoustical Society of America 122 (6), 3725–3731.

Parks, S. E., Hamilton, P. K., Kraus, S. D., Tyack, P. L., 2005. The gunshot sound produced by male North Atlantic right whales (*Eubalaena glacialis*) and its potential function in reproductive advertisement. Marine Mammal Science 21 (3), 458–475.

Parks, S. E., Johnson, M., Nowacek, D., Tyack, P. L., 2011b. Individual right whales call louder in increased environmental noise. Biology Letters 7 (1), 33–35.

Parks, S. E., Urazghildiiev, I., Clark, C. W., 2009. Variability in ambient noise levels and call parameters of North Atlantic right whales in three habitat areas. Journal of the Acoustical Society of America 125 (2), 1230–1239.

Patricio, S., Soares, C., Sarmento, A., 2009. Underwater noise modelling of wave energy devices. In: Proceedings of the 8th European Wave and Tidal Energy Conference (EWTEC).

Payne, R., Webb, D., 1971. Orientation by means of long range acoustic signaling in baleen whales. Annals of the New York Academy of Sciences 188 (1), 110–141.

Payne, R. S., McVay, S., 1971. Songs of humpback whales. Science 173 (3997), 585–597.

Pettit, E. C., 2012. Passive underwater acoustic evolution of a calving event. Annals of Glaciology 53 (60), 113–122.

Picciulin, M., Sebastianutto, L., Codarin, A., Farina, A., Ferrero, E. A., 2010. In situ behavioural responses to boat noise exposure of *Gobius cruentatus* (Gmelin, 1789; fam. Gobiidae) and *Chromis chromis* (Linnaeus, 1758; fam. Pomacentridae) living in a Marine Protected Area. Journal of Experimental Marine Biology and Ecology 386 (1-2), 125–132.

Pirotta, E., Laesser, B. E., Hardaker, A., Riddoch, N., Marcoux, M., Lusseau, D., 2013. Dredging displaces bottlenose dolphins from an urbanised foraging patch. Marine Pollution Bulletin 74 (1), 396–402.

Pirotta, E., Thompson, P., Miller, P., Brookes, K., Cheney, B., Barton, T., Graham, I., Lusseau, D., 2014. Scale-dependent foraging activity of bottlenose dolphins modelled using passive acoustic data. Functional Ecology 28 (1), 206–217.

Popper, A. N., Fewtrell, J., Smith, M. E., McCauley, R. D., 2003. Anthropogenic sound: Effects on the behavior and physiology of fishes. Marine Technology Society Journal 37 (4), 35–40.

Popper, A. N., Hastings, M. C., 2009a. The effects of anthropogenic sources of sound on fishes. Journal of Fish Biology 75 (3), 455–489.

Popper, A. N., Hastings, M. C., 2009b. The effects of human-generated sound on fish. Integrative Zoology 4 (1), 43–52.

Porter, M. B., 1992. The KRAKEN normal mode program. Tech. rep., DTIC Document.

Porter, M. B., 2011. The BELLHOP manual and user's guide: Preliminary draft. Heat, Light, and Sound Research, Inc. La Jolla, CA, USA, http://oalib.hlsresearch.com/Rays/HLS-2010-1.pdf, Tech. rep.

Purser, J., Radford, A. N., 2011. Acoustic noise induces attention shifts and reduces foraging performance in three-spined sticklebacks (*Gasterosteus aculeatus*). Plos One 6 (2), e17478.

Radford, C., Jeffs, A., Tindle, C., Montgomery, J., 2008. Temporal patterns in ambient noise of biological origin from a shallow water temperate reef. Oecologia 156 (4), 921–929.

Radford, C. A., Stanley, J. A., Tindle, C. T., Montgomery, J. C., Jeffs, A. G., 2010. Localised coastal habitats have distinct underwater sound signatures. Marine Ecology Progress Series 401, 21–29.

Rako, N., Fortuna, C. M., Holcer, D., Mackelworth, P., Nimak-Wood, M., Pleslić, G., Sebastianutto, L., Vilibić, I., Wiemann, A., Picciulin, M., 2013. Leisure boating noise as a trigger for the displacement of the bottlenose dolphins of the Cres-Lošinj archipelago (northern Adriatic Sea, Croatia). Marine Pollution Bulletin 68 (1-2), 77–84.

Reid, J. B., Evans, P. G., Northridge, S. P., 2003. Atlas of cetacean distribution in north-west European waters. Joint Nature Conservation Committee, Peterborough, UK.

Reinhall, P. G., Dahl, P. H., 2011. Underwater Mach wave radiation from impact pile driving: Theory and observation. Journal of the Acoustical Society of America 130 (3), 1209–1216.

Richards, S. D., Harland, E. J., Jones, S. A. S., 2007. Underwater noise study supporting Scottish Executive Strategic Environmental Assessment for Marine Renewables, QINETIQ Report 06/02215/2. Tech. rep.

Richardson, W. J., Fraker, M. A., Würsig, B., Wells, R. S., 1985. Behaviour of bowhead whales *Balaena mysticetus* summering in the Beaufort Sea: Reactions to industrial activities. Biological Conservation 32 (3), 195–230.

Richardson, W. J., Greene, C. R., Malme, C. I., Thompson, D. H., 1995. Marine Mammals and Noise. Academic Press, San Diego, CA.

Richardson, W. J., Würsig, B., 1997. Influences of man-made noise and other human actions on cetacean behaviour. Marine and Freshwater Behaviour and Physiology 29 (1), 183–209.

Richardson, W. J., Würsig, B., Greene, C. R., 1986. Reactions of bowhead whales, *Balaena mysticetus*, to seismic exploration in the Canadian Beaufort Sea. Journal of the Acoustical Society of America 79 (4), 1117–1128.

Rogers, E. O., Genderson, J. G., Smith, W. S., Denny, G. F., Farley, P. J., 2004. Underwater acoustic glider. In: Proceedings of the International Geoscience and Remote Sensing Symposium (IGARSS '04). Vol. 3. pp. 2241–2244.

Rolland, R. M., Parks, S. E., Hunt, K. E., Castellote, M., Corkeron, P. J., Nowacek, D. P., Wasser, S. K., Kraus, S. D., 2012. Evidence that ship noise increases stress in right whales. Proceedings of the Royal Society B: Biological Sciences 279 (1737), 2363–2368.

Ross, D., 1976. Mechanics of Underwater Noise. Pergamon Press, NY.

Roussel, E., 2002. Disturbance to Mediterranean cetaceans caused by noise. Tech. rep., A report to the ACCOBAMS Secretariat, Monaco, 2002. Section 13, 18 pp.

Rudnick, D. L., Davis, R. E., Eriksen, C. C., Fratantoni, D. M., Perry, M. J., 2004. Underwater gliders for ocean research. Marine Technology Society Journal 38 (2), 73–84.

Sara, G., Dean, J., D'Amato, D., Buscaino, G., Oliveri, A., Genovese, S., Ferro, S., Buffa, G., Martire, M., Mazzola, S., 2007. Effect of boat noise on the behaviour of bluefin tuna *Thunnus thynnus* in the Mediterranean Sea. Marine Ecology Progress Series 331, 243–253.

Scheidat, M., Castro, C., Gonzalez, J., Williams, R., 2004. Behavioural responses of humpback whales (*Megaptera novaeangliae*) to whalewatching boats near Isla de la Plata, Machalilla National Park, Ecuador. Journal of Cetacean Research and Management 6 (1), 63–68.

Scottish Government, 2011. 2020 Routemap for Renewable Energy in Scotland, Scottish Government, Edinburgh, Scotland.

Scrimger, J. A., 1985. Underwater noise caused by precipitation. Nature 318 (6047), 647–649.

Scrimger, J. A., Evans, D. J., McBean, G. A., Farmer, D. M., Kerman, B. R., 1987. Underwater noise due to rain, hail, and snow. Journal of the Acoustical Society of America 81 (1), 79–86.

Scrimger, P., Heitmeyer, R. M., 1991. Acoustic source-level measurements for a variety of merchant ships. Journal of the Acoustical Society of America 89 (2), 691–699.

Shahidul Islam, M., Tanaka, M., 2004. Impacts of pollution on coastal and marine ecosystems including coastal and marine fisheries and approach for management: A review and synthesis. Marine Pollution Bulletin 48 (7-8), 624–649.

Shortis, M., Harvey, E., Seager, J., 2007. A review of the status and trends in underwater videometric measurement. In: Proceedings of SPIE 6471.

Simpson, S. D., Meekan, M., Montgomery, J., McCauley, R., Jeffs, A., 2005. Homeward sound. Science 308 (5719), 221–221.

Širović, A., Hildebrand, J. A., Wiggins, S. M., McDonald, M. A., Moore, S. E., Thiele, D., 2004. Seasonality of blue and fin whale calls and the influence of sea ice in the Western Antarctic Peninsula. Deep Sea Research Part II: Topical Studies in Oceanography 51 (17), 2327–2344.

Širović, A., Wiggins, S. M., Oleson, E. M., 2013. Ocean noise in the tropical and subtropical Pacific Ocean. The Journal of the Acoustical Society of America 134 (4), 2681–2689.

Slabbekoorn, H., Bouton, N., van Opzeeland, I., Coers, A., ten Cate, C., Popper, A. N., 2010. A noisy spring: The impact of globally rising underwater sound levels on fish. Trends in Ecology & Evolution 25 (7), 419–427.

Sousa-Lima, R. S., Norris, T. F., Oswald, J. N., Fernandes, D. P., 2013. A review and inventory of fixed autonomous recorders for passive acoustic monitoring of marine mammals. Aquatic Mammals 39 (1), 23–53.

Sousa-Lima, R. S., Paglia, A. P., Da Fonseca, G. A., 2002. Signature information and individual recognition in the isolation calls of Amazonian manatees, *Trichechus inunguis* (Mammalia: Sirenia). Animal Behaviour 63 (2), 301–310.

Southall, B. L., 2005. Shipping Noise and Marine Mammals: A Forum for Science, Management, and Technology. Final Report of the National Oceanic and Atmospheric Administration (NOAA) International Symposium, 18-19 May 2004.

Southall, B. L., Bowles, A. E., Ellison, W. T., Finneran, J. J., Gentry, R. L., Greene, Charles R., J., Kastak, D., Ketten, D. R., Miller, J. H., Nachtigall, P. E., Richardson, W. J., Thomas, J. A., Tyack, P. L., 2007. Marine mammal noise exposure criteria: Initial scientific recommendations. Aquatic Mammals 33 (4), 411–521.

Stimpert, A. K., Au, W. W. L., Parks, S. E., Hurst, T., Wiley, D. N., 2011. Common humpback whale (*Megaptera novaeangliae*) sound types for passive acoustic monitoring. Journal of the Acoustical Society of America 129 (1), 476–482.

Stimpert, A. K., Wiley, D. N., Au, W. W. L., Johnson, M. P., Arsenault, R., 2007. 'Megapclicks': Acoustic click trains and buzzes produced during night-time foraging of humpback whales (*Megaptera novaeangliae*). Biology Letters 3 (5), 467–470.

Stone, G. S., Florez-Gonzalez, L., Katona, S., 1990. Whale migration record. Nature 346, 705.

Strasberg, M., 1979. Nonacoustic noise interference in measurements of infrasonic ambient noise. Journal of the Acoustical Society of America 66 (5), 1487–1493.

Tasker, M., Amundin, M., André, M., Hawkins, A., Lang, W., Merck, T., Scholik-Schlomer, A., Teilmann, J., Thomsen, F., Werner, S., Zakharia, M., 2010. Marine Strategy Framework Directive - Task Group 11 Report Underwater noise and Other Forms of Energy. EUR 24341 EN - Joint Research Centre, Luxembourg: Office for Official Publications of the European Communities, 55pp.

Tavolga, W. N., 1958. Underwater sounds produced by two species of toadfish, *Opsanus tau* and *Opsanus beta*. Bulletin of Marine Science 8 (3), 278–284.

Tegowski, J., Deane, G., Lisimenka, A., Blondel, P., 2012. Spectral and statistical analyses of ambient noise in Spitsbergen Fjords and identification of glacier calving events. In: 11th European Conference on Underwater Acoustics, Edinburgh, Scotland.

Theobald, P., Robinson, S., Lepper, P., Hayman, G., Humphrey, V., Wang, L., Mumford, S., 2011. The measurement of underwater noise radiated by dredging vessels during aggregate extraction operations. In: 4th International Conference on Underwater Acoustic Measurements, Technologies and Results, Kos, Greece.

Thorne, P. D., 1986. Laboratory and marine measurements on the acoustic detection of sediment transport. Journal of the Acoustical Society of America 80 (3), 899–910.

Thorp, W. H., 1967. Analytic description of the low-frequency attenuation coefficient. Journal of the Acoustical Society of America 42 (1), 270.

Tolstoy, M., Diebold, J., Doermann, L., Nooner, S., Webb, S., Bohnenstiehl, D., Crone, T., Holmes, R., 2009. Broadband calibration of the R/V Marcus G. Langseth four-string seismic sources. Geochemistry, Geophysics, Geosystems 10 (8), 1–15.

Toropova, C., Meliane, I., Laffoley, D., Matthews, E., Spalding, M., (Eds.), 2010. Global Ocean Protection: Present Status and Future Possibilities. International Union for Conservation of Nature and Natural Resources, Gland, Switzerland.

Tougaard, J., Carstensen, J., Teilmann, J., Skov, H., Rasmussen, P., 2009a. Pile driving zone of responsiveness extends beyond 20 km for harbor porpoises (*Phocoena phocoena* (L.)). Journal of the Acoustical Society of America 126 (1), 11–14.

Tougaard, J., Henriksen, O. D., Miller, L. A., 2009b. Underwater noise from three types of offshore wind turbines: Estimation of impact zones for harbor porpoises and harbor seals. Journal of the Acoustical Society of America 125 (6), 3766–3773.

Tougaard, J., Wright, A., Madsen, P. T., (In Press). Noise exposure criteria for harbour porpoises. In: Effects of Noise on Aquatic Life II. Springer, NY.

Trevorrow, M. V., Vasiliev, B., Vagle, S., 2008. Directionality and maneuvering effects on a surface ship underwater acoustic signature. Journal of the Acoustical Society of America 124 (2), 767–778.

Tyack, P. L., 2008. Implications for marine mammals of large-scale changes in the marine acoustic environment. Journal of Mammalogy 89 (3), 549–558.

Urick, R. J., 1983. Principles of Underwater Sound, 3rd Edition. McGraw-Hill, NY.

Urick, R. J., 1986. Ambient noise in the sea. Peninsula Publishing, Los Altos, CA.

Vabø, R., Olsen, K., Huse, I., 2002. The effect of vessel avoidance of wintering Norwegian spring spawning herring. Fisheries Research 58 (1), 59–77.

Vagle, S., Large, W. G., Farmer, D. M., 1990. An evaluation of the WOTAN technique of inferring oceanic winds from underwater ambient sound. Journal of Atmospheric and Oceanic Technology 7 (4), 576–595.

Van der Graaf, A., Ainslie, M. A., Andre, M., Brensing, K., Dalen, J., Dekeling, R., Robinson, S., Tasker, M., Thomsen, F., Werner, S., 2012. European Marine Strategy Framework Directive - Good Environmental Status (MSFD GES): Report of the Technical Subgroup on Underwater noise and other forms of energy. Tech. rep.

Van der Schaar, M., Ainslie, M. A., Robinson, S. P., Prior, M. K., André, M., 2014. Changes in 63 Hz third-octave band sound levels over 42 months recorded at four deep-ocean observatories. Journal of Marine Systems 130, 4–11.

Van Parijs, S. M., Clark, C. W., Sousa-Lima, R. S., Parks, S. E., Rankin, S., Risch, D., Van Opzeeland, I. C., 2009. Management and research applications of real-time and archival passive acoustic sensors over varying temporal and spatial scales. Marine Ecology Progress Series 395, 21–36.

Vasconcelos, R. O., Amorim, M. C. P., Ladich, F., 2007. Effects of ship noise on the detectability of communication signals in the Lusitanian toadfish. Journal of Experimental Biology 210 (12), 2104–2112.

VENUS, 2013. http://venus.uvic.ca/ (Last accessed 30 Sep 2013).

Versluis, M., Schmitz, B., von der Heydt, A., Lohse, D., 2000. How snapping shrimp snap: Through cavitating bubbles. Science 289 (5487), 2114–2117.

Wale, M. A., Simpson, S. D., Radford, A. N., 2013a. Noise negatively affects foraging and antipredator behaviour in shore crabs. Animal Behaviour 86 (1), 111–118.

Wale, M. A., Simpson, S. D., Radford, A. N., 2013b. Size-dependent physiological responses of shore crabs to single and repeated playback of ship noise. Biology Letters 9 (2), 20121194.

Wales, S. C., Heitmeyer, R. M., 2002. An ensemble source spectra model for merchant ship-radiated noise. Journal of the Acoustical Society of America 111 (3), 1211–1231.

Wardle, C., Carter, T., Urquhart, G., Johnstone, A., Ziolkowski, A., Hampson, G., Mackie, D., 2001. Effects of seismic air guns on marine fish. Continental Shelf Research 21 (8), 1005–1027.

Watwood, S. L., Miller, P. J., Johnson, M., Madsen, P. T., Tyack, P. L., 2006. Deep-diving foraging behaviour of sperm whales (*Physeter macrocephalus*). Journal of Animal Ecology 75 (3), 814–825.

Welch, P., 1967. The use of fast Fourier transform for the estimation of power spectra: A method based on time averaging over short, modified periodograms. IEEE Transactions on Audio and Electroacoustics 15 (2), 70–73.

Wenz, G. M., 1961. Some periodic variations in low-frequency acoustic ambient noise levels in the ocean. Journal of the Acoustical Society of America 33 (1), 64–74.

Wenz, G. M., 1962. Acoustic ambient noise in the ocean: Spectra and sources. Journal of the Acoustical Society of America 34 (12), 1936–1956.

Wiggins, S., 2003. Autonomous acoustic recording packages (ARPs) for long-term monitoring of whale sounds. Marine Technology Society Journal 37 (2), 13–22.

Wiggins, S. M., Hildebrand, J. A., 2007. High-frequency Acoustic Recording Package (HARP) for broad-band, long-term marine mammal monitoring. In: Symposium on Underwater Technology and Workshop on Scientific Use of Submarine Cables and Related Technologies. pp. 551–557.

Williams, R., Trites, A. W., Bain, D. E., 2002. Behavioural responses of killer whales (*Orcinus orca*) to whale-watching boats: Opportunistic observations and experimental approaches. Journal of Zoology 256 (2), 255–270.

Wilson, B., Carter, C., Norris, J., 2011. Going with the flow: A method to measure and map underwater sound in tidal-stream energy sites. Proceedings of the Institute of Acoustics 33 (5), 78.

Wilson, O. B., Wolf, S. N., Ingenito, F., 1985. Measurements of acoustic ambient noise in shallow water due to breaking surf. Journal of the Acoustical Society of America 78 (1), 190–195.

Wladichuk, J., 2010. Investigation of ambient noise in the underwater coastal environment and its potential for use as a navigational aid by grey whales, *Eschrichtius robustus*, foraging in British Columbia, Canada. Ph.D. thesis, University of Bath.

Woźniak, B., Dera, J., 2007. Light Absorption in Sea Water. Springer, NY.

Wright, A. J., Deak, T., Parsons, E. C. M., 2011. Size matters: Management of stress responses and chronic stress in beaked whales and other marine mammals may require larger exclusion zones. Marine Pollution Bulletin 63 (1-4), 5–9.

Wright, A. J., Soto, N. A., Baldwin, A. L., Bateson, M., Beale, C. M., Clark, C., Deak, T., Edwards, E. F., Fernaández, A., Godinho, A., Hatch, L. T., Kakuschke, A., Lusseau, D., Martineau, D., Romero, M. L., Weilgart, L. S., Wintle, B. A., Notarbartolo-di Sciara, G., Martin, V., 2007a. Do marine mammals experience stress related to anthropogenic noise? International Journal of Comparative Psychology 20 (2), 274–316.

Wright, A. J., Soto, N. A., Baldwin, A. L., Bateson, M., Beale, C. M., Clark, C., Deak, T., Edwards, E. F., Fernández, A., Godinho, A., Hatch, L. T., Kakuschke, A., Lusseau, D., Martineau, D., Romero, M. L., Weilgart, L. S., Wintle, B. A., Notarbartolo-di Sciara, G., Martin, V., 2007b. Anthropogenic noise as a stressor in animals: A multidisciplinary perspective. International Journal of Comparative Psychology 20 (2), 250–273.

Wysocki, L. E., Dittami, J. P., Ladich, F., 2006. Ship noise and cortisol secretion in European freshwater fishes. Biological Conservation 128 (4), 501–508.

Zelick, R., Mann, D. A., Popper, A. N., 1999. Acoustic Communication in Fishes and Frogs. In: Comparative Hearing: Fish and Amphibians. Springer, NY, pp. 363–411.

Supplementary Material to Section 4.1

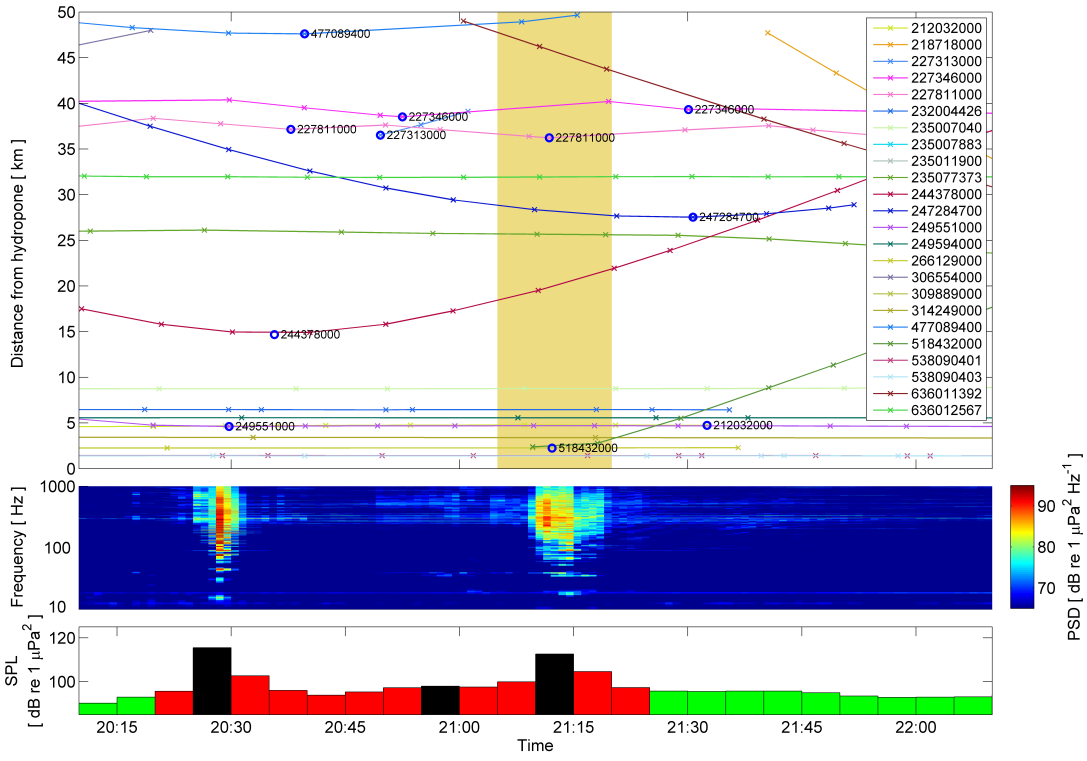

Figure A-1: False Negative 1/5. The CPA at ∼35 km belongs to an 18-m fishing vessel (227811000), while the CPA at ∼2 km is a 77-m cargo ship (518432000). [*Top*: Range from hydrophone vs. time. Crosses denote individual AIS transmissions; lines connect transmissions from the same vessel; circles indicate closest points of approach, labelled with the MMSI number. Shaded area denotes 15-minute time window around current SPL peak. Horizontal lines indicate AIS transmissions from stationary vessels. *Middle*: Power spectral density of concurrent acoustic data. *Bottom*: Broadband (0.01-1 kHz) SPL, showing 'background' (green), 'intermittent' (red), and 'intermittent' peaks (black)].

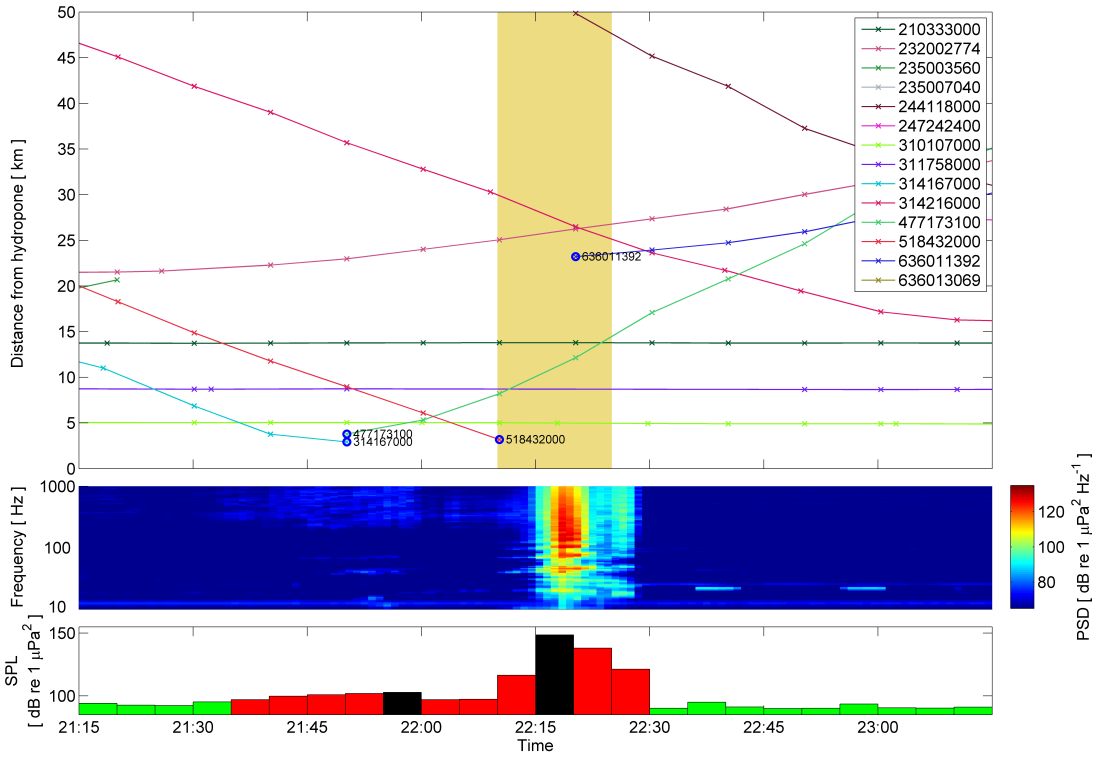

Figure A-2: False Negative 2/5. The magnitude of the SPL peak (148.6 dB re 1 μPa^2) and the trajectory of the closer vessel, a 77-m cargo ship (518432000), suggest that the closer vessel was the source of this peak. [*Top*: Range from hydrophone vs. time. Crosses denote individual AIS transmissions; lines connect transmissions from the same vessel; circles indicate closest points of approach, labelled with the MMSI number. Shaded area denotes 15-minute time window around current SPL peak. Horizontal lines indicate AIS transmissions from stationary vessels. *Middle*: Power spectral density of concurrent acoustic data. *Bottom*: Broadband (0.01-1 kHz) SPL, showing 'background' (green), 'intermittent' (red), and 'intermittent' peaks (black)].

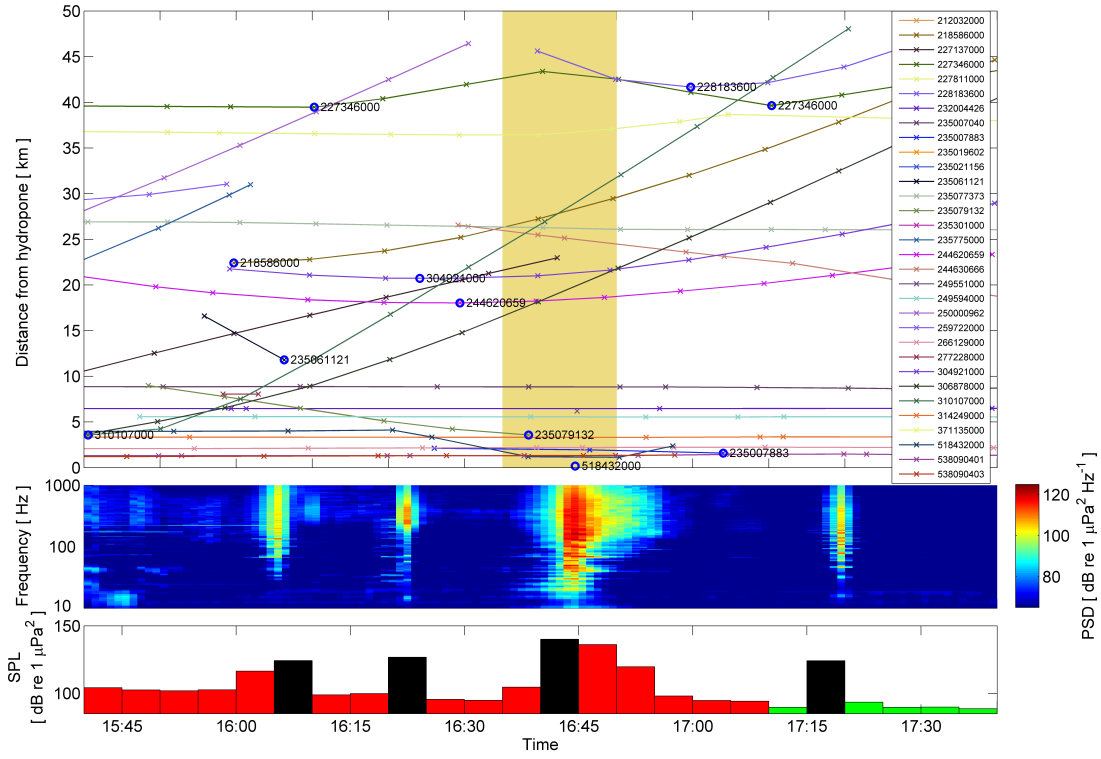

Figure A-3: False Negative 3/5. The spatial and temporal proximity of the closer CPA to the deployment, the magnitude of the SPL peak (140.1 dB re 1 μPa^2), and the fact that the further CPA is a 14-m recreational vessel (235079132) suggest that that the closer vessel (518432000) is the source of this peak. [*Top*: Range from hydrophone vs. time. Crosses denote individual AIS transmissions; lines connect transmissions from the same vessel; circles indicate closest points of approach, labelled with the MMSI number. Shaded area denotes 15-minute time window around current SPL peak. Horizontal lines indicate AIS transmissions from stationary vessels. *Middle*: Power spectral density of concurrent acoustic data. *Bottom*: Broadband (0.01-1 kHz) SPL, showing 'background' (green), 'intermittent' (red), and 'intermittent' peaks (black)].

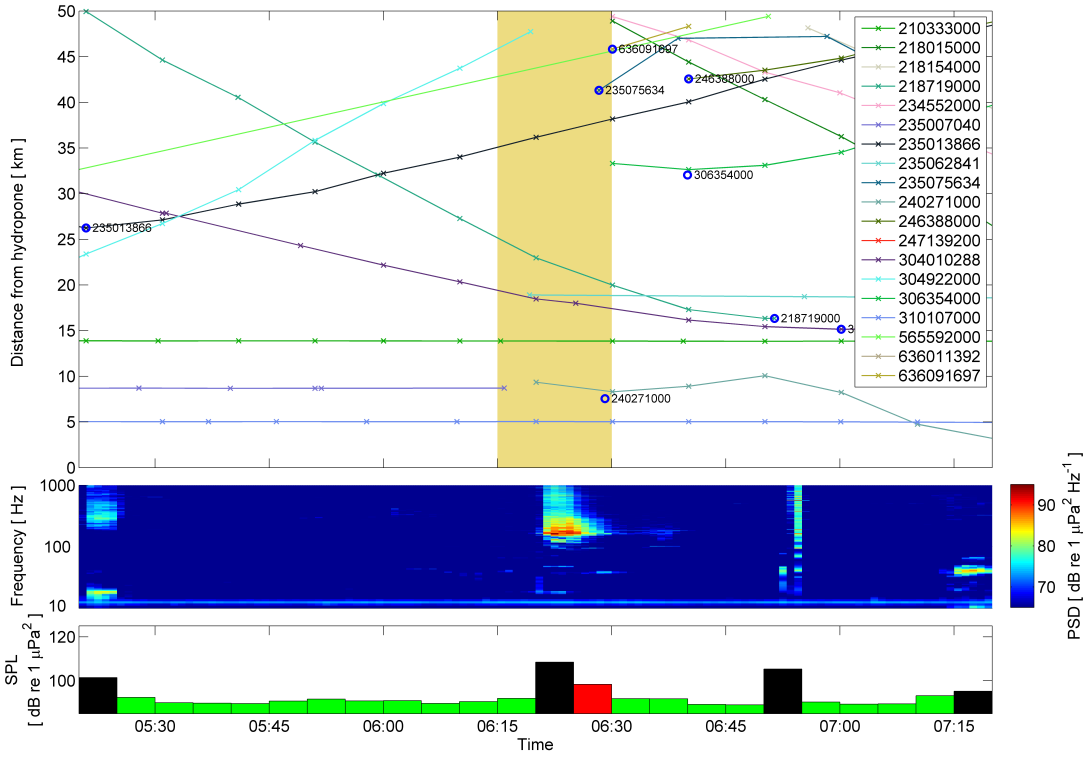

Figure A-4: False Negative 4/5. The further CPA at ∼40 km is a 13-m catamaran (235075634), while the nearer CPA is a 190-m bulk carrier (240271000). [*Top*: Range from hydrophone vs. time. Crosses denote individual AIS transmissions; lines connect transmissions from the same vessel; circles indicate closest points of approach, labelled with the MMSI number. Shaded area denotes 15-minute time window around current SPL peak. Horizontal lines indicate AIS transmissions from stationary vessels. *Middle*: Power spectral density of concurrent acoustic data. *Bottom*: Broadband (0.01-1 kHz) SPL, showing 'background' (green), 'intermittent' (red), and 'intermittent' peaks (black)].

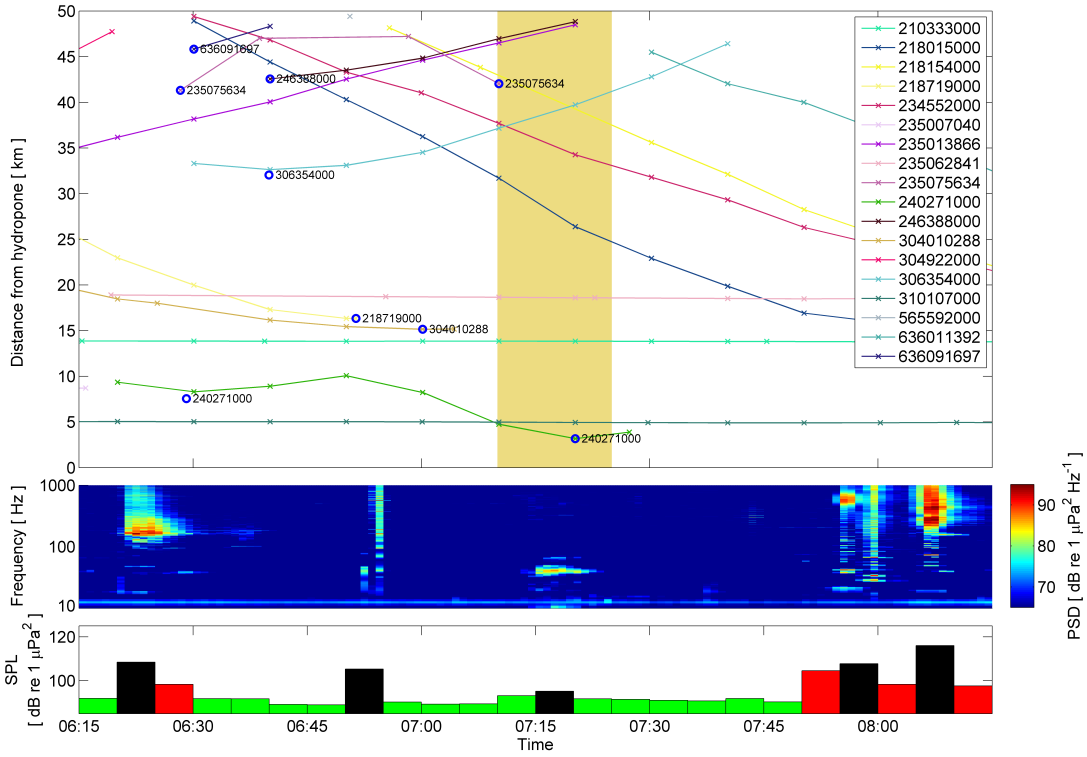

Figure A-5: False Negative 5/5. The further CPA at ∼40 km is a 13-m catamaran (235075634), while the nearer CPA is a 190-m bulk carrier (240271000). [*Top*: Range from hydrophone vs. time. Crosses denote individual AIS transmissions; lines connect transmissions from the same vessel; circles indicate closest points of approach, labelled with the MMSI number. Shaded area denotes 15-minute time window around current SPL peak. Horizontal lines indicate AIS transmissions from stationary vessels. *Middle*: Power spectral density of concurrent acoustic data. *Bottom*: Broadband (0.01-1 kHz) SPL, showing 'background' (green), 'intermittent' (red), and 'intermittent' peaks (black)].

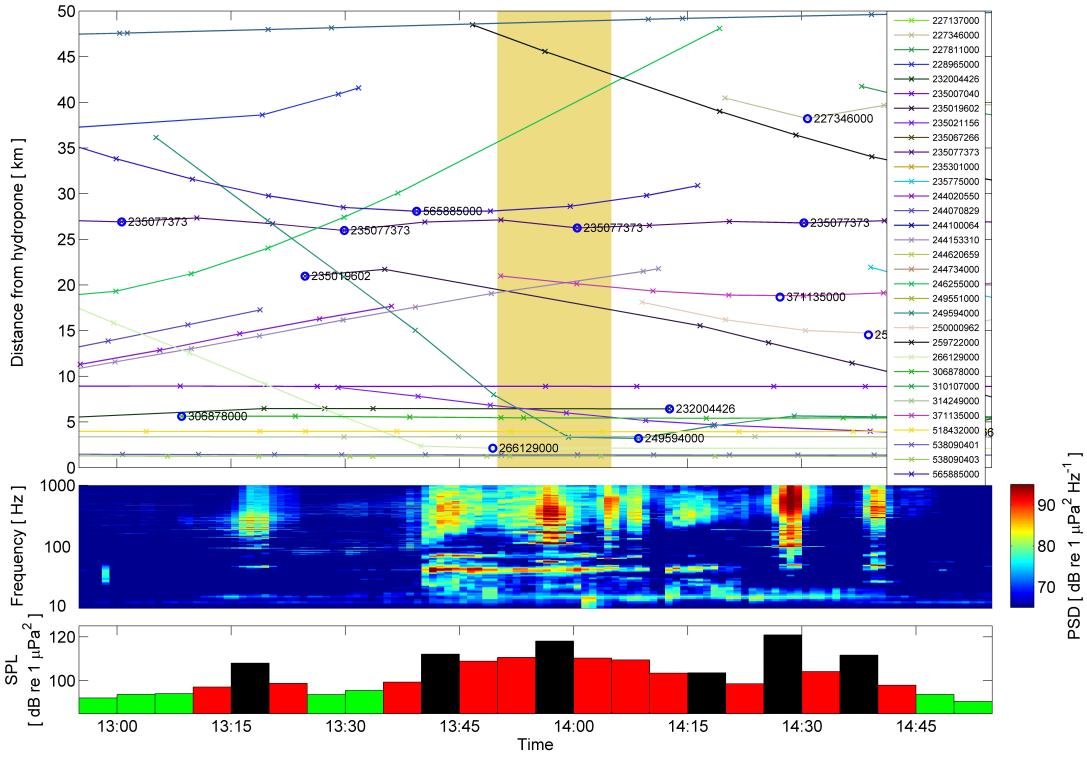

Figure A-6: False Positive 1/3. The CPA within the time window is an 87-m research vessel (235077373), while the much nearer CPA is a 144-m tanker (266129000). [*Top*: Range from hydrophone vs. time. Crosses denote individual AIS transmissions; lines connect transmissions from the same vessel; circles indicate closest points of approach, labelled with the MMSI number. Shaded area denotes 15-minute time window around current SPL peak. Horizontal lines indicate AIS transmissions from stationary vessels. *Middle*: Power spectral density of concurrent acoustic data. *Bottom*: Broadband (0.01-1 kHz) SPL, showing 'background' (green), 'intermittent' (red), and 'intermittent' peaks (black)].

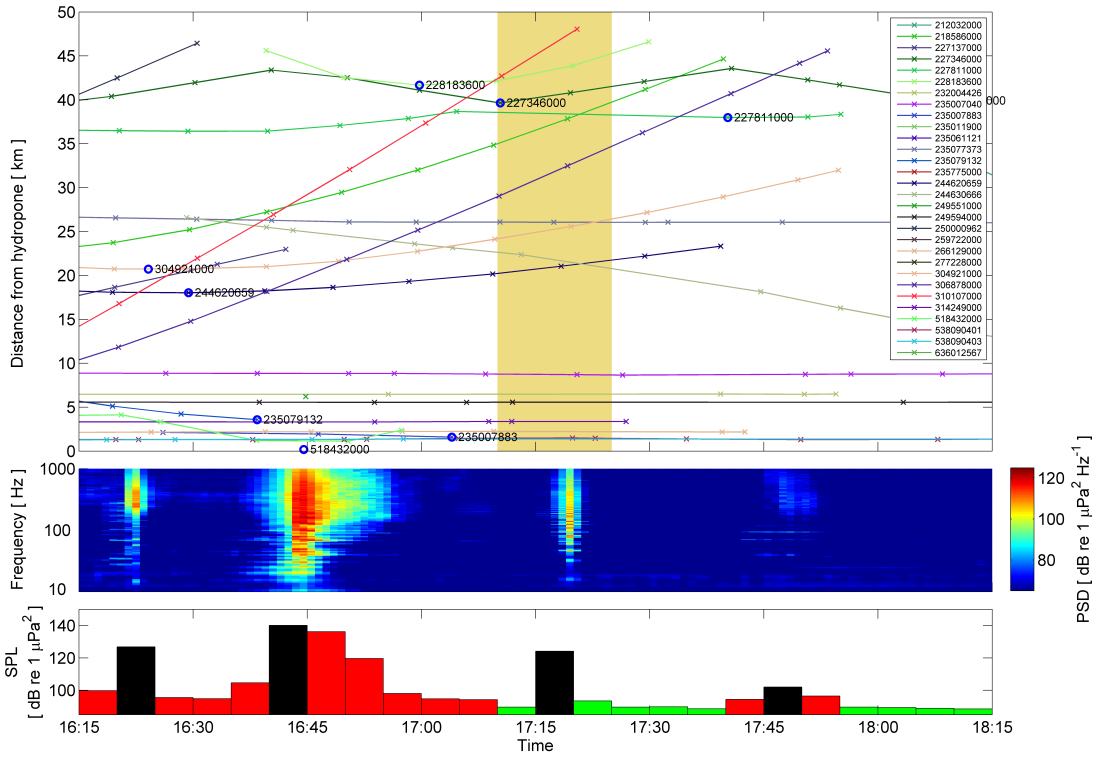

Figure A-7: False Positive 2/3. The CPA at ∼40 km is a 19-m fishing vessel (227346000). Due to the speed of the transit, it is probable that this peak was due to a small vessel close to the deployment not transmitting AIS data. [*Top*: Range from hydrophone vs. time. Crosses denote individual AIS transmissions; lines connect transmissions from the same vessel; circles indicate closest points of approach, labelled with the MMSI number. Shaded area denotes 15-minute time window around current SPL peak. Horizontal lines indicate AIS transmissions from stationary vessels. *Middle*: Power spectral density of concurrent acoustic data. *Bottom*: Broadband (0.01-1 kHz) SPL, showing 'background' (green), 'intermittent' (red), and 'intermittent' peaks (black)].

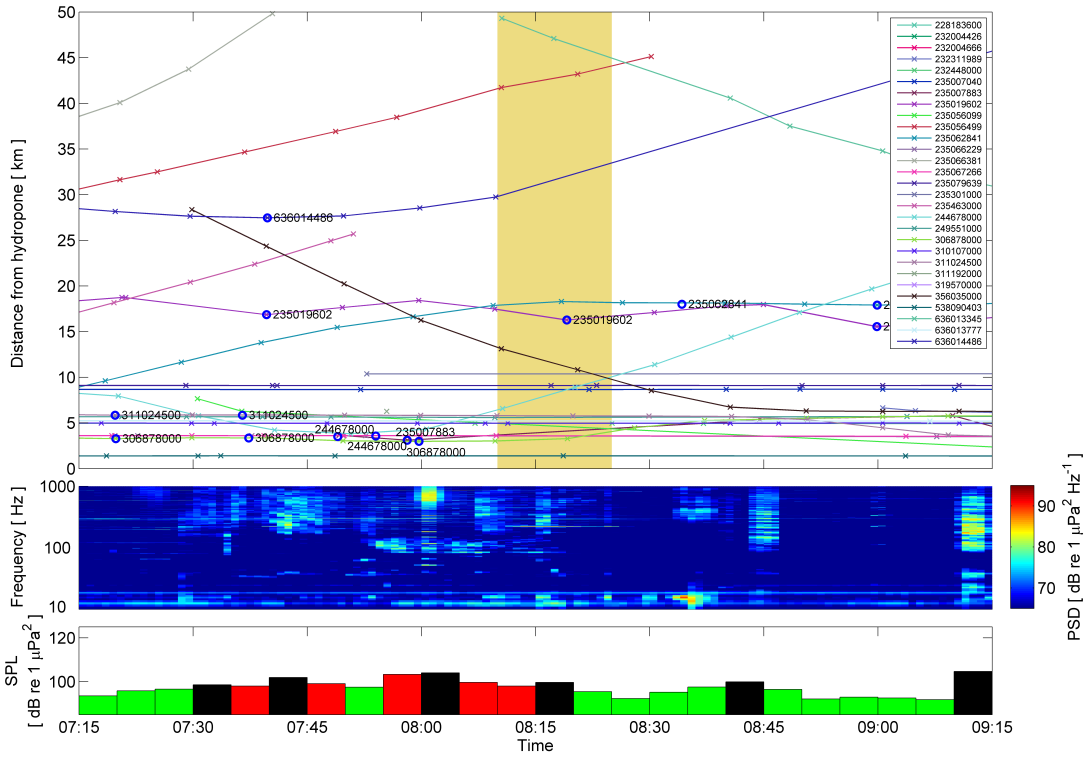

Figure A-8: False positive 3/3. The CPA at ∼15 km is a 10-m fishing vessel (235019602). The relatively continuous noise visible in the spectrogram may be due to nontransiting vessels within the Bay. [*Top*: Range from hydrophone vs. time. Crosses denote individual AIS transmissions; lines connect transmissions from the same vessel; circles indicate closest points of approach, labelled with the MMSI number. Shaded area denotes 15-minute time window around current SPL peak. Horizontal lines indicate AIS transmissions from stationary vessels. *Middle*: Power spectral density of concurrent acoustic data. *Bottom*: Broadband (0.01-1 kHz) SPL, showing 'background' (green), 'intermittent' (red), and 'intermittent' peaks (black)].

Supplementary Material to Section 4.2

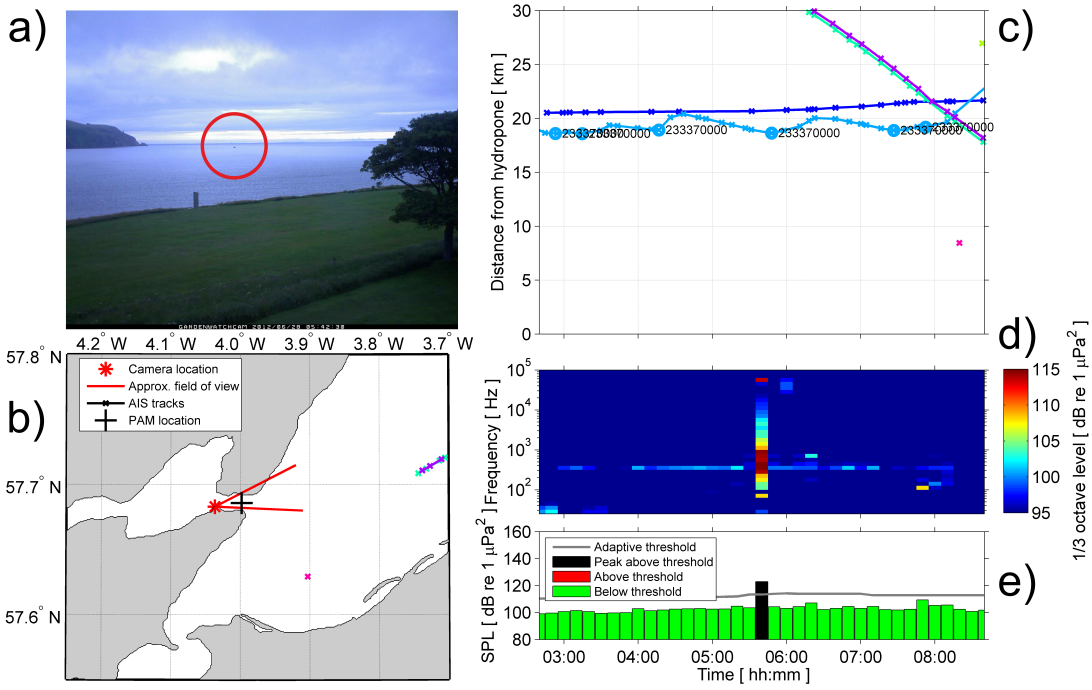

Figure B-1: Unidentified vessel example. Noise peak at 05:40 does not correspond to the CPA of an AIS-tracked transit, but time-lapse footage captures passage of a small vessel not transmitting an AIS signal past the hydrophone. (a) Still of time lapse footage showing vessel; (b) Map of AIS movements in period centred on CPA. Black cross denotes location of PAM unit in The Sutors, circles indicate CPAs labelled with Maritime Mobile Service Identity (MMSI) number; (c) Range of AIS transmissions from PAM unit versus time; (d) 1/3 octave spectrum of concurrent acoustic data; (e) Broadband level in frequency range 0.1-1 kHz, showing peak identification using adaptive threshold.

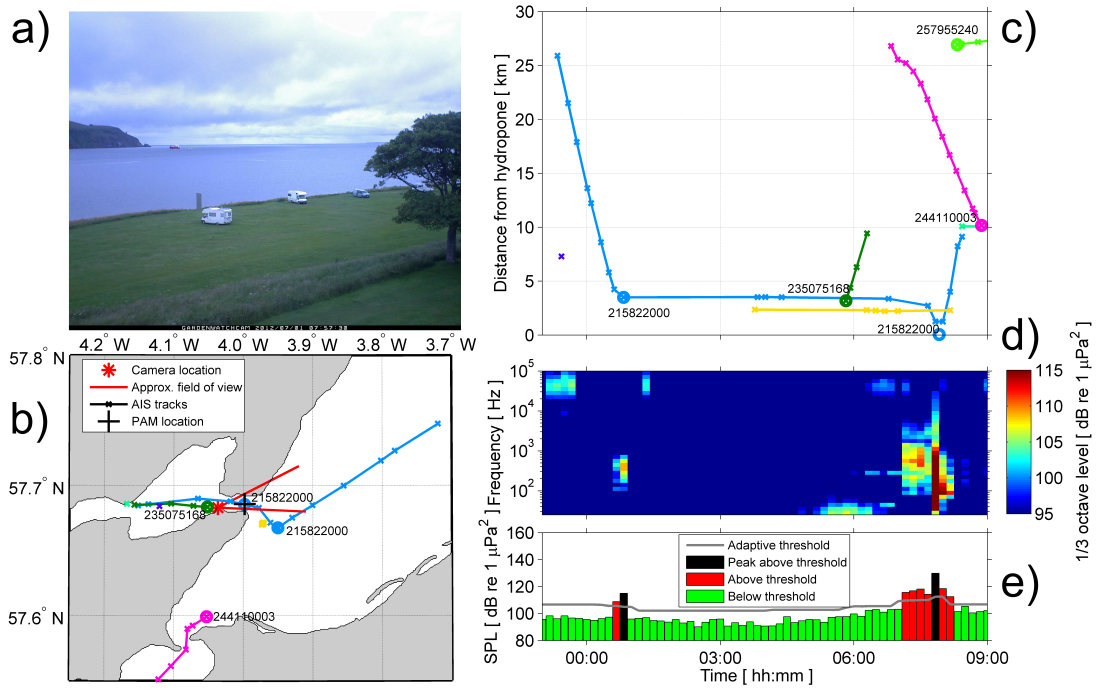

Figure B-2: Decelerating vessel example. First noise peak [see part (e)] occurs as vessel decelerates to a halt at 00:50, while second peak corresponds to CPA at 07:50 as vessel transits into the Cromarty Firth. (a) Still of time lapse footage showing vessel; (b) Map of AIS movements in period centred on CPA. Black cross denotes location of PAM unit in The Sutors, circles indicate CPAs labelled with Maritime Mobile Service Identity (MMSI) number; (c) Range of AIS transmissions from PAM unit versus time; (d) 1/3 octave spectrum of concurrent acoustic data; (e) Broadband level in frequency range 0.1-1 kHz, showing peak identification using adaptive threshold.

The following videos are also provided on the accompanying DVD:

SuppMat_Video1_TheSutors.mp4

Rig tow at The Sutors. Footage shows shipping activity at The Sutors from 26-27 Sep 2012. Audio composed of concatenated real-time samples of acoustic data, filtered and compressed for audibility. Video panels correspond to components of Fig. 4.14, p84.

SuppMat_Video2_Chanonry.mp4

Chanonry ship passage. Footage shows an example ship passage at Chanonry on 18 Aug 2012. Audio consists of temporally-compressed acoustic data, filtered for audibility. Video panels correspond to components of Fig. 4.14, p84.